

**Studies on anti-obesity compounds in Okinawan  
traditional bioresources: Identification and its activity  
enhancement.**

**沖縄県の伝統的な生物資源に含まれる抗肥満活性成分に関する研究－化学構造とその活性増強法－**

**Abu Yousuf Hossin**

**2021**

**Studies on anti-obesity compounds in Okinawan  
traditional bioresources: Identification and its activity  
enhancement.**

**沖縄県の伝統的な生物資源に含まれる抗肥満活性成分に関する研究－化学構造とその活性増強法－**

**Abu Yousuf Hossin**

A dissertation submitted to the United Graduate School of  
Agricultural Sciences, Kagoshima University, Japan

In partial fulfillment of the requirements  
for the degree of

**DOCTOR OF PHILOSOPHY**

**2021**

## Acknowledgments

It is with immense gratitude that I acknowledge the support and guidance received by my Major Advisory Supervisor, Prof. Hirosuke Oku, Tropical Biosphere Research Center (TBRC), Center of Molecular Biosciences (COMB), University of the Ryukyus. Prof. Oku has been my inspiration and guidance in my life during the stay in Japan.

This dissertation would not have been possible without the guidance of Dr. Associate Prof. Masashi Inafuku University of the Ryukyus and Faculty of Agriculture who in one way or another contributed and extended his valuable support in the completion of this study.

It gives me great pleasure in acknowledging Asst. Prof. Hironori Iwasaki, Faculty of Agriculture, University of the Ryukyus and Prof. Koji Nagao, Faculty of Agriculture, Saga University; for their immense comments, suggestions and support throughout my research period. Special thanks to my thesis reviewer Prof. De-Xing Hou, Faculty of Agriculture, Kagoshima University.

My sincere gratitude goes to Nakamura, for his advice, kind consideration of me at the very beginning of research as a friend.

Special thanks to all of my previous and present lab members for their support and for making my lab experience a memorable one. Special thanks to all staff members at the Center of Molecular Biosciences for their kind assistance during my study period.

Grateful thanks and deepest gratitude to Dr. Md. Harun-Ur-Rashid, and Dr. Shahanas Parveen Associate Professor, Department of Genetics and Plant Breeding, Sher-e-Bangla Agricultural University, Dhaka-1207, Bangladesh, for their, continuous inspiration, and helpful suggestion during the period of this research.

I recognize this research would not have been possible without the financial assistance of Amino Up Company Limited, Sapporo, Japan, and express my heartfelt gratitude for the financial support given to me.

Finally, I take this opportunity to praise the “Allah” for making me this capable, my parents, brother, and sisters for their invaluable support, unconditional love, and help emotionally throughout my stay in Japan and for bearing all the tough times they went through with me.

**DEDICATED  
TO  
ALL MY TEACHERS**

The dissertation here to attached, entitled “**Studies on anti-obesity compounds in Okinawan traditional bioresources: Identification and its activity enhancement.**” prepared and submitted by Abu Yousuf Hossin in partial fulfillment of the requirement for the degree of Doctor of Philosophy in Agriculture is now accepted.

## **EVALUATION COMMITTEE MEMBERS OF DISSERTATION**

---

**Dr. Hirosuke Oku**

Professor

Center of Molecular Biosciences  
University of the Ryukyus, Japan  
(Major Advisor)

---

**Dr. Koji Nagao**

Professor

Faculty of Agriculture  
Saga University, Japan  
(Vice Advisor)

---

**Dr. Hironori Iwasaki**

Associate Professor

Center of Molecular Biosciences  
University of the Ryukyus, Japan  
(Vice Advisor)

---

**Dr. De-Xing Hou**

Professor

Faculty of Agriculture  
Kagoshima University, Japan  
(Vice Advisor)

---

**Dr. Masashi Inafuku**

Associate Professor

Faculty of Agriculture  
University of the Ryukyus, Japan  
(Vice Advisor)

## Table of contents

List of figures.....	vi
List of tables.....	x
List of Publications .....	xi
List of abbreviations.....	xii
Abstract.....	xiv
Outline of the studies.....	xviii

## Chapter I: General Introduction

<b>1.1. Introduction .....</b>	<b>2</b>
1.1.1. The global perspective on obesity epidemic .....	2
1.1.2. Prevalence of obesity and occurrence in Japan.....	4
1.1.3. In vitro cell culture models and transcriptional regulation of adipogenesis .....	6
1.1.4. Causes for obesity .....	9
1.1.5. Treatments for obesity.....	9
1.1.6. Physiological roles of adipose tissue during obesity.....	10
1.1.7. Anti-obesogenic effects of plant products and their mechanism of action .....	11
1.1.8. Importance of plant derivative natural products on anti-obesity .....	12
1.1.9. Impact of tropical medicinal plants on human health .....	13

1.1.10. Natural products nanoparticulation with PLGA.....	14
---	----

## **Chapter II: Anti-obesity activity of dihydropyranocoumarins and its enhancement by nanoparticulation with polylactic-co-glycolic acid: An in vivo study**

<b>2.1. Introduction.....</b>	<b>17</b>
<b>2.2. Materials and methods .....</b>	<b>19</b>
2.2.1. Purification of DPCs from PJT .....	19
2.2.2. Preparation of nano-DPCs.....	19
2.2.3. Ethical approval.....	20
2.2.4. Experimental animals.....	20
2.2.5. Experimental design.....	20
2.2.6 Biochemical analysis .....	24
2.2.7. Histological analysis.....	24
2.2.8. Quantitative real-time polymerase chain reaction.....	24
2.2.9. Concentration analysis of DPCs and nano-DPCs in epididymal WAT .....	27
2.2.10. Statistical analyses.....	27
<b>2.3. Results.....</b>	<b>29</b>
2.3.1. Purified DPCs and DPC incorporated in nanoparticle as nano-DPCs.....	29
2.3.2. DPCs and nano-DPCs effects of on growth parameters .....	31

2.3.3. DPCs and nano-DPCs effects on serum and hepatic parameters .....	34
2.3.4. DPCs and nano-DPCs effects on lipid accumulation in epididymal adipose tissues .....	34
2.3.5. DPCs and nano-DPCs effects on lipid metabolism-related gene expressions in epididymal WAT .....	38
2.2.6. PLGA nanoparticulation effect of DPCs in WAT accumulation .....	38
<b>2.4. Discussion.....</b>	<b>40</b>
<b>2.5. Conclusion.....</b>	<b>43</b>
 <b>Chapter III: Anti-obesity effect of <i>Cirsium brevicaule</i> A. GRAY Root (CbR) on 3T3–L1</b>	
<b>3.1. Introduction .....</b>	<b>45</b>
<b>3.2. Materials and methods.....</b>	<b>48</b>
3.2.1. Plant material .....	48
3.2.2. Extraction and purification of CbR.....	48
3.2.3. Purification and structure identification of fractionated CbR extract .....	50
3.2.4. Cell culture and treatments.....	50
3.2.5. Oil Red O Staining.....	52
3.2.6. Statistical analyses.....	52
<b>3.3. Results.....</b>	<b>53</b>
3.3.1. Effect of CbR extract on 3T3–L1cells .....	53



3.3.2. Effect of partially purified CbR methanol extract on 3T3–L1 cells .....	54
3.3.3. Effects of CbR methanol extract fractions on 3T3–L1 cells.....	56
3.3.4. Screening of F1 fraction .....	58
3.3.5. Chemical structure identification of active compound from CbR.....	61
3.3.6. Screening of F2 fraction.....	61
<b>3.4. Discussion.....</b>	<b>64</b>
<b>3.5. Conclusion.....</b>	<b>64</b>
 <b>Chapter IV: Anti-adipogenic effect of syringin via AMPK and Akt signaling pathways</b>	
<b>4.1 Introduction.....</b>	<b>66</b>
<b>4.2. Materials and methods.....</b>	<b>67</b>
4.2.1. Syringin purification .....	67
4.2.2. Cell culture and treatments .....	67
4.2.3. Quantitative real-time polymerase chain reaction.....	68
4.2.4. Western blot analyses .....	70
4.2.5. Statistical analyses .....	72
<b>4.3. Results</b>	
4.3.1. Effect of syringin during the differentiation time points of adipogenesis.....	73
4.3.2. Effects of syringin on differentiation and lipid accumulation of 3T3–L1 cells.....	74
4.3.3. Effects of syringin on lipid metabolism related genes and proteins regulation.....	77

4.3.4. Effects of syringin on signaling pathways .....	79
<b>4.4. Discussion.....</b>	<b>81</b>
<b>4.5. Conclusion.....</b>	<b>84</b>
 <b>Chapter V: General conclusion.....</b>	 <b>85</b>
<b>References .....</b>	<b>92</b>

## List of Figures

Figure No.	Title	Page No.
Fig.1-1	Worldwide prevalence of obesity	03
Fig.1-2	Obesity growth rate from 2013 to 2019 in japan	04
Fig.1-3	Highest and lowest obese adult male population prevalence regions in Japan.	05
Fig.1-4	Induction of adipogenesis by a cascade of transcription factors	08
Fig.1-5	Hydrolysis of PLGA	15
Fig.2-1	<i>Peucedanum japonicum</i> Thunb (PJT)	17
Fig.2-2	HPLC chromatogram of DPCs	29
Fig.2-3	Chemical information and content of dihydropyrancoumarins (DPCs) used in this study	33
Fig.2-4	Effects of dietary dihydropyrancoumarins (DPCs) and DPC-encapsulated polylactic-co-glycolic acid nanoparticles (nano-DPCs) on growth parameters	32

Fig.2–5	Effects of dietary dihydropyranocoumarins (DPCs) and DPC-encapsulated polylactic-co-glycolic acid nanoparticles (nano-DPCs) on serum parameters	33
Fig.2–6	Effects of dietary dihydropyranocoumarins (DPCs) and DPC-encapsulated polylactic-co-glycolic acid nanoparticles (nano-DPCs) on hepatic parameters	35
Fig.2–7	Effects of dietary dihydropyranocoumarins (DPCs) and DPC-encapsulated polylactic-co-glycolic acid nanoparticles (nano-DPCs) on adipocyte size in epididymal white adipose tissues	36
Fig.2–8	Effects of dietary dihydropyranocoumarins (DPCs) and DPC-encapsulated polylactic-co-glycolic acid nanoparticles (nano-DPCs) on lipid metabolism-related gene expression in epididymal white adipose tissue	37
Fig.2–9	Concentration of dihydropyranocoumarins (DPCs) in epididymal white adipose tissue (WAT) collected 24 h after oral administration of DPCs or polylactic-co-glycolic acid (PLGA) nanoparticles with DPCs (nano-DPCs)	39
Fig.3–1	<i>Cirsium brevicaule</i> A. GRAY	47
Fig.3–2	Flowchart for the extraction of active anti-obesity compounds from <i>Cirsium brevicaule</i> A GRAY root (CbR) with low polar to high polar solvent.	49

Fig.3-3	Time schedule for the treatment with crude extract or its fractions during the cellular differentiation of 3T3-L1	51
Fig.3-4	Effects of CbR extracts on 3T3-L1 cells	53
Fig.3-5	Effects of extracts and fractions from CbR on 3T3-L1 cells.	55
Fig.3-6	Effect of fractions from CbR on 3T3-L1 cells.	57
Fig. 3-7	HPLC chromatogram of CbR methanol extract fractions	58
Fig.3-8	Effect of fractions from CbR on 3T3-L1 cells.	59
Fig.3-9	Isolation of active components from CbR and their chemical structure	60
Fig.3-10	Flowchart for the bioactivity-guided purification of anti-obesity compounds from CbR.	62
Fig. 3-11	HPLC profiling CbR methanol extract and effects of on intracellular lipid accumulation in 3T3-L1 cells	63
Fig.4-1	Effect of syringin on intercellular lipid accumulation in 3T3-L1 cells	73
Fig.4-2	Effect of syringin on adipogenic differentiation and lipid accumulation in 3T3-L1 cells.	75
Fig.4-3	Effect of syringin on adipogenic differentiation through the regulation of adipogenic factors in 3T3-L1 cells	76

Fig.4-4	Effect of syringin on the expression of adipogenesis-related genes and proteins	78
Fig.4-5	Effects of syringin on AMPK, ACC, and Akt phosphorylation during the differentiation of 3T3-L1 adipocytes	80
Fig. 5-1	Summary illustration of suppressive effects of DPCs and Nano-DPC on high fat diet induce obese mice fat burning pathway	87
Fig. 5-2	Summary illustration of the suppressive effects of syringin on adipogenesis and lipogenesis related gene parameters <i>in vitro</i>	91

---

## List of Tables

<b>Table No.</b>	<b>Title</b>	<b>Page No.</b>
Table 2–1	Composition of experimental diets used in this study	22
Table 2–2	Administration procedure of dihydropyranocoumarins (DPC) and its total dosages in this study.	23
Table 2–3	TaqMan gene expression assays used for the quantitative real time PCR analysis	26
Table 2–4	Total food, energy intake and fecal lipid excretion	32
Table 4–1	TaqMan gene expression assays used for the quantitative real time PCR analysis.	69
Table 4–2	List of antibodies used in this western blotting	71
Table 5–1	Summary of pteryxin characteristics	88
Table 5–2	Summary of peucedanocoumarin III (PCIII) characteristics	89
Table 5–3	Summary of syringin characteristics	90

## List of Publications

1. **Hossin, A.Y.**; Inafuku, M.; Oku, H. Dihydropyranocoumarins Exerted Anti-Obesity Activity In Vivo and its Activity Was Enhanced by Nanoparticulation with Polylactic-Co-Glycolic Acid. *Nutrients* **2019**, *11*, 3053. doi.org/10.3390/nu11123053
2. **Hossin, A.Y.**; Inafuku, M.; Takara, K.; Nugara, R.N.; Oku, H. Syringin: A Phenylpropanoid Glycoside Compound in *Cirsium brevicaule* A. GRAY Root Modulates Adipogenesis. *Molecules* **2021**, *26*, 1531. doi.org/10.3390/ molecules26061531



## Abbreviations

ACC	Acetyl CoA carboxylase
ACOX	Acyl-coenzyme A oxidase
ACTB	Actin, beta, cytoplasmic
ADIPOQ	Adiponectin
Akt	Protein kinase B
AMPK	AMP-activated protein kinase
BAT	Brown adipose tissue
BCS	Bovine calf serum
BMI	Body mass index
C/EBP $\alpha$	CCAAT/enhancer binding protein alpha
CbR	<i>Cirsium brevicaule</i> A. GRAY Root
CBAG	<i>Cirsium brevicaule</i> A. GRAY leaf
CC	Column chromatography
CPT1	Carnitine palmitoyltransferase 1
DEX	Dexamethasone
DMEM	Dulbecco's modified Eagle's medium
DPC	Dihydropyranocoumarin
EI-MS	Electron ionization mass spectrometry
FABP4	Fatty acid binding protein 4
FAS	Fatty acid synthase
FBS	Fetal bovine serum
FFA	Free fatty acids
GAPDH	Glyceraldehyde-3-phosphate dehydrogenase
GLUT	Glucose transporter
HDL	High density lipoprotein
HFD	High fat diet
HPLC	High-performance liquid chromatography
HRP	Horseradish peroxidase
IBMX	3-isobutyl-1-methylxanthine

LC-MS	Liquid chromatography-mass spectrometry
LIPE	Hormone-sensitive lipase
LPL	Lipoprotein lipase
<i>mRNA</i>	<i>Messenger RNA</i>
pAb	Polyclonal antibody
PCIII	Peucedanocoumarin III
PGC1 $\alpha$	Peroxisome proliferator activated receptor gamma coactivator 1-alpha
PJT	<i>Peucedanum japonicum</i> Thunb
PLGA	Polylactic-co-glycolic acid
PPAR $\gamma$	Peroxisome proliferator activated receptor gamma
PTX	Pteryxin
PVDF	Polyvinylidene difluoride
qPCR	Quantitative reverse transcriptase real-time polymerase chain reaction
SCD	Stearoyl-CoA desaturase
SREBP	Sterol regulatory element-binding protein
TC	Total Cholesterol
T2D	Type 2 diabetes
TG	Triglyceride
mAb	Monoclonal antibody
MSCs	Mesenchymal stem cells
NCS	Newborn calf serum
UCP	Uncoupling protein
UPLC	Ultraperformance liquid chromatography
WAT	White adipose tissue
WHO	World health organization

## Abstract

Supplementation of diet with functional components is an effective way to manage obesity and overweight. Therefore, this study aims to characterize the anti-obesity properties of Okinawan folk medicine and attempt the enhancement of their bioactivities.

The first experiment examined the anti-obesity mechanisms of dihydropyrancoumarins (DPCs). In the previous studies, DPCs were isolated from an Okinawan traditional herb, *Peucedanum japonicum* Thunb. (PJT), as anti-obesity compounds with cultured adipocytes. However, it is not known whether DPCs exert anti-obesity activity *in vivo*. I also assessed the effect of nanoparticulation of DPCs into polylactic-co-glycolic acid (PLGA) on their bioavailability and functionality. Dietary intake of DPCs significantly suppressed the body weight gain and fat accumulation in white adipose tissues (WAT) of mice fed a high-fat diet. DPCs intake also significantly decreased the mean size of adipocytes and upregulated mRNA levels of thermogenesis-related genes in WAT. Similar results were observed in mice received a small amount of DPCs (1% equivalence of regular dose) when encapsulating in PLGA nanoparticles, but not non-nanoparticulated form. These results suggested that DPCs' anti-obesity properties are caused by an increase in energy expenditures, and that a PLGA-based nanoparticulate system is a powerful tool to enhance their activities.

Next, I focused on anti-obesity properties of *Cirsium brevicaule* A. GRAY (CBAG), whose aerial parts and root are traditionally used as both food and herbal medicine in Okinawa. Our previous study demonstrated the anti-obesity properties of CBAG leaves, but not evaluated the biological activities of CBAG root (CbR). This study therefore evaluated and characterized the anti-obesity properties of CbR by testing its activities in adipocyte cultures. Dried CbR powder was serially extracted with solvents of various polarities, and these crude extracts were tested for

inhibitory effects on lipid accumulation in 3T3–L1 cells. Treatment of 3T3–L1 cells with a methanol extract of CbR reduced cellular lipid accumulation the most. The methanol extract was then fractionated, and these fractions were subjected to further activity analyses. The phenylpropanoid glycosidic molecule syringin (PubChem ID: 5316860) was identified as an active compound in CbR. Syringin suppressed lipid accumulation of 3T3–L1 cells in a dose-dependent manner without cytotoxicity. This compound also significantly reduced the gene expressions of the master regulator of adipogenesis and other differentiation markers, and effectively enhanced the phosphorylation of the AMP-activated protein kinase and acetyl-CoA carboxylase. These results indicated that syringin has potent anti-obesity effects due to the attenuation of adipocyte differentiation, adipogenesis, and the promotion of lipid metabolism.

In conclusion, the results of present studies provide insight into the anti-obesity characteristics of DPCs and syringin, suggesting the great potential of PJT and CBAG as functional foods against obesity. In addition, this study pointed to the great potential for a PLGA-based nanoparticle encapsulation of bioactive compounds such as DPC in the oral delivery of anti-obesity agents.

# 沖縄県の伝統的な生物資源に含まれる抗肥満活性成分に関する研究－化学構造とその活性増強法－

肥満等の生活習慣病の予防や改善において、食事による機能性成分摂取は有効な手段となる。従って、本研究は沖縄県で伝統的に野菜／薬草として利用されている生物資源の抗肥満活性とその活性発現機序を明らかにすると同時に、その活性増強に資する技術を開発することを目的とした。

これまでの研究では、沖縄県の伝統的な食資源であるボタンボウフウ (*Peucedanum japonicum* Thunb, PJT) に含まれるジヒドロピラノクマリン (DPC) 化合物が抗肥満活性を有することを、培養脂肪細胞を用いた評価系により明らかにしている。本研究では、動物試験にてPJTより単離したDPC化合物の抗肥満活性を評価すると共に、その作用機序を明らかにすることで、長命草の機能性食素材としての可能性を探った。また、その生体内利用率を向上させるために、DPC化合物をポリ乳酸-グリコール酸共重合体 (PLGA) でナノ粒子技術の有効性を検証した。その結果として、高脂肪食摂取マウス (C57BL/6J) の体重増加量と白色脂肪組織 (WAT) 重量は、DPC化合物の混餌投与 (1.94 mg/day) によって有意に抑制されることが明らかとなった。更には、DPC化合物投与群のWATの脂肪細胞サイズは有意に減少し、それらの熱産生関連遺伝子のmRNAレベルは有意に亢進していたことから、DPC化合物が脂肪細胞の熱産生亢進を介した抗肥満効果をもたらす機能性食成分であることが示唆された。また、PLGAナノ粒子化DPC化合物は、その投与量が少量 (混餌投与の100分の1量) であるにも関わら

ず、上記混餌投与と同様の抗肥満活性を示したことから、**PLGA**を基盤としたナノ粒子化システムは**DPC**化合物の生物活性を増強するために有効な技術であることが示唆された。

次に本研究では、沖縄に広く自生するシマアザミ (*Cirsium brevicaule* A. GRAY、**CBAG**) の生物活性に着目した。これまでの研究では、**CBAG**の葉の抗肥満作用は確認されていたが、根 (**CbR**) の生物活性は評価されていない。**CbR**乾燥粉末から得た種々の粗抽出物が**3T3-L1**細胞の脂肪蓄積に与える影響を評価したところ、メタノール抽出物が最も高い抑制活性を示したことから、更なる分画作業を繰り返して活性成分の単離と同定を試みた。その結果として、フェニルプロパノイド配糖体である「シリンギン (PubChem ID: 5316860)」が活性本体であることが明らかとなった。同化合物は、**3T3-L1**細胞における脂質合成のマスターレギュレーター遺伝子や分化マーカー遺伝子の発現を有意に低下させることが明らかとなり、更には**AMPK**やアセチル-CoAカルボキシラーゼのリン酸化を有意に亢進することが明らかとなった。従って、シリンギンは脂肪細胞の分化や脂質代謝の抑制を介して抗肥満効果をもたらす機能性成分であることが示唆された。

本研究により、沖縄県の伝統的な生物資源である **PJT** と **CBAG** が抗肥満効果をもたらす機能性食素材であることが明らかとなり、それらの活性寄与成分も明らかとなった。更には、**PLGA** を基盤としたナノ粒子化が抗肥満剤の開発に有用であることが明らかとなった。

## Outline of the studies

1. The effects of nanoparticulation on anti-obesity activities of dihydropyrano coumarins (DPCs), which are derivated from *Peucedanum japonicum* Thunb (PJT) was investigated in mice. Gene expression analyses were given special attention to reveal the underlying mechanisms related to DPCs (Chapter II).
2. The effects of *Cirsium brevicaule* A. GRAY root (CbR) on the development of obesity were investigated *in vitro* using 3T3-L1 cells. To identify the active compound, I examined anti-obesity activities in various extracts of CbR, and fractioned and subjected to further activity analyses (Chapter III).
3. The effects of syringin, which was isolated as an active compound from CbR in Chapter III, and its mechanisms were examined (Chapter IV). The main focus of this study was to elucidate the compound responsible for inhibiting adipogenesis, and to examine the activity against anti-obesity *in vitro*.

# **CHAPTER I**

## **General Introduction**



## **1.1. Introduction**

### **1.1.1. The global perspective on obesity epidemic**

Obesity is characterized by excess body fat storage due to a long-term high caloric intake and less energy expenditure. Obesity is frequently accompanied by serious threats to health such as cardiovascular disease, type 2 diabetes, sleep apnea, cancer, and hypertension. In the last few decades, the dietary behavior and lifestyle of the world population have undergone significant changes. This change directly impacts on human health as a result of global disease pattern transition, with fewer infectious diseases and more chronic diseases [1].

Obesity is most often defined according to Body Mass Index (BMI) and is calculated as weight in kilograms divided by height in meters squared ( $\text{kg/m}^2$ ). Following current recommendations, overweight is defined as a  $\text{BMI} \geq 25$  and obesity as a  $\text{BMI} \geq 30$  [2]. According to National Health and Nutrition Examination Survey (NHANES), from 2009 to 2010, the mean age-adjusted BMI for 20-year-old Americans was 28.7. More than 1.9 billion adults worldwide are overweight, with over 650 million of them being obese. Notably, a significant increase in obese children under 5-year-old reached 39 million in 2020 [3] (Figure 1–1). This is an alarmingly high number considering the potentially severe consequences.

Twin adoption studies found that adopted children had body sizes more similar to their biological parents than their adopted parents, and suggested that familial aggregation of obesity was primarily due to genetics rather than environmental factors [4,5]. Meanwhile, there is evidence that the environment and the complex interplay between environment and genes play significant roles in developing obesity [6,7], although genetic factors are important. Nowadays, the environment has been obesogenic due to access easily to foods high in saturated fat and refined

sugar, and also due to our comfortable lives with heated houses, easy transport by car, video games, and television. Several studies have also found that industrial chemicals and pesticides are persistent organic pollutants (POPs), such as e.g. polychlorinated bisphenyls (PCBs) which accumulate in human adipose tissues [8,9]. It has been shown that POPs affect hepatic, reproductive, and immune systems, and also relate to metabolic syndrome, including type 2 diabetes, insulin resistance, dyslipidemia, and obesity [10,11].

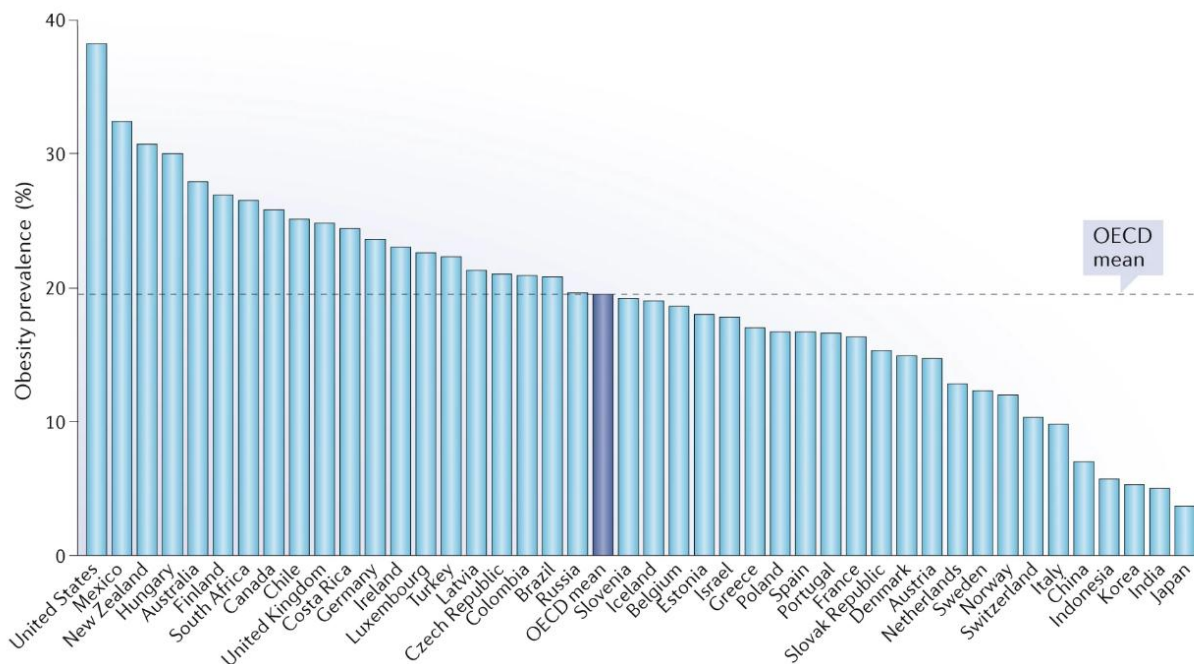


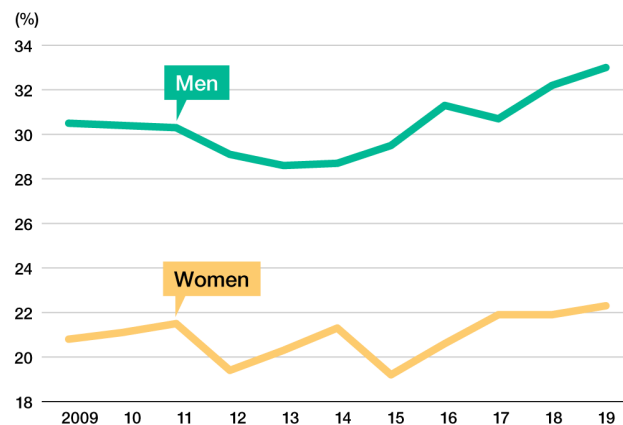
**Figure 1–1 worldwide prevalence of obesity.**

Prevalence of obesity (BMI  $\geq 30\text{kg/m}^2$ ) varies countries to countries (Organization for Economic Cooperation and Development (OECD), 2017; percentage of adults with obesity from measured data). In 2015, across OECD countries, the mean prevalence of obesity in adults was 19.5% (dotted line) and ranged from 30% in the United States. Adapted with permission from ref.40, the OECD [12].

### 1.1.2. Prevalence of obesity and occurrence in Japan

As shown above, The WHO has defined a BMI  $\geq 25$  as overweight and a BMI  $\geq 30$  as obesity. Meanwhile, the Japan Society on Obesity Study has benchmarked 25 as the obese limit of BMI [13] because humans with BMI  $\geq 25$  have more visceral fat and are at increased risk of type 2 diabetes and cardiovascular diseases. According to a survey conducted by the Japan Ministry of Health, Labor and Welfare, male obesity has been upward in between 2013 to 2019 analyzed by ([www.nippon.com/en/japan-data/h00853/](http://www.nippon.com/en/japan-data/h00853/)) (Figure 1–2). Nevertheless, it has been revealed that 30% of men and 40% of women are unable to change their food habits and lifestyle due to maintaining their job responsibilities, housework, and childcare.

**Percentage Overweight Among Respondents Aged 20 or Older**



**Percentage Overweight by Age Group**

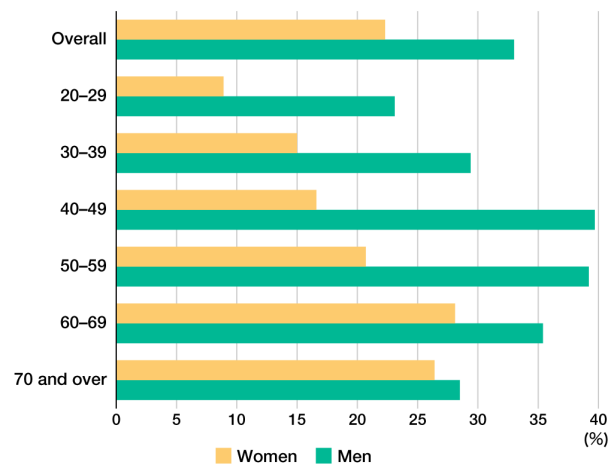


**Figure 1-2** Obesity growth rate from 2013 to 2019 in Japan  
Data from the Ministry of Health, Labor and welfare. ([www.nippon.com/en/japan-data/h00853/](http://www.nippon.com/en/japan-data/h00853/))

A survey in 2010 showed that obesity risk was higher in 40-year-old adults and over, and similar trends have been observed in recent studies [14]. Furthermore, it also revealed that Okinawa was ranked as No. 1 for the highest prevalence of obesity amongst the 47 prefectures in Japan in 2010 (Figure 1–3). The second highest prevalence was observed in Miyazaki, and the least were in Tottori, Shiga, Fukui, and Yamaguchi [15]. The following figure illustrates the selected highest and lowest prevalence of obesity in prefectures in Japan.

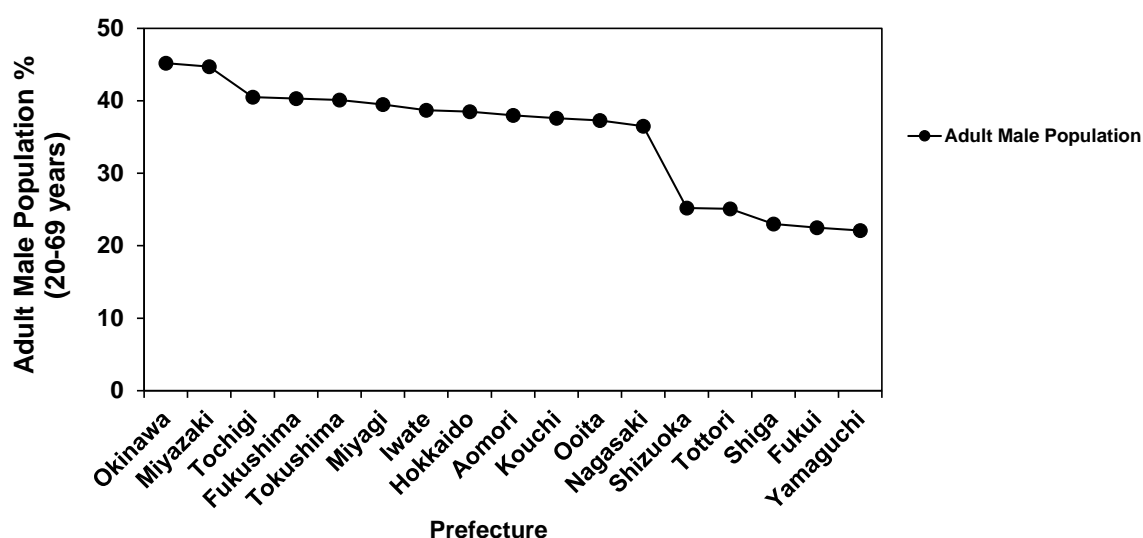


**Figure 1–3** Highest and lowest obese adult male population prevalence regions in Japan

Source: Ministry of Health, Labor and Welfare; 2010

### 1.1.3. In vitro cell culture models and transcriptional regulation of adipogenesis

General adipocytes and cephalic adipocytes are differentiated from mesoderm-derived mesenchymal stem cells (MSCs), and neuroectodermal-derived neural crest cells, respectively [16]. Adipogenesis could be divided into two phases: a determination phase and a differentiation phase has shown below.

**Determination phase:** The MSCs lose their pluripotency and become committed adipocyte progenitors, preadipocytes, determined to the adipogenic fate. These preadipocytes subsequently undergo adipocyte differentiation when receiving appropriate signals.

**Differentiation phase:** Adipogenesis is exceedingly coordinated cellular differentiation process. In this process, fibroblastic progenitors are transformed into spherical fat-loaded adipocytes, which acquire the abilities carrying out fatty acid uptake, triglyceride synthesis and transport, adipokine secretion.

Nowadays, adipogenesis is understood in a detailed manner, with new modulators being discovered continually. The broad literature studies on adipogenesis have been conducted mainly using *in vitro* cell culture models and genetically modified animals. Many *in vitro* models have been established for studying adipocyte differentiation. Among them, more frequently used are mouse cell lines 3T3–L1 pre-adipocytes and 3T3–F442 for white adipocytes [17-19], and hibernoma cell line HIB-1B for brown adipocytes [20]. Of available human models, the Simpson Golabi Behmel syndrome (SGBS) cell line [21] and the human multipotent adipose-derived stem (hMADS) cell line are to be mentioned. The hMADS cell line has been published as a model of both white and brite adipocyte differentiation depending on the length of treatment with ligands of the transcription factor PPAR $\gamma$  [22,23]. As shown in figure 1–6, to induce the differentiation of

3T3–L1 preadipocyte into white adipocytes, they are stimulated with a hormonal mixture of insulin (INS), the synthetic glucocorticoid dexamethasone (DEX), and a cAMP elevating agent like 3-isobutyl-1-methylxanthine (IBMX) in fetal bovine serum (FBS). This stimulus initiates a cascade of events modulating a temporal program of transcription and cell morphology. Following to induction, the cells re-enter the cell cycle undergoing at least two rounds of mitosis. This process is called clonal expansion. During this activation phase, specific adipogenic transcription factors emerge. Some of the initial transcription factors induced are C/EBP $\beta$  and C/EBP $\delta$ . Most of the modulating activities in the cell differentiation phase are converging to induce the nodal transcription factors, PPAR $\gamma$  and C/EBP $\alpha$ . The expression of these two key factors is characterized by a second permanent withdrawal from the cell cycle, followed by the gradual acquisition of a mature adipocyte phenotype (Figure 1–6) [24]. Numerous literatures from both *in vivo* and *in vitro* studies on adipose biology have been demonstrated that PPAR $\gamma$  and the C/EBP family are primordial transcription factors that control adipogenesis. In the differentiation process, C/EBP $\beta$  and C/EBP $\delta$  are induced early, and they play a pivotal role in the induction of PPAR $\gamma$ , which is the superior transcription factor in adipogenesis. C/EBP $\alpha$  is subsequently induced by PPAR $\gamma$ , forming a feed-forward loop between them, and maintaining and establishing the mature adipocyte by transactivating a group of genes important for adipocyte function.

In general, *in vitro* cell lines associated with adipogenesis are good models that synchronously and faithfully reproduce most of the features of *in vivo* differentiation, therefore at the same time allowing for the controllable situation. However, there are some limitations. Immortalized cells become out of their natural microenvironment. The close interconnection with the vasculature and adipose stromal cells is lost, and paracrine signals from neighboring cells in the tissue and endocrine and neural signals from important metabolic organs.

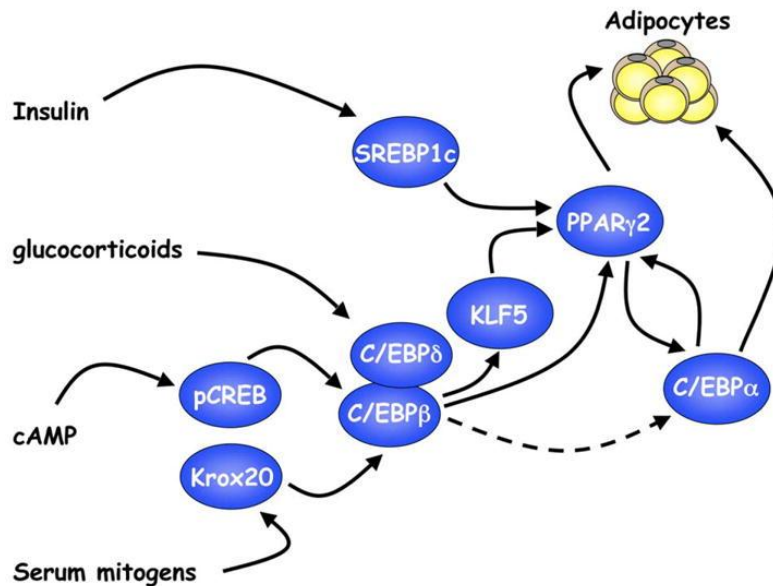


**Figure 1–4 Induction of adipogenesis by a cascade of transcription factors**

Exposure to a cocktail of adipogenic inducers comprised of insulin, glucocorticoids, agents that elevate cAMP (isobutylmethylxanthine), and fetal bovine serum activates the expression of several transcription factors converging on PPAR $\gamma$  in preadipocyte. PPAR $\gamma$  induces C/EBP $\alpha$  expression, and these transcription factors dominate terminal adipogenesis. This illustration is referred from [25].

#### **1.1.4. Causes for obesity**

Energy imbalance in the body is a pivotal cause of obesity and overweight. If the energy intake exceeds the energy expenditure, it will cause excess body fat to be stored. Fat-enriched food containing saturated fatty acids, which may affect body weight by controlling satiety and metabolic efficiency and modulating insulin secretion and action [26]. On the other hand, there are a wide range of factors that influence obesity, such as an inattentive life style and a busy social environment [27]. People who live a physically inactive life watch TV for hours, sit in front of a computer, or even rely on a car instead of walking. This kind of lifestyle results in less calories being consumed and retain more energy in the body. In addition, genes, family history, health condition, sleep, and certain medicines used to treat depression have also been known to contribute to obesity [28-30].

#### **1.1.5. Treatments for obesity**

According to the National Institute of Health, USA, a weight loss between 5–10% of initial body weight has been recommended from baseline as the threshold. With success, further weight loss can be attempted [31]. There are many different types of obesity medications available [32]. One of them is orlistat, which inhibits lipase from pancreas, thereby reducing the absorption of fat in the intestines [33,34] and the other is sibutramine, an appetite suppressant [35]. However, both medicines have side-effects, such as increased blood pressure, constipation, dry mouth, headache, and insomnia [34,36,37]. Studies in various anti-obesity medications have focused on high withdrawal rates.

The attempts to treat general overweight and obesity are often close to feckless. The pillar in treating obesity remains lifestyle modification to reduce caloric intake and increase energy



expenditure via exercise. However, it is difficult for most people to change their lifestyles and achieve long-term compliance.

Natural resources are a central theme of research at the interface of chemistry and biology. Natural products have low side effects on toxicities and therapeutic consequences compared to synthetic drugs. To treat obesity and its continuation, it is necessary to keep researching for new treatments. In this context, the possibilities of treating obesity with natural products have been focused, and considered to be an excellent alternative strategy.

#### **1.1.6. Physiological roles of adipose tissue during obesity**

Adipose tissue is a complex organ that regulates energy homeostasis typically in the body; however, excessive accumulation of fat in them is considered as obesity [38,39]. Furthermore, the adipose tissue functions as an endocrine organ, secreting a variety of factors, such as free fatty acids (FFA), leptin, adiponectin, tumor necrosis factor- $\alpha$  (TNF- $\alpha$ ), and interleukin (IL)-6, which ultimately affect the metabolic homeostasis. In this manner, adipocytes had been used as a study model since the 1970s because of their authentic key features compared to other cell lines [18]. Whereas various studies focused on the adipogenesis by developing white adipose tissue (WAT) [40-42], recent studies have also focused on the brown adipose tissue (BAT), which physiological role is the opposite to that of WAT [43,44]. Thus, the studies are focusing on adipose tissues, at least in mice, are considered to provide beneficial information on adiposity, insulin resistance, and hyperlipidemia [45-47].

### 1.1.7. Anti-obesogenic effects of plant products and their mechanism of action

The literatures have proven that upregulation or downregulation of hundreds of transcriptional factors, hormones, and enzymes can cause obesity [32]. In the management of obesity, various phytochemicals/plant products contribute to beneficial effects through their diverse actions [32]. Their mechanism of action is following may include of their mechanism of action.

**a. Increase in energy expenditure:** WAT stores energy in the form of lipids; on the other hand, BAT converts the stored lipids to energy as heat (thermogenesis). Uncoupling proteins (UCPs) are central activator of thermogenesis, and induction of UCP expression by natural anti-obesogenic phytochemicals is considered to be one of the potential routes for obesity resolution [48,49].

**b. Control in adipocyte differentiation:** Adipose tissues control energy balance and lipid homeostasis. Adipose tissue has two primary conditions: hyperplasia (increased cell number) and hypertrophy (increased cell size). Adipocytes store triglycerides (TG) and release them when needed in response to energy demands. Inhibiting the function of the major adipogenic factors, such as PPAR $\gamma$ , C/EBP, and SREBP families may be necessary for developing anti-obesity therapies [48,50].

**c. Inhibition of pancreatic lipase activity:** Pancreatic lipase is the most crucial enzyme that hydrolyzes TG into monoglycerides and fatty acids. This enzyme hydrolyzes 50–70 % of total dietary fat intake [51], and the inhibition of this enzyme is one of the approaches against obesity. Therefore, lipase inhibition has been extensively studied to evaluate the potential of natural products to inhibit dietary fat absorption [52-54].

**d. Appetite suppressants:** The state of satiety is regulated by various neurological and hormonal signals in the human body. Nervous system signaling peptides such as histamine and dopamine are correlated with the state of satiety. To inhibit weight gain, plant products that activate the sympathetic nervous system and enhance adrenaline levels can effectively improve the feeling satiety [55,56].

**e. Regulation of lipid metabolism:** Modulating the expression of transcriptional factors and enzymes, which are involved in lipid metabolism (lipogenesis and lipolysis) can be achieved by plant products [57]. For example, activation of the  $\beta$ -adrenergic receptor causes non-shivering thermogenesis in brown adipocytes and lipolysis in white adipocytes [58].

#### **1.1.8. Importance of plant-derived natural products on anti-obesity**

Food habit and type of food has a positive correlation with obesity and obesity associated metabolic syndrome. The growing threat of obesity and metabolic syndrome to global health has encouraged researchers and scientists to find new, effective and safe anti-obesity agents, especially from natural sources. These natural products are mostly derived from edible part of the plants, including fruits, vegetables, grains, and herbs. The nutritional and biological benefits of these natural products are profoundly contributed by the presence of an abundant amount of unsaturated fatty acids, fibers, and phytochemicals[59]. Currently anti-obesity products in market can be classified into three categories:

- (1) Food ingredients,
- (2) Herbal ingredients, and
- (3) Other functional supplements.

People usually consume developing functional products in their daily life which is the most popular segment in the functional supplement industry. Recently traditional Chinese medical experts use herbal remedies that usually are mixtures of different herbs, such as turmeric and mulberry leaf, to treat obese patients. Herbal therapies are popular in Asia, and are spreading worldwide.

Nowadays, the human behavior of changing food habit and lifestyle has increased the incidence of obesity and even has become a risk factor to the population of children [60]. Medicinal use of plants arises from ethnopharmacological and ethnobotanical approaches. These knowledge, thus anything “traditional” has become something of great importance to science. Those approaches have helped in the selection of species to be studied, and in the development of phytotherapeutic medicines based on ethnopharmacological investigation [61]. The potential of natural products in the treatment of obesity is still unexplored, and could be a great alternative for the development of safe and effective anti-obesity drugs.

#### **1.1.9. Impact of tropical medicinal plants on human health**

Over the last few decades, there has been a remarkable and steady increase in the number of plant-derived medicines worldwide [62]. Plant secondary metabolites (PSMs) are used for plant defense system against pathogenic attacks and environmental stresses. Moreover, PSMs are also increasingly being used as medicinal ingredients and food additives for therapeutic purposes.[63]. PSMs synthesis and their accumulation are strongly modulated by variety of environmental factors, such as temperature [64], light [65], soil water [66], soil fertility and salinity[67], and for most plants; therefore, a change in an individual factor may alter the content of PSMs even if other factors remain constant. Climate change is challenging for plants and animals adaptation, but

according to Murren *et al.*, plants have phenotypic plasticity that allows individuals to alter their phenotypes in response to the environment they encounter [68].

Plant-derived natural products have always fascinated many scientists because they are biocompatible and can be safe and effective therapeutic agents. Recent studies found that historical basis of drug discovery knowledge is valuable resources for target-based drug discovery [69,70]. Most of the medicinal properties of tropical plants have yet to be assessed, and they are very interesting subjects for research.

#### **1.1.10. Natural products nanoparticulation with PLGA**

The great pharmacological potentials of plant derivative natural compounds are restricted their efficacy due to the molecule presents some drawbacks are hydrophobic properties, rapid hydrolysis in alkaline media and light instability. The hydrophobic compounds results in pharmacokinetic restrictions such as low absorption and bioavailability by oral route, extensive metabolism and rapid elimination [71,72]. To overcome this barrier, nanoparticulation of plant derivative compounds may modify pharmacokinetic parameters. It has been reported that natural compounds are loaded in nanoparticles improved in absorption, bioavailability, and plasma circulation time, with reduction of clearance, consequently increasing the drug's mean half-life [73-76].

Polymer nanoparticles are solid and spherical structures ranging around 100 nm to less than 1  $\mu\text{m}$  in size, which are prepared from natural or synthetic polymers, such as polylactic-co-glycolic acid (PLGA), polyvinyl alcohol (PVA), polyethylene glycol (PEG), poly-L-lactic acid (PLA), polycaprolactone (PCL), and chitosan are the most common polymers [77-79]. Among them, PLGA has attracted considerable attention because of its special properties such as biodegradability [80],

biocompatibility [81], prevention of inclusion degradation, and sustained release of inclusion [82], and having possibility for modifying surface properties to target specific organs or cells [83]. PLGA polymers hydrolysis occurs by metabolic system and produce two monomers which are lactic acid and glycolic acid. Those endogenous monomers are easily metabolized via the Krebs cycle (Figure 1-5) and eliminates as CO<sub>2</sub> and water through respiration, urine and feces [84,85]. Moreover, the preparation methods of PLGA-based nanoparticles are well-developed for their formulations and adapted for various types of compounds. Therefore, PLGA has been approved to use as an injectable drug delivery carrier by Food and Drug Administration (FDA) and European Medicine Agency (EMA) [78].

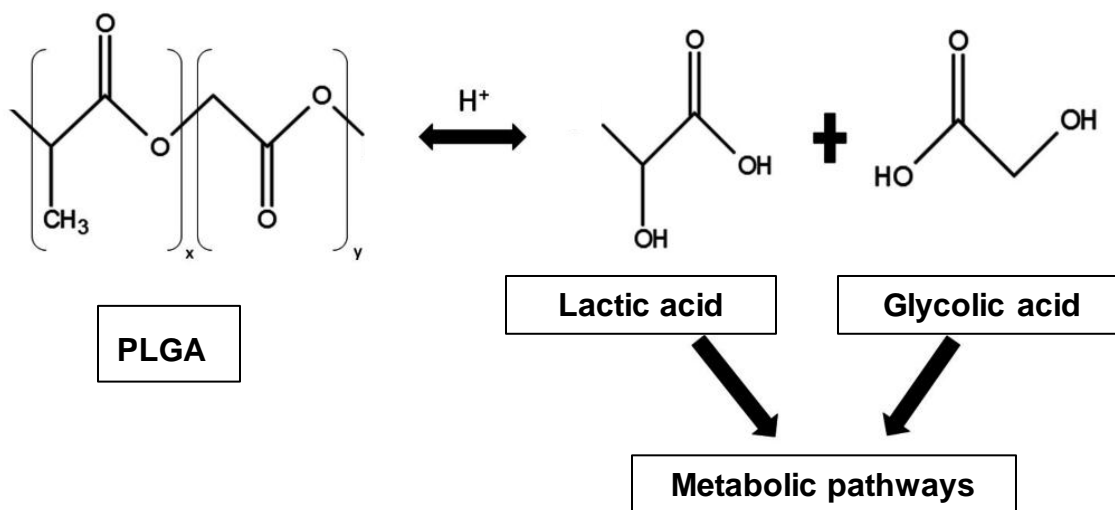


**Figure 1–5** Hydrolysis of PLGA. This illustration is referred from [84].

Several studies found that PLGA nanoparticles improved the bioavailability of plant derivative natural compounds such as curcumin after oral administration [86-88].

## **CHAPTER II**

Anti-obesity activity of dihydropyranocoumarins  
and its enhancement by nanoparticulation with  
polylactic-co-glycolic acid: An in vivo study

## 2.1. Introduction

In last few decades, obesity has become one of the most prevalent health issues [12]. It has a close relationship with non-communicable diseases, such as fatty liver disease, type 2 diabetes, and other critical metabolic disorders [89]. Lifestyle and a high-calorie diet are the most prominent factors involved in the development of obesity. Therefore, obesity constitutes a major public health problem worldwide and reaching a pandemic level.

Several pharmaceutical substances have been developed to treat this condition by reducing nutrient absorption or by enhancing thermogenesis and lipid turnover [90,91]; however, practical use of these medicines has been hampered by their side effects. In this context, the supplementation of the daily diet with natural anti-obesity agents has been considered to effective for managing obesity, as well as calorie control and exercise. Considering the side effects and safety, medicinal plants traditionally used for many years and their active compounds merit investigation to develop more natural and safer anti-obesity agents.

*Peucedanum japonicum* Thunb (PJT), belonging to the family of Apiaceae, grows on the coastal and cliff areas near the ocean throughout southern Japan and China. The leaves of PJT have been used as a leafy vegetable and garnish, (Figure 2–1), and are called “Choumeisou” in Japanese which means a long-life herb in Okinawa, Japan.



**Figure 2–1** *Peucedanum japonicum* Thunb (PJT)



A study by Nukitrangsan found that dietary intake of PJT powder inhibited lipid absorption in mice fed a high-fat diet (HFD) [92]. Another study on anti-obesity activities of PJT found its usefulness as a natural agent to reduce obesity [93]. Further examination was carried out to identify the active compounds, and revealed at last that several types of dihydropyranocoumarins (DPCs) exert the inhibitory effects on lipid accumulation in 3T3–L1 adipocytes and that dietary intake of DPC concentrate prepared from PJT decrease the relative weight of WAT in HFD-fed mice[94]. It has been reported that several types of coumarin are isolated from *Peucedanum* plants and have various physiological activities [94-97]; however, a few studies has reported the anti-obesity effects of any coumarins. Therefore, I conducted further studies on the molecular mechanism of the anti-obesity effect of DPCs and the enhancement of its activity.

The nutritional value of food can be improved by adding bioactive compounds; however, most of their positive effects are impaired by their poor bioavailability, limited water solubility, and metabolic transformations [98]. One strategy for reducing these limitations is to integrate these bioactive compounds into nanoparticles. Delivery systems using nanoparticles have been investigated as a possible approach through which to markedly improve the bioavailability of drug and food bioactive [98,99]. Carrier systems of biodegradable particulates are of interest as a potential means by which to orally deliver compounds to improve their bioavailability [84]. As mentioned in chapter I, PLGA has attracted the most attention among the various polymers because of its favorable characteristics and its approvals by the U.S. FDA and EMA for drug delivery applications [78,100,101]. In the present study, I therefore investigated the following:

- ❑ To improve the purity of DPCs and evaluate its anti-obesity activity
- ❑ Maximize DPCs bioavailability and functionality by nanoparticulation with PLGA.

## **2.2. Materials and Methods**

### **2.2.1. Purification of DPCs from PJT**

The PJT leaves were collected from Yonaguni, an island in Okinawa Prefecture, Japan. Dried PJT leaves were incubated with 10 times volume of 50% ethanol at room temperature overnight and subsequently stored for 2 days at 4 °C. The filtrates were applied to a column (2.0 cm I.D. × 30 cm) of DIAION HP20 (Mitsubishi Rayon Aqua Solutions Co. Ltd., Tokyo, Japan) to adsorb the objective coumarins. The eluent by 75% ethanol was used as CC in the in vivo study. The products were further concentrated using a Hi-Flash column ODS-SM (YAMAZEN Corp., Osaka, Japan) and subsequently evaporated and dissolved in 99.5% ethanol to a final concentration of 10 mg/mL. To isolate each compound, fractional extracts were applied to an Inertsil ODS-3 column (20 mm I.D. × 250 mm, GL Sciences, Inc., Tokyo, Japan) and analyzed using the Shimadzu LC-20A HPLC system (Shimadzu Corp.). The collected fractions were evaporated and dissolved in ethanol at 2 mg/mL. Purity of the fractions was determined using HPLC on a COSMOSIL 2.5Cholest column, and their structures were identified using a Bruker UltraShield 400 MHz NMR spectrometer (Bruker Corporation, Billerica, MA, USA).

### **2.2.2. Preparation of nano-DPCs**

Isolated DPCs were also nanoparticulated with PLGA as nano-DPCs. The vehicle PLGA nanoparticles and nano-DPCs are used in this study were prepared by SENTAN Pharma Inc. (Fukuoka, Japan), and the particle mean size were approximately 304 nm and 266 nm, respectively (Figure 2–3). DPCs contents in nano-DPCs were measured by HPLC system as mentioned above.

### **2.2.3 Ethical approval**

This study was carried out according to experimental animal protocols were approved by the animal experiment committee at University of the Ryukyus, Okinawa Japan, and the experiments were performed according to the ethical guidelines of the University for Animal Experiments.

### **2.2.4. Experimental animals**

In this study, twenty-four 4-week-old male C57BL/6 mice were used which were purchased from Japan SLC, Inc. (Shizuoka, Japan). The mice were individually housed in plastic cages under specific pathogen-free condition and maintained at 24°C in a 12 h light-dark cycle. The mice were fed on a normal commercial chow diet for 7 days to acclimate them to their environment, followed by they were randomly divided into experimental groups for each experiment.

### **2.2.5. Experimental design**

To elucidate the anti-obesity effects of DPCs and its augmentation by nanoparticulation with PLGA. All experimental mice after 1-week acclimation randomly divided into four groups (n = 6 for each group): control, regular dose DPC (regular dose), low dose DPC (low dose), and low dose nanoparticulated DPC (nano-DPC) groups (Table 2–2). Experimental diets and DPC doses were optimized according to our previous study [94]. The experimental HFD containing 20% fat was prepared as the AIN-76 formulation and its composition is summarized in (Table 2–1). Approximately 39% of the total calories in HFD were derived from fat. Table 2–2 summarizes the

administration procedures of DPCs in this experiment. The animals fed HFD were supplemented with DPCs either by diet or gavage. The control group was fed with only HFD without any supplementation of DPCs. The administration of DPCs to regular and low dose groups were done by the diet while to nano-DPC group was by gavage. In the case of supplementation by the diet, DPCs was added at the expense of sucrose.

In nano-DPC group, nano-DPCs suspended in water were orally administered by gavage to mice (2 times/week). All groups except for nano-DPC group received the vehicle PLGA nanoparticles by gavage (2 times/week). All mice were given ad libitum access to the experimental diet and water for 10 weeks. The feces were collected for 3 d at the end of the feeding period and lyophilized. The mice were starved for 12 h before euthanasia under anesthesia by exsanguination from the heart. The liver and WAT were immediately excised, and the sera were prepared from the blood. Part of the excised epididymal WAT was fixed in 10% neutral formalin solution, and the remaining tissue and sera were frozen in liquid nitrogen and stored at  $-80^{\circ}\text{C}$  until use.

**Table 2–1** Composition of experimental diets used in this study

	Experimental group			
	Control	Regular dose	Low dose	Low dose
		DPC	DPC	nano-DPC
Composition of experimental diet (g/100g)				
Casein	20.00	20.00	20.00	20.00
$\beta$ -corn starch	15.00	15.00	15.00	15.00
Cellulose	5.00	5.00	5.00	5.00
AIN-76 mineral mix	3.50	3.50	3.50	3.50
AIN-76 vitamin mix	1.00	1.00	1.00	1.00
DL-methionine	0.30	0.30	0.30	0.30
Choline bitartrate	0.20	0.20	0.20	0.20
Corn oil	20.00	20.00	20.00	20.00
Purified DPC	0.00	0.069	0.00069	0.00
Sucrose	to make 100			

Eighteen male 6-week-old ICR mice were used to examine the effect of PLGA nanoparticle encapsulation on bioavailability of oral DPCs in this study. After giving them 1 week to acclimate to their environment, the mice were randomly divided into two groups (n = 9 for each group). The mice were starved for 12 h and then orally administered with purified DPC suspension with vehicle PLGA nanoparticle or nano-DPCs (DPC dosage: 4 mg/kg body weight) by gavage. After treatment for 24 h, the mice were euthanized under anesthesia by exsanguination from the heart. Epididymal WAT was immediately excised, frozen in liquid nitrogen, and stored at -80°C until use.

**Table 2-2** Administration procedure of dihydropyranocoumarins (DPC) and its total dosages in this study.

	Experimental group			
	Control	Regular dose	Low dose	nano-DPC
		DPC	DPC	
Total DPC dosage (mg) <sup>§</sup>				
by diet	0	146 ± 1	1.47 ± 0	0
by gavage	0	0	0	1.48 ± 0
Oral administration by gavage (µg/injection) <sup>†</sup>				
Nano-DPC	0	0	0	615 <sup>‡</sup>
Vehicle PLGA Nanoparticles	541	541	541	0

<sup>§</sup> Data are shown as the means ± SEM.

<sup>†</sup> Nano-DPC, DPC-encapsulated polylactic-co-glycolic acid (PLGA) nanoparticles. Nano-DPC and vehicle PLGA nanoparticles were orally administered twice a week.

<sup>‡</sup> 615 µg nano-DPC contains 73.8 µg DPCs.

### **2.2.6. Biochemical analysis**

Total cholesterol (TC), triglycerides (TG), aminotransferase activities and glucose levels in serum were determined using a commercial enzymatic kit (Wako Pure Chemical Industries, Ltd., Osaka, Japan). Serum leptin levels were measured using enzyme-linked immunosorbent assay kits (Morinaga Institute Biological Science, Inc. Kanagawa, Japan). Lipids in the liver and feces were extracted using a previously described method [102], and their concentration were determined using the commercial kits described above. All experiment using commercial kits were followed according to the manufacturers' protocol

### **2.2.7. Histological analysis**

Epididymal WAT was fixed in paraffin and embedded tissue was stained with hematoxylin and eosin to measure cell size using a microscope according to previously described procedures [103]. The stained section was viewed at 10× magnification and photographed using a digital camera (Olympus BX41, NY, USA). Analyses of the adipocyte area of at least 100 adipocytes per section was conducted using Adiposoft for Image J (<https://imagej.nih.gov/ij/>).

### **2.2.8. Quantitative real-time polymerase chain reaction**

Total RNA was extracted from the isolated epididymal WAT using a TRIzol reagent and according to PureLink RNA mini kit protocol (Thermo Fisher Scientific, Waltham, MA, USA). First-strand cDNA was synthesized using 2 µg total RNA as a template. For quantitative real-time polymerase chain reaction, the primers and probe sets (Table 2–3) were purchased from Integrated DNA Technologies, Inc. (Coralville, IA, USA). To measure the relative abundance of target

transcripts, amplifications were performed using PrimeTime Gene Expression Master Mix (Integrated DNA Technologies, Inc.) with the StepOne Real-Time PCR System (Thermo Fisher Scientific), and the amounts of the target transcripts were normalized to those of ACTB and GAPDH.



**Table 2–3** TaqMan gene expression assays used for the quantitative real time PCR analysis.

<b>Gene</b>	<b>Description</b>	<b>Gene expression assay reference</b>
ACC1	Acetyl-coenzymeA (CoA) carboxylase 1	Mm.PT.58.12492865
$\beta$ -actin	ACTB	Mm.PT.58.33257376.gs
C/EBP $\alpha$	CCAAT/enhancer binding protein (C/EBP), alpha	Mm.PT.58.30061639.g
CPT1a	Carnitine palmitoyltransferase 1A	Mm.PT.58.10147164
CPT2	Carnitine palmitoyltransferase 2	Mm.PT.58.13124655
FABP4	Fatty acid binding protein 4	Mm.PT.58.43866459
GAPDH	Glyceraldehyde-3-phosphate dehydrogenase	Mm.PT.39a.1
FASN	Fatty acid synthase	Mm.PT.58.14276063
LIPE	Hormone-sensitive lipase	m.PT.58.6342082
LPL	Lipoprotein lipase	Mm.PT.58.46006099
ACOX	Peroxisomal acyl-coenzyme A oxidase 1	Mm.PT.58.50503784
PPAR $\alpha$	Peroxisome proliferator-activated receptor $\alpha$	Mm.PT.58.9374886
PPAR $\gamma$	Peroxisome proliferator activated receptor gamma	Mm.PT.58.31161924
PGC1a	PPAR $\gamma$ coactivator 1 $\alpha$	Mm.PT.58.16192665
SCD1	Stearoyl-Coenzyme A desaturase 1	Mm.PT.58.8351960
GLUT4	Glucose transporter type 4	Mm.PT.58.9683859
SREBP1	Sterol regulatory element-binding protein 1	Mm.PT.58.8508227
UCP1	Uncoupling protein 1	Mm.PT.58.7088262
UCP2	Uncoupling protein 2	Mm.PT.58.11226903
UCP3	Uncoupling protein 3	Mm.PT.58.9090376

PrimeTime qPCR Probe Assays (Integrated DNA Technologies, Inc.)

### **2.2.9. Concentration analysis of DPCs and nano-DPCs in epididymal WAT**

One hundred milligrams of excised epididymal WAT were used in experiment and the tissue homogenized in chloroform/methanol (2/1) with 50 ng visnadine (Sigma-Aldrich Corp., St. Louis, MO, USA) as an internal standard. After adding distilled water to the homogenate and centrifuging, the chloroform layer was collected and evaporated. The extracted lipid was filtered and subjected to liquid chromatography-mass spectrometry (LC-MS) analysis. The chromatographic analysis was conducted on a Waters Acquity Ultraperformance liquid chromatography (UPLC) H-Class system coupled to a Waters Xevo TQD mass spectrometer (Waters, Milford, MA, USA). In the LC system, a 10 by 2.1-mm Titan C18 UHPLC column (particle size: 1.9  $\mu$ m) was used at 40°C, and the mobile phase was 65% acetonitrile with 0.1% formic acid at flow rate 0.4 mL/min. The operating parameters for MS were as follows: capillary voltage, 3.00 kV; cone voltage, 55 V; source temperature, 150°C; desolvation temperature, 500°C; desolvation gas flow, 1000 L/h; and cone gas, 150 L/h. Quantification was conducted in positive electrospray ionization and multiple reaction monitoring (MRM) modes. MRM transitions were  $m/z$  409.2  $\rightarrow$  309.2 for peucedanocoumarin III (PCIII) and pteryxin (PTX) and  $m/z$  411.2  $\rightarrow$  351.1 for visnadine as the internal standard. Quantitative data analyses were conducted using the Waters MassLynx with TargetLynx application managers.

### **2.2.10. Statistical analyses**

Data are expressed as the mean  $\pm$  standard error of the mean (SEM). The statistical significance of the difference between the two experimental groups was determined using the Student's *t*-test. To determine the significance of the differences among the means for more than

three groups, the differences among the mean values were subsequently inspected using the Tukey's honestly significant difference test.  $p < 0.05$  was set as the level of significance.

## 2.3. Results

### 2.3.1. Purified DPCs and DPC incorporated in nanoparticle as nano-DPCs

DPCs were purified from PJT. HPLC analyses showed that purified DPC extract has two major peaks: PCIII (41.7%, v/v) and PTX (57.3%, v/v) (Figure 2–2). Nano-DPCs were incorporated with  $12.0 \pm 0.2\%$  of DPCs: PCIII, 5.04%; PTX, 6.96%.

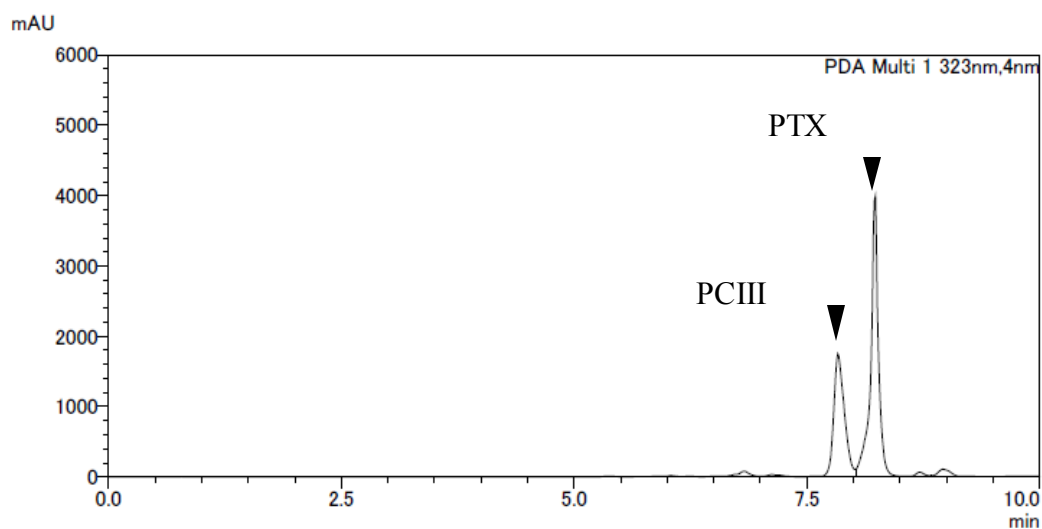
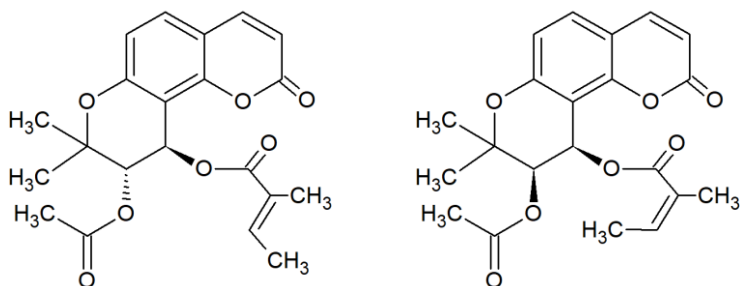


**Figure 2-2** HPLC chromatogram of DPCs (concentrated)

Notes: PCIII: peucedanocoumain III, PTX: pteryxin.



Compound	Peucedanocoumarin III (PCIII)	Pteryxin (PTX)
PubChem CID	1032882	5281425
Content in purified DPC	41.8%	57.4%
Content in DPC-NPs	5.04%	6.96%

**Figure 2–3** Chemical information and content of dihydropyranocoumarins (DPCs) used in this study. Notes: DPC, dihydropyranocoumarin and nano-DPC, DPC-encapsulated polylactic-co-glycolic acid nanoparticles.

### 2.3.2. DPCs and nano-DPCs effects of on growth parameters

The mice in the regular and low dose groups were fed the experimental HFD containing DPCs at 0.069% and 0.00069%, respectively, which meant that mice in the regular dose DPC group took a total of  $146 \pm 1$  mg DPCs, while the mice in low dose DPC group received only 1% of that amount (Table 2–2). As a result, the total intake of DPCs in the nano-DPC group mice fed the control HFD but also administered nano-DPCs twice a week was comparable to that in the low dose DPC group mice (Table 2–2).

The total food and energy intake, and the fecal TG content over the final 3 experimental days almost similar results were observed among all experimental groups (Table 2–4) however, significant decreases in the final body weight and body weight gain were observed in the regular dose and nano-DPC groups than in the control and low dose groups (Figure 2–4A). The relative weights of epididymal, omental, and subcutaneous WAT in the regular dose group were significantly lower compared to control and low dose groups (Figure 2–4B). Similar results were observed in the nano-DPC group, but their epididymal WAT showed a tendency to decrease (Figure 2–4B). The weight of relative perirenal WAT in mice of the regular dose and nano-DPC groups also showed a tendency to decrease compared with that of the control and low dose groups (Figure 2–4B).

Table 2–4. Total food, energy intake and fecal lipid excretion

	Experimental group			
	Control	Regular dose DPC	Low dose DPC	nano-DPC
Total food intake (g)	199 ± 1	197 ± 1	198 ± 1	199 ± 1
Total energy intake (kcal)	914 ± 5	904 ± 8	912 ± 3	914 ± 4
Fecal lipid excretion (mg/3days)	395 ± 32	384 ± 16	359 ± 23	362 ± 11

Data are shown as the means ± SEM.

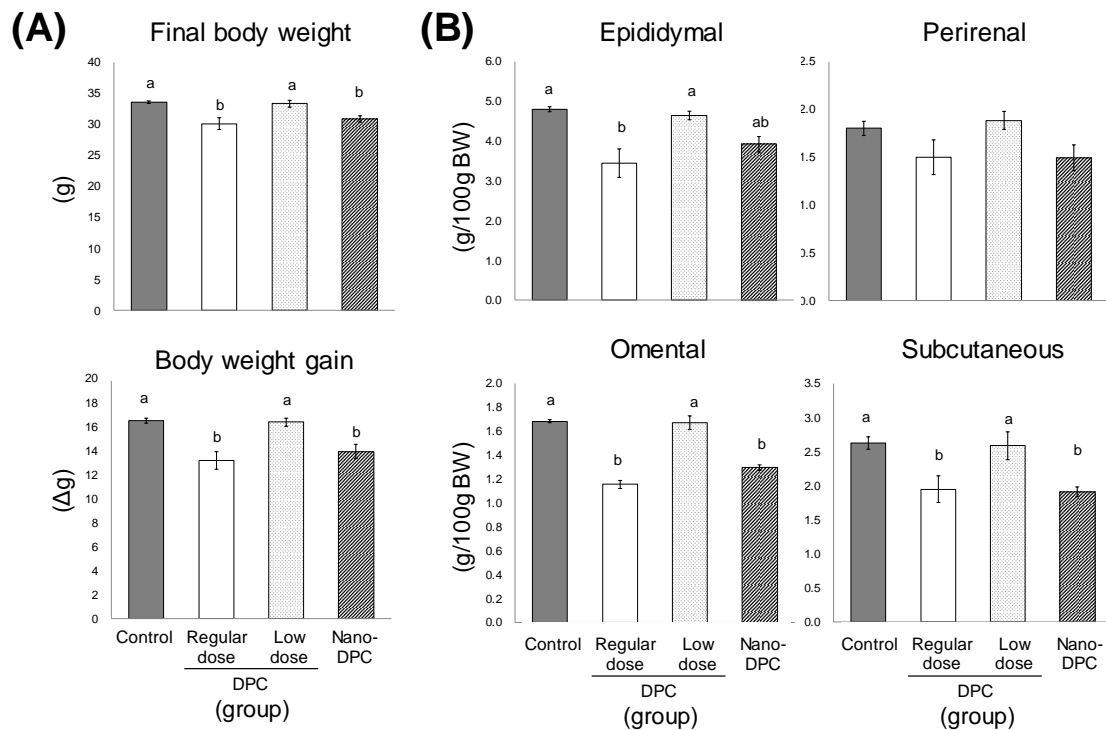


**Figure 2–4** Effects of dietary dihydropyranocoumarins (DPCs) and DPC-encapsulated polylactic-co-glycolic acid nanoparticles (nano-DPCs) on growth parameters. (A) Final body weight and body weight gain and (B) relative weights of white adipose tissues. Notes: Each value represents the mean ± SEM for six mice. Different letters indicate significant differences among each experimental group using Tukey's honestly significant difference test ( $p < 0.05$ ).

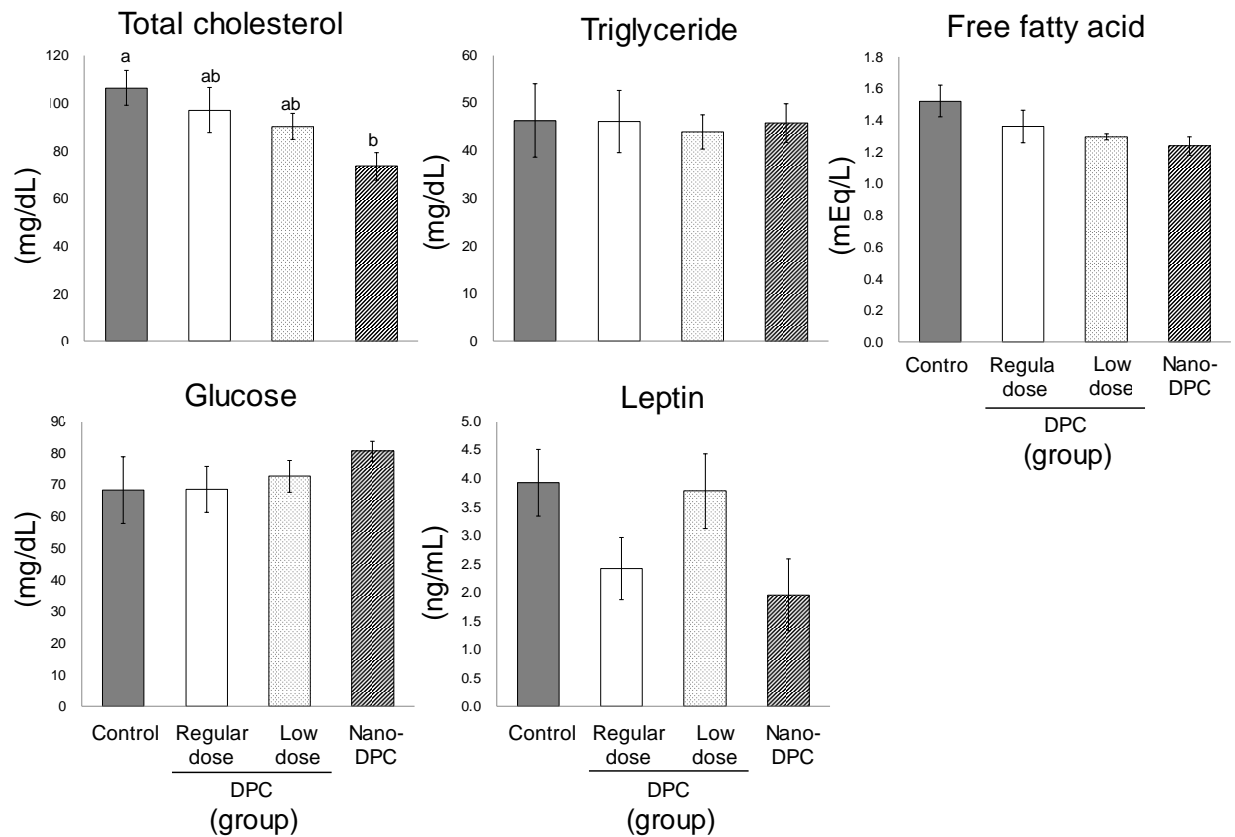


**Figure 2-5** Effects of dietary dihydropyranocoumarins (DPCs) and DPC-encapsulated poly(lactic-co-glycolic acid) nanoparticles (nano-DPCs) on serum parameters. Each value represents the mean  $\pm$  SEM for six mice. Different letters indicate significant differences among each experimental group using Tukey's honestly significant difference test ( $p < 0.05$ )



### **2.3.3. DPCs and nano-DPCs effects on serum and hepatic parameters**

In the serum levels of TG, free fatty acid, and glucose no significant difference were observed among all experimental groups; (Figure 2–5) whereas serum TC level in mice of the nano-DPC group significantly decreased compared with that of the control group. Serum leptin levels in regular dose and nano-DPC groups also tended to decrease compared with those in the control and low dose groups. Although the raw weight of the liver was largely comparable among all experimental groups (data not shown), its relative weight in mice of regular dose and nano-DPC groups was significantly lower than that of the control and low dose groups (Figure 2–6A). Oral intake of DPCs by diet and oral injection of nano-DPCs by gavage had no effect on hepatic lipid levels (Figure 2–6B). For the hepatopathy indicators, serum alanine aminotransferase (ALT) activity in the nano-DPC group mice significantly decreased, and a decreasing tendency in aspartate aminotransferase (AST) activity was also observed in those mice compared with those in the control group mice (Figure 2–6C).

### **2.3.4. DPCs and nano-DPCs effects on lipid accumulation in epididymal adipose tissues**

DPCs treated mice significantly decreased the size of adipocyte in epididymal WAT (Figure 2–7A). Mice in the regular dose and nano-DPC groups had significantly smaller adipocytes than the control group mice (Figure 2–7B). In the regular dose and nano-DPC groups, the proportion of large adipocytes ( $> 6000 \mu\text{m}^2$ ) significantly decreased and that of small adipocytes ( $< 2000 \mu\text{m}^2$ ) tended to increase compared to those in the control group (Figure 2–7C). Although the relative weights of epididymal WAT were largely comparable between the control and low dose group mice, a tendency for the mean adipocyte size to decrease was observed in low dose group (Figure

2–7B). The percentage of large adipocytes ( $> 8000 \mu\text{m}^2$ ) in the low dose group mice was significantly lower than that in the control group mice (Figure 2–7C).

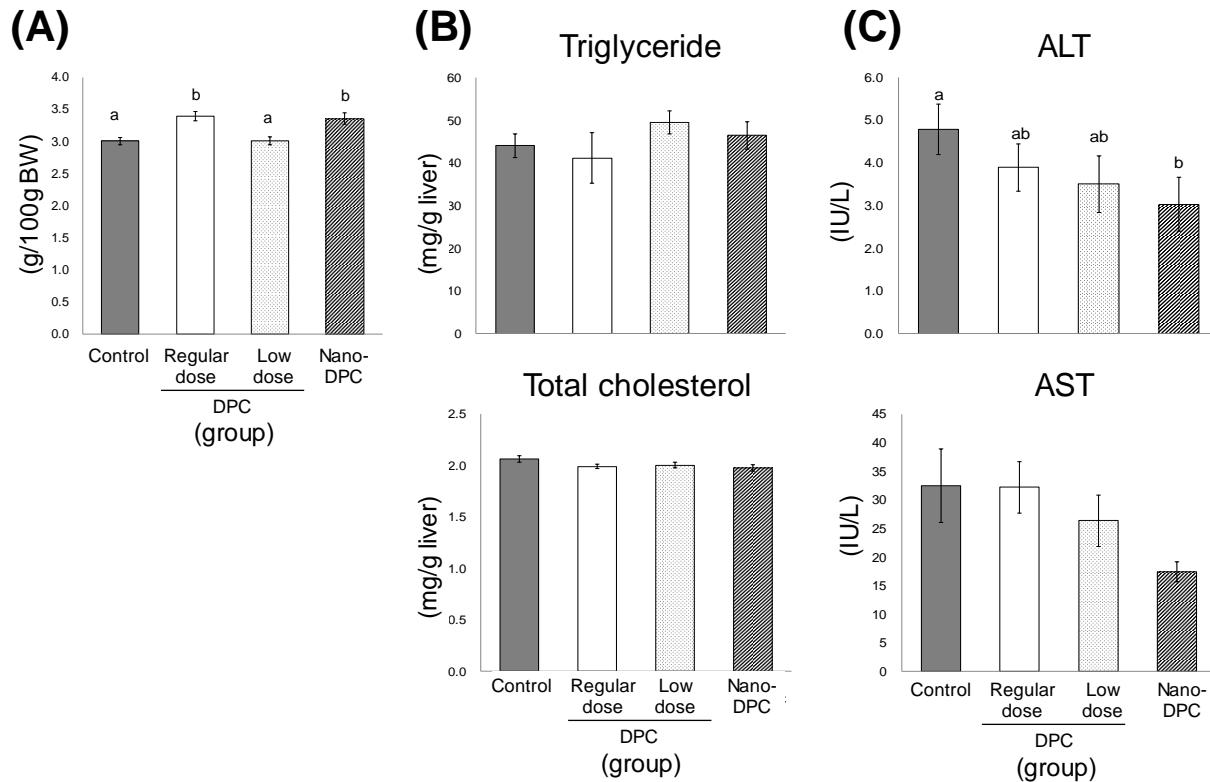


**Figure 2–6** Effects of dietary dihydropyranocoumarins (DPCs) and DPC-encapsulated polylactic-co-glycolic acid nanoparticles (nano-DPCs) on hepatic parameters. (A) Relative liver weight, (B) hepatic lipid contains, and (C) alanine transaminase activities. Notes: ALT, alanine aminotransferase and AST, aspartate aminotransferase. Each value represents the mean  $\pm$  SEM for six mice. Different letters indicate significant differences among each experimental group using Tukey's honestly significant difference test ( $p < 0.05$ ).

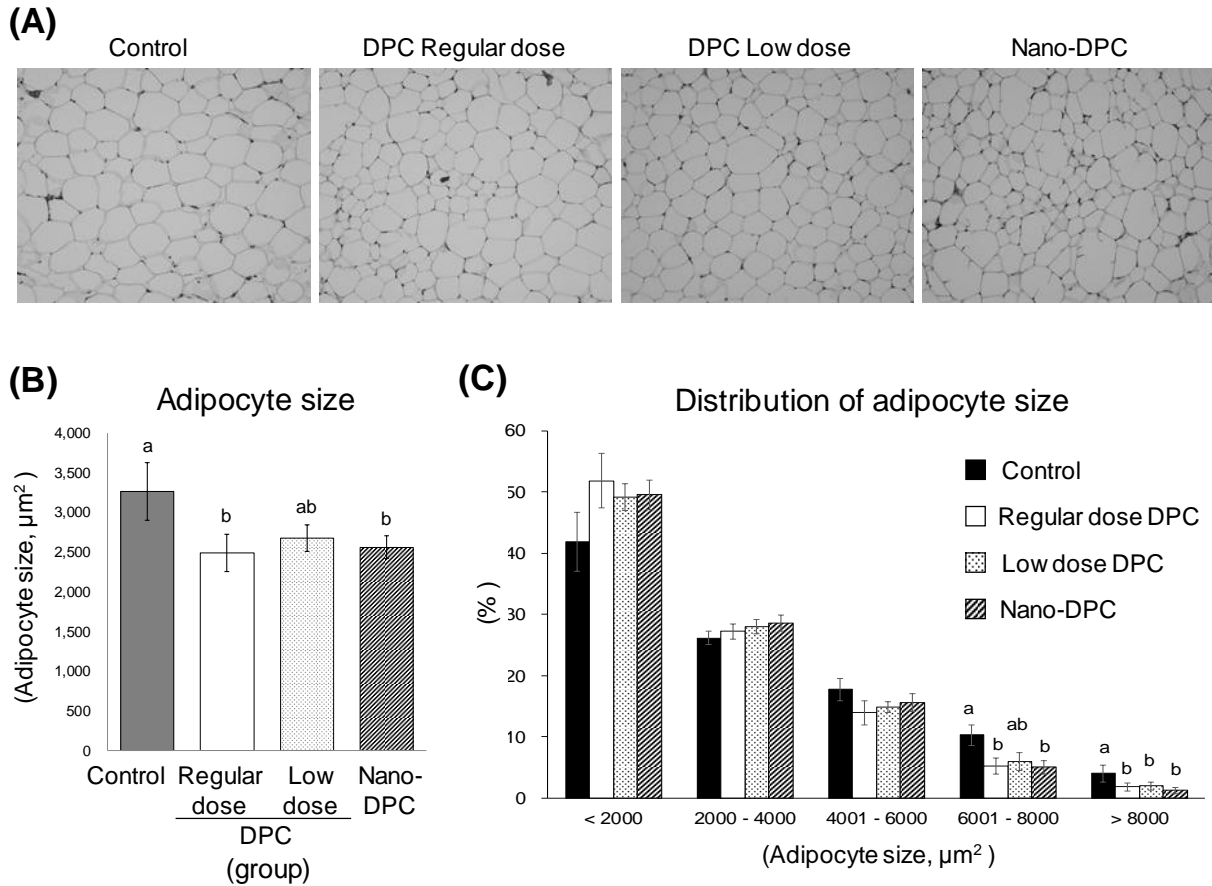


**Figure 2-7** Effects of dietary dihydropyranocoumarins (DPCs) and DPC-encapsulated polylactic-co-glycolic acid nanoparticles (nano-DPCs) on adipocyte size in epididymal white adipose tissues. **(A)** Histological images of epididymal WAT, **(B)** mean of adipocytes size, and **(C)** distribution of adipocyte size. Notes: Each value represents the mean  $\pm$  SEM for six mice. Different letters indicate significant differences among each experimental group using Tukey's honestly significant difference test ( $p < 0.05$ ).

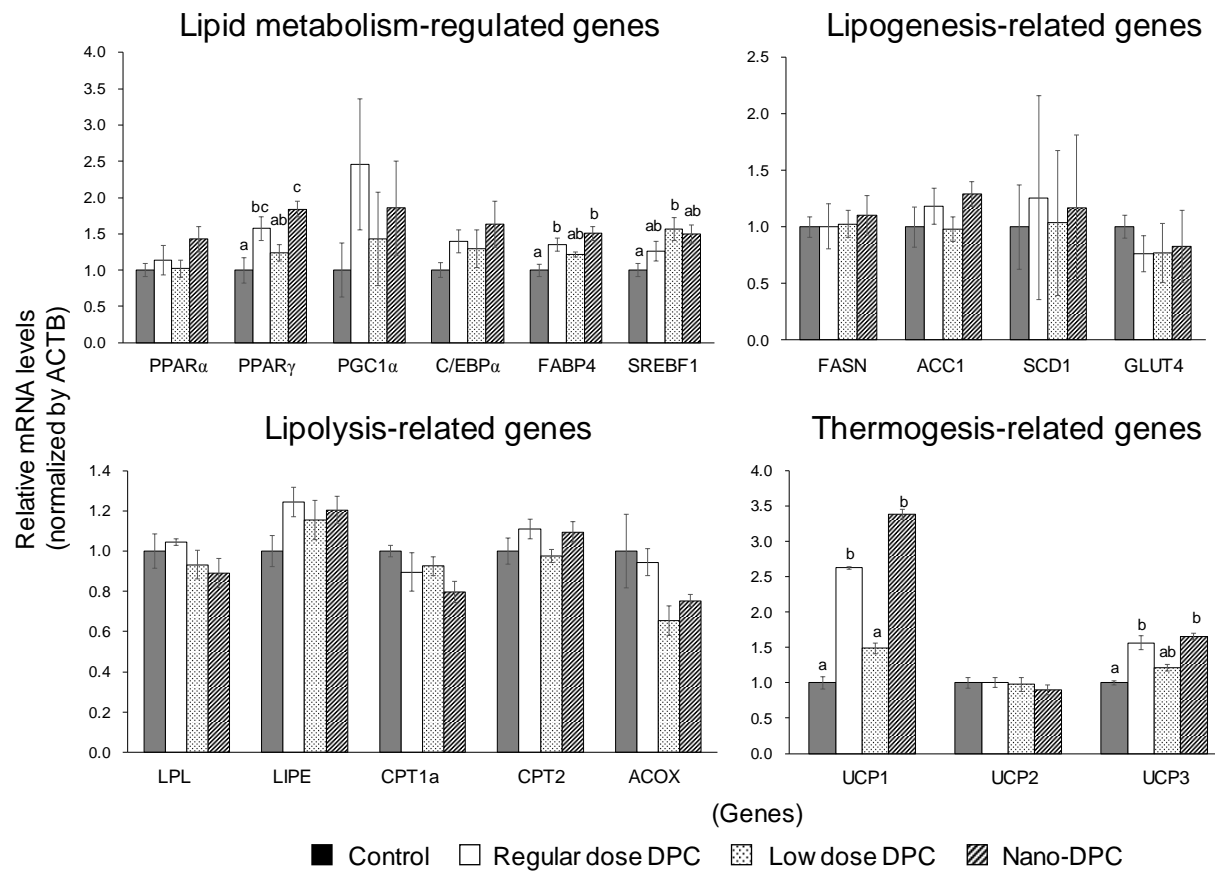


**Figure 2-8** Effects of dietary dihydropyrancoumarins (DPCs) and DPC-encapsulated polylactic-co-glycolic acid nanoparticles (nano-DPCs) on lipid metabolism-related gene expression in epididymal white adipose tissue. Notes: Each value represents the mean  $\pm$  SEM from at least three independent experiments. Different letters indicate significant differences among each experimental group using Tukey's honestly significant difference test ( $p < 0.05$ ).

### **2.3.5. DPCs and nano-DPCs effects on lipid metabolism-related gene expressions in epididymal WAT**

To evaluate the molecular mechanisms of DPCs and nano-DPCs effect on epididymal WAT in a genetic level, I have analyzed the mRNA levels of lipid metabolism-related genes (Figure 2–8). The relative mRNA expressions of PPAR $\gamma$  and FABP4 in mice of regular dose and nano-DPC groups were significantly higher than those of the control group. Increasing tendencies were also observed in mRNA levels of PGC1 $\alpha$  and C/EBP $\alpha$  in the mice fed DPCs. In mice of low dose group, mRNA levels of SREBF1 significantly increased compared with that of the control group. Significant differences were not observed in relative mRNA levels of lipogenesis and lipolysis-related genes, and dietary intake of DPCs and oral administration of nano-DPCs significantly increased thermogenesis-related gene expressions in WAT. The relative mRNA levels of UCP1 in WAT in mice of the regular dose and nano-DPC groups significantly increased by 2.5 to 3.5fold compared with those of the control and low dose groups. Gene expression of UCP3 in mice of the regular dose and nano-DPC groups also significantly increased compared to that in the control group mice, but not compared to that in the low dose group mice.

### **2.3.6. PLGA nanoparticulation effect of DPCs in WAT accumulation**

To understand the effect of PLGA nanoparticulation of DPCs on WAT, I compared the DPC content in WAT after a single oral administration of DPCs and nano-DPCs by gavage. The PCIII content in WAT in mice administered with nano-DPCs showed an approximately 3-fold higher level than when using a DPC suspension with vehicle PLGA nanoparticles (Figure 2–9). Similar results were also observed in the PTX contents in WAT.

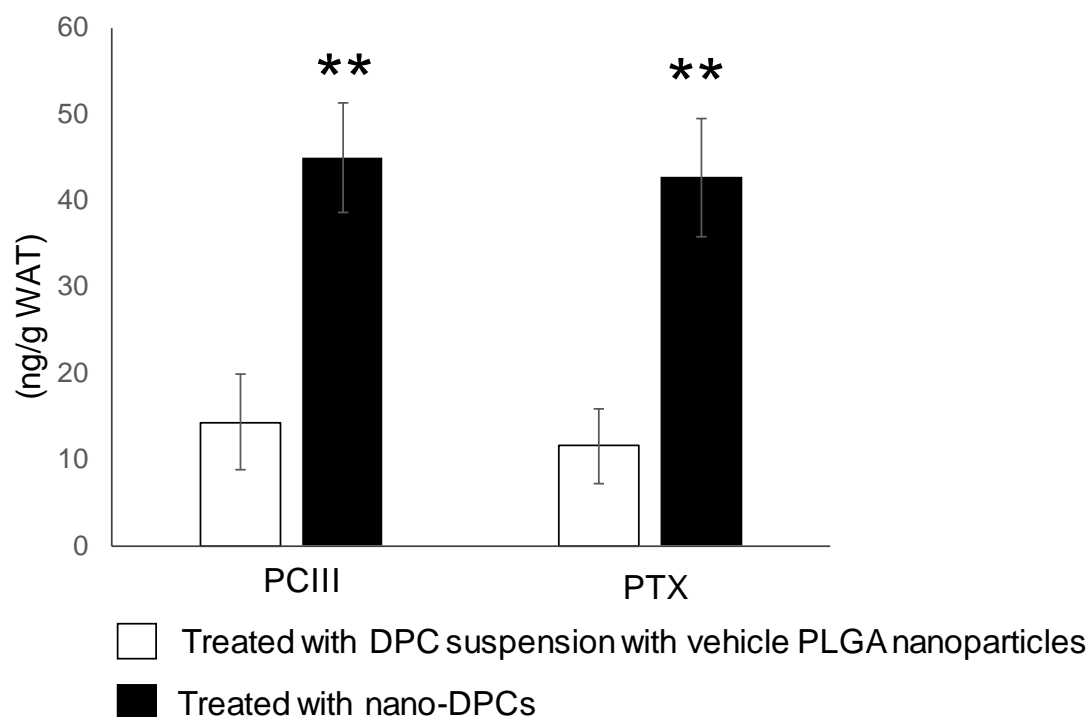


**Figure 2–9** Concentration of dihydropyranocoumarins (DPCs) in epididymal white adipose tissue (WAT) collected 24 h after oral administration of DPCs or polylactic-co-glycolic acid (PLGA) nanoparticles with DPCs (nano-DPCs). Notes: Each value represents the mean  $\pm$  SEM for 9 mice. The asterisk shows significant differences as compared with the mice treated with DPC suspension with vehicle PLGA nanoparticles using the Student's *t*-test (\*\*  $p < 0.01$ ).

## 2.4. Discussion

In present study, I investigated the anti-obesity effect of DPCs, such as mainly PCIII and PTX, on HFD-fed mice. Previous study did not remove the possibility that other ingredients in DPCs concentrate have anti-obesity effects [94]; however, this study has clearly showed that dietary intake of pure DPCs prevents fat accumulation in WAT, and suggested that DPCs are a significant factor in the anti-obesity effects of PJT. In addition, thus results suggested that DPCs' anti-obesity properties are caused by an increase in energy expenditures resulting from increased UCPs, and that PLGA-based nanoparticulate system is a powerful tool by which to enhance DPC activities.

Adipose tissue is the most flexible endocrine organ that can expand and reconstruct itself throughout life. Adipose tissue can grow and expand either by hypertrophy or hyperplasia [104]. Hypertrophy of adipocytes can increase hypoxia and mechanical stress to neighboring cells and the extracellular matrix. As a result in reduced adipose tissue functions, which contributes to the early onset of metabolic disease, and persistently elevated levels of nutrients in the blood, which causes leads to the fat accumulation in ectopic tissues, such as skeletal muscle, heart, and the liver [105,106]. On the other hand, hyperplastic growth is considered to be a healthy and adaptive mechanism by which to maintain proper functions of stromal vascular fraction (SVF), responses to anti-inflammatory hormone adiponectin, insulin-sensitizing and other metabolism-modulatory adipokines [105,107]. Indeed, a study found that treatment with thiazolidinediones, an insulin-sensitizing drug leads to enhancement of overall adipose tissue growth, it induces the conversion of hypertrophic into hyperplastic adipose tissue [108]. In hyperplasia of adipocytes, mature adipocytes are generated from preadipocytes during adipogenesis, C/EBP $\alpha$  and FABP4 are the principal regulator of this process [109,110]; therefore, it is known that hypertrophic obesity is also more strongly associated with insulin resistance and metabolic complications than hyperplastic

obesity [111]. Present study showed that C/EBP $\alpha$  and FABP4 gene expressions significantly increased or tended to increase in epididymal WAT of the mice fed HFD containing DPCs (Figure 2-8). Dietary intake of DPCs also led to decreases in the average size of epididymal white adipocytes (Figure 2-7). One recent study has reported that dietary intake of suksdorfin, which has a structure similar to that of the DPCs used in this study, induces adipogenesis in WAT in obese, diabetic *KK-Ay* mice [112]. Thus, these results suggested that the dietary intake of DPCs can induce the conversion of hypertrophic into hyperplastic obesity in HFD-fed mice. It has also suggested that other ingredients in PJT can exert anti-lipogenic effects on WAT because our previous study observed significant decreases in mRNA levels of lipogenesis-related genes in the epididymal WAT of mice fed HFD containing DPC concentrates from PJT (DPC contents: ~62.2%) [94]. In addition, it should be noted that these phenomena were observed in the low dose group, in which mice fed 1% of the amount of DPCs fed to regular dose group (Table 2-2).

As mentioned above, the dietary intake of DPCs and oral administration of nano-DPCs significantly decreased hypertrophic white adipocytes (Figure 2-7); however, significant decreases in the mass of epididymal WAT were observed in mice of regular dose and nano-DPC groups, but not in the low dose group mice (Figure 2-4B). This decreased WAT mass contained, as a results significant upregulated mRNA levels of thermogenesis-related genes, such as UCP1 and UCP3 (Figure 2-8). It is well known that UCPs increase proton leakage across the mitochondrial inner membrane and thereby dissipates the proton motive force as heat instead of synthesizing ATP [113]. Adipocytes are broadly divided into white adipocytes and brown adipocytes. Brown adipocytes are characterized by multilocular lipid droplets and have thermogenic properties mainly through the mitochondrial UCP1 in brown adipose tissues; whereas, white adipocytes store neutral fat as energy in WAT [114]. It has been reported that



adaptive stimuli, such as cold exposure and adrenergic stimulation, can induce browning, which converts white adipocytes into brown-like adipocytes (recently called “beige” adipocytes) in WAT [115]. These beige adipocytes resemble white adipocytes in WAT have extremely low basal expression of UCP1, but beige adipocytes similar to classic brown adipocytes with high UCP1 expression; therefore, it is suggested that their generation increases energy expenditure and can prevent obesity [116-118]. At the molecular level, WAT browning is regulated by multiple factors and signaling pathways. PGC-1 $\alpha$  is known as a cold-induced interacting partner of PPAR $\gamma$  in adipocyte browning [119]. Consistent with our findings on the upregulations of PPAR $\gamma$ , PGC-1 $\alpha$ , and UCP1 expression in WAT (Figure 2–8), I observed that the dietary intake of DPCs or oral treatment with nano-DPCs enhanced energy expenditure and caused significant decreases in epididymal WAT mass in regular dose and nano-DPC group mice (Figure 2–4). In addition, these results suggested that the biological activities of DPCs are factors in the conversion of white into beige adipocytes.

Several studies reported that, PLGA nanoparticles have markedly improved the bioavailability of several compounds, such as curcumin after oral administration [101,120,121]. A recent study has demonstrated that incorporation into PLGA nanoparticles markedly enhance the therapeutic effects of  $\gamma$ -oryzanol on glucose and lipid metabolism in obese diabetic mice [122]. In this study, I observed that treatment with small amount of DPC (1% of DPC amount in regular dose) had no effect on WAT weight, but had significant anti-obesity effects on mice when the same amount of DPCs encapsulated into PLGA nanoparticles (Figures 2–4 and 2–7). Moreover, PLGA nanoparticle encapsulation significantly increased the DPC concentration in WAT 24 h after oral administration (Figure 2–9). These results might demonstrate the enormous potential for PLGA nanoparticles to act as carriers for the oral delivery of DPCs. Moreover, significant decreases in

serum levels of cholesterol and hepatopathy indicators were observed in mice treated with DPCs encapsulated into PLGA, but not in those treated with DPCs alone (Figures 2–5 and 2–6). It has been reported that the compound has been encapsulated into PLGA nanoparticles is distributed mainly in the liver and intestine in mice over a longer period time than the non-encapsulated compound after oral administration [122]; therefore, it is suggested that PLGA nanoparticle encapsulation expands the therapeutic potential of DPCs to prevent the development of obesity and its related diseases, although further studies are needed to confirm this effect.

## **2.5. Conclusions**

This study clearly demonstrated that DPCs, such as PCIII and PTX, contributes to the beneficial effects of PJT on the development of obesity, and also nano-DPCs enhanced DPCs accumulation and concentration in WAT. As a results DPCs and nano-DPCs prevents HFD-induced weight gain, by converted hypertrophic to hyperplastic obesity, improved serological markers and enhanced energy expenditures. PLGA nanoparticle encapsulation was helpful in enhancing the efficacy of oral intake of DPCs to develop natural and safe anti-obesity agents. Thus, this study suggests that DPCs to be used as an anti-obesity drug in pharmaceutical industry nano-DPCs technique can be consider for the development of new therapeutics.

## CHAPTER III

Anti-obesity effect of *Cirsium brevicaule* A.  
GRAY Root (CbR) extract on 3T3-L1

### 3.1. Introduction

In chapter II, I showed that anti-obesity activity of *Peucedanum japonicum* Thunb (PJT) derived DPCs and the usefulness of nanoparticle encapsulation on DPC activity; whereas, in this study, I focused on anti-obesity properties of the other tropical bioresource, *Cirsium brevicaule* A. GRAY (CBAG).

Genus *Cirsium* (thistle) belongs to the Asteraceae family and more than 200 species of thistle are well distributed around the world. Some *Cirsium* species are used as edible plants and medicinal plants in the traditional medicine, although many species are often considered as invasive weeds against which massive means of control are deployed in general [123,124]. It is well known that *Cirsium* species contain a variety of natural products and their main secondary metabolites are flavonoids and glycosides [125,126]. Lot of studies have reported that compounds from *Cirsium* species and their extracts show many different biological activities such as antioxidant, antidiabetic, anti-inflammatory, hepatoprotective, and anticancer activities [123].

It has been reported that flavones isolated from *C. japonicum* enhance adipocyte differentiation by inducing PPAR $\gamma$  activation in 3T3–L1 cells [127,128]. An antidiabetic effect of *C. japonicum* was also revealed in diabetic rats, suggesting their potential benefit as an alternative in treating diabetes mellitus [128]. Mori *et al.* demonstrated that the crude extracts of *C. oligophyllum* inhibited lipid accumulation in white adipose tissue in rats [129]. Nonpolar crude extracts of *C. pascuarensense*, and *C. vulgare* and *C. ehrenbergii* have been shown to confer antidiabetic and hepatoprotective activities, respectively [130,131].

*C. brevicaule* A. GRAY (CBAG), is a wild perennial herb, grows in rocky gravels or forest margins along maritime coastlines [132], and is distributed in southern-Japan and China. Stems, leaves and roots of CBAG are traditionally used as a food and herbal medicine in the Okinawa Islands and Amami Islands of Japan. The *Cirsium brevicaule* group is characterized as follows [133]: (1) well-developed rosette-like basal leaves, (2) subscapos habit, (3) a few large and erect capitula, (4) large strongly spiny (5) erect and not sticky involucre, and (6) habitat preference in rocky gravels or forest margin along maritime coast.

Our previous study [134] showed that dietary intake of CBAG leaves (CbL) significantly decreased hepatic lipid accumulation in mice fed a high-fat diet and treatment of 3T3-L1 cells with nonpolar crude extract of CbL significantly reduced cellular lipid accumulation. In contrast, there are few scientific data on the biological activities of CBAG root (CbR) are available (Figure 3-1).

In China, the roots or entire plants of more than ten *Cirsium* species (*C. japonicum*, *C. eriophoroideum*, *C. esculentum*, *C. griseum*, *C. lineare*, *C. maackii*, *C. pendulum*, *C. setosum*, *C. souliei*, and *C. valassovianum*) have been used as folk medicines for symptoms of various diseases [126]. Previous study has investigated the antioxidant activities of the methanol and water extracts of the roots of *C. japonicum*, and also confirmed that both extracts have high phenolic and flavonoid contents and beneficial activities *in vitro* against diabetes [135]. I, therefore, evaluated the biological activities of CbR pertaining to metabolic syndrome, and tried to concentrate its active compound in this study.



**Figure 3–1***Cirsium brevicaule* A. GRAY

Shoot (left); root (right)

## 3.2. Materials and methods

### 3.2.1. Plant material

*Cirsium brevicaule* A. Gray was botanically classified by Asa Gray [48]; a voucher specimen of the plant was deposited in the Amami Museum (Kagoshima, Japan) by Hayao Ohno (voucher specimen number: 1582). The CbR used in this study was harvested on Tokunoshima Island in Kagoshima Prefecture, Japan. Freeze-dried CbR was generously provided by Healthy Island Co. (Kagoshima, Japan).

### 3.2.2. Extraction and fractionation of CbR

Dried powder was serially extracted by incubation with a total of 9 volumes of hexane, chloroform, methanol, and water for 1 h at 37 °C (Figure 3–2). To identify the antiadipogenic compounds, the methanol extract was dried and re-dissolved in chloroform:methanol (9:1, v/v) (Figure 3–5A), these soluble and insoluble fractions were screened for its adipogenic effect by the lipid accumulation assay. Chloroform:methanol 9:1 soluble fraction was having maximum lipid accumulation inhibition activity in 3T3–L1 cells.

The chloroform:methanol 9:1 soluble fraction was further subjected to open column chromatography (CC) for rough fractionation. CC was performed on Hi-FLASH silica gel open-column (Yamazen Corp., Osaka, Japan). The starting eluent was chloroform:methanol (9:1, v/v) followed by a gradual shift in the mixing ratio to 0:10 (v/v) to yield 5 fractions F–1 to F–5 (Figure 3–6A).





### **3.2.3. Purification and structure identification of fractionated CbR extract**

On the basis of low polarity F-1 was further subjected to HPLC with (chloroform:methanol, 9:1, v/v) in a silica gel column (Cosmosil 5SL-II, Nacalai Tesque, Inc., Kyoto, Japan) (Figure 3-7A). The active fractions were evaporated to a complete dry, dissolved in methanol, and further purified through an HPLC reverse-phase C18 column (GL Sciences Inc., Tokyo, Japan) with methanol containing 0.1% formic acid (Figure 3-7A). All extracts and isolated fractions were evaporated or freeze-dried in vacuo, and stored at -80 °C until further use. Powders were dissolved in dimethyl sulfoxide before use for the treatments. To identify the chemical structure of the purified active compound, NMR spectra were measured on a Bruker AVANCE 400 (Bruker Biospin, Rheinstetten, Germany). <sup>1</sup>H-NMR, <sup>13</sup>C-NMR, HSQC, and HMBC were measured using a 5-mm probe. The operating frequencies were 400.13 MHz for <sup>1</sup>H-NMR and 100.62 MHz for <sup>13</sup>C-NMR spectra. Samples were measured at 299 K in CDCl<sub>3</sub> with TMS as standard. ESI-MS was also performed on a LC-MS (Xevo TQD, Waters Corp., Milford, MA, USA) in positive-ion mode.

### **3.2.4. Cell culture and treatments**

Dulbecco's modified Eagle's medium (DMEM) and human insulin were purchased from Wako Pure Chemical Industries Ltd. Fetal bovine serum (FBS) and newborn calf serum (NCS) were purchased from AusGeneX PTY Ltd. (Oxenford, Australia) and Global Life Science Technologies Japan Co. Ltd. (Tokyo, Japan), respectively, and these sera were inactivated at 56 °C for 30 min before use. Dexamethasone, 3-isobutyl-1-methylxanthine, and syringin were purchased

from Sigma-Aldrich, Inc. (MO, USA). Cells were purchased from the JCRB Cell Bank (Tokyo, Japan) and cultured in a humidified atmosphere of 95% air and 5% CO<sub>2</sub> at 37 °C.

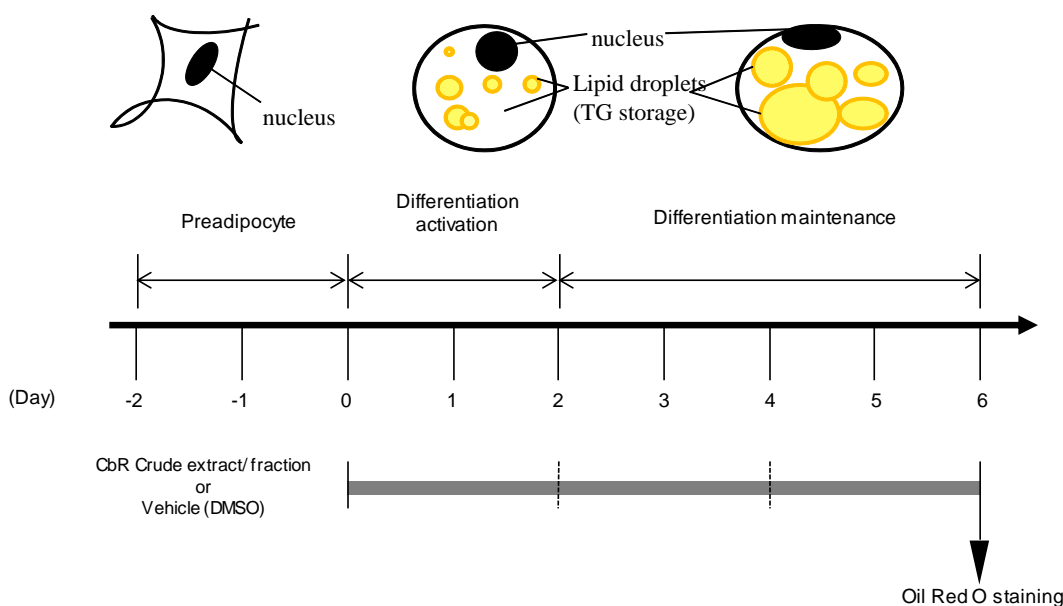


**Figure 3–3** Time schedule for the treatment with crude extract or its fractions during the cellular differentiation of 3T3–L1.

3T3–L1 preadipocytes were maintained in DMEM with low glucose (1 g/L) containing 10% NCS and avoided complete confluence before initiating differentiation. For adipogenesis, preadipocytes were cultured in 24-well plates at a density of  $4 \times 10^4$  cells per well. The confluent preadipocytes were maintained for another 2 days. Differentiation was induced by standard differentiation inducers: 0.5 mM 3-isobutyl-1-methylxanthine (IBMX), 0.25  $\mu$ M dexamethasone (DEX), and 10  $\mu$ g/mL insulin in DMEM with high glucose (4.5 g/L) containing 10% FBS for 48 h (from day 0 to 2). The culture medium was then changed to DMEM with high glucose

supplemented with 10% FBS and 10 µg/mL insulin from day 2 to 6. Cells were cultured in the culture media supplemented with each extract or isolated fractions from day 0 to 6. On day 6, lipid by Oil Red O (Figure 3-3).

### **3.2.5. Oil Red O Staining**

3T3–L1 cells were washed two times with PBS and fixed in 10% formalin in PBS for 10 minutes at room temperature. After washing the cells twice with PBS, cells were stained with Oil Red O staining solution for 10 minutes (0.3% Oil Red O in isopropanol, diluted 3:2 in water and filtered with a 0.45µm filter; Wako HP). After staining, cells were washed with 60% isopropanol then stained dye was extracted with isopropanol for quantification by absorbance readout at 520 nm.

### **3.2.6. Statistical Analyses**

Data are expressed as the mean  $\pm$  standard error of the mean (SEM). The statistical significance of the difference between the two experimental groups was determined using the Student's *t*-test. To determine the significance of the differences among the means for more than three groups, the data were analyzed using one-way analysis of variance, and the differences among the mean values were subsequently inspected using the Dunnett's significant difference test. The level of significance was set to  $p < 0.05$ .

### 3.3. Results

#### 3.3.1. Effect of CbR extract on 3T3–L1 cells

The CbR was extracted with hexane, chloroform, methanol and water, among them methanol extract in the highest extraction yield (5.5%, w/w) followed by hexane extract (3.5%, w/w), water extract (1.5%, w/w), chloroform extract (0.5%, w/w) from dried CbR powder. Lipid accumulation in 3T3–L1 adipocyte was significantly decreased when treated with chloroform extract or methanol extract whereas, there are no effect were observed in hexane and water extract (Figure 3–4).

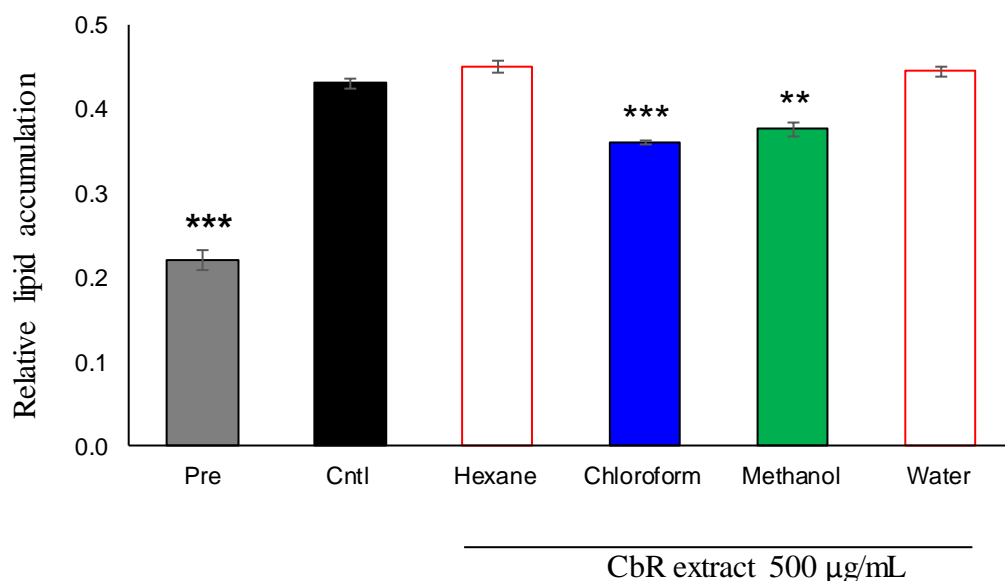


**Figure 3–4** Effects of extracts from CbR on 3T3-L1 cells. Inhibitory effects of the CbR crude extract on cellular lipid accumulation. The results are presented as means  $\pm$  SEM from three independent experiments. The asterisk (\*) indicates a significant difference between control and treatment groups by Dunnett's test. \*\* $p < 0.01$ , and \*\*\* $p < 0.001$  vs control (Cntl) and preadipocytes (pre).

### **3.3.2. Effect of partially purified CbR methanol extract on 3T3–L1 cells**

Methanol extract has been chosen for higher yield and purifications were carried out for anti-adipogenic active compound. To isolate the most active anti-adipogenic compound, methanolic extract was partially purified on the basis of polarity. Stronger anti-adipogenic active compounds are soluble in low polar solution Chloroform : MeOH 9:1. (Figure 3–5B).

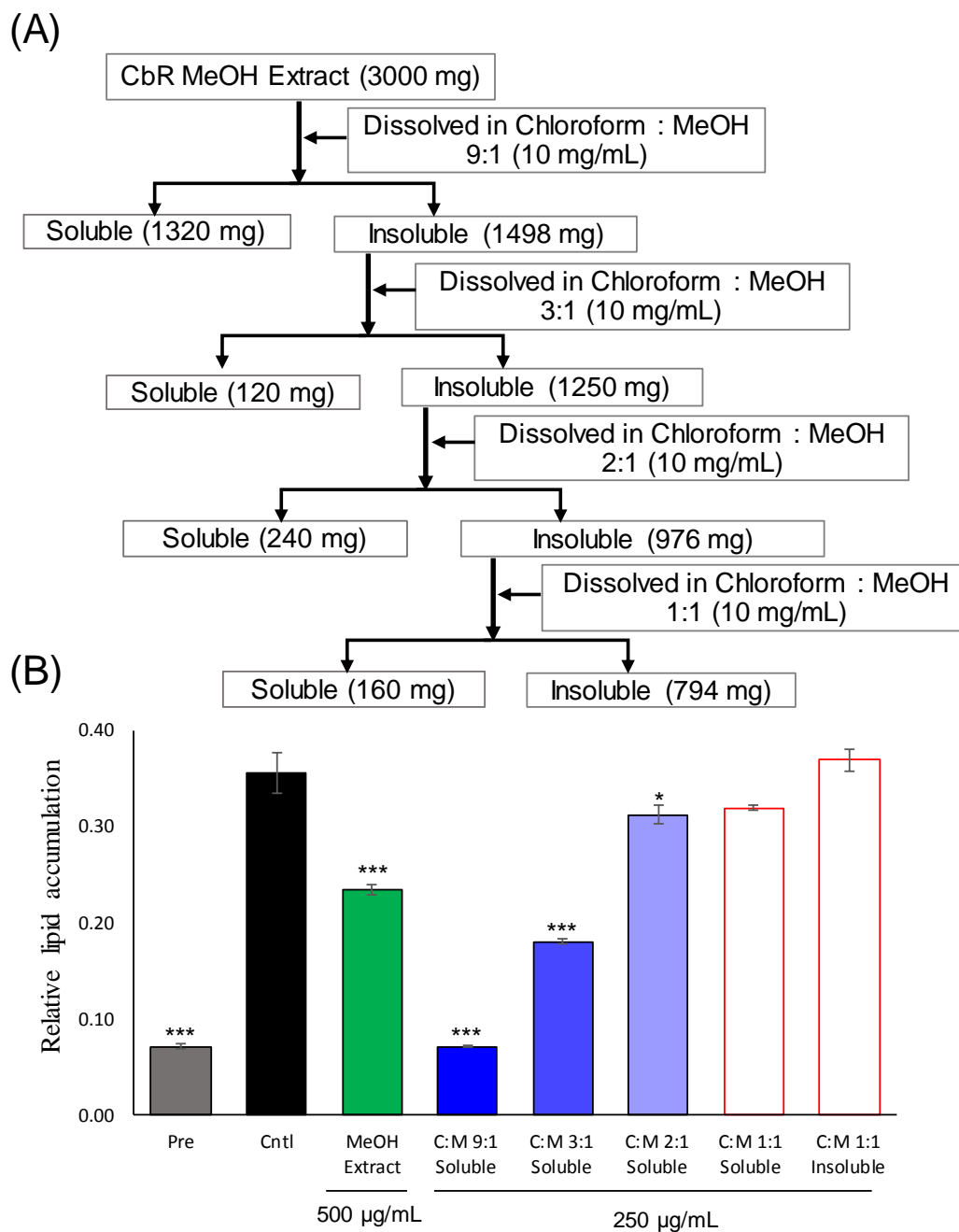


**Figure 3–5** Effect of CbR methanol extract fractions on 3T3–L1 cells. (A) A Flowchart for the liquid-liquid partition on the basis of solvent polarity of CbR methanol extract. (B) Inhibitory effects of the CbR methanol extract and of its fractions on cellular lipid accumulation. The results are presented as means  $\pm$  SEM from three independent experiments. The asterisk (\*) indicates a significant difference between control and treatment groups by Dunnett's test. \* $p < 0.05$ , \*\* $p < 0.01$ , and \*\*\* $p < 0.001$  vs control (Cntl) and preadipocytes (pre).

### **3.3.3. Effects of CbR methanol extract fractions on 3T3–L1 cells**

Methanol extract was partially purified with chloroform: methanol 9:1, which was followed by further fractionated into F–1 to F–5 through a silica gel open column. Among these five divided fractions, treatments with a dose of 100µL/ml lower-polarity fraction, F–1 and F–2, significantly inhibited the lipid accumulation in 3T3–L1 cells whereas no significant effect was observed in comparatively high polar fractions such as F–3, F–4 and F–5 (Figure 3–6 B).

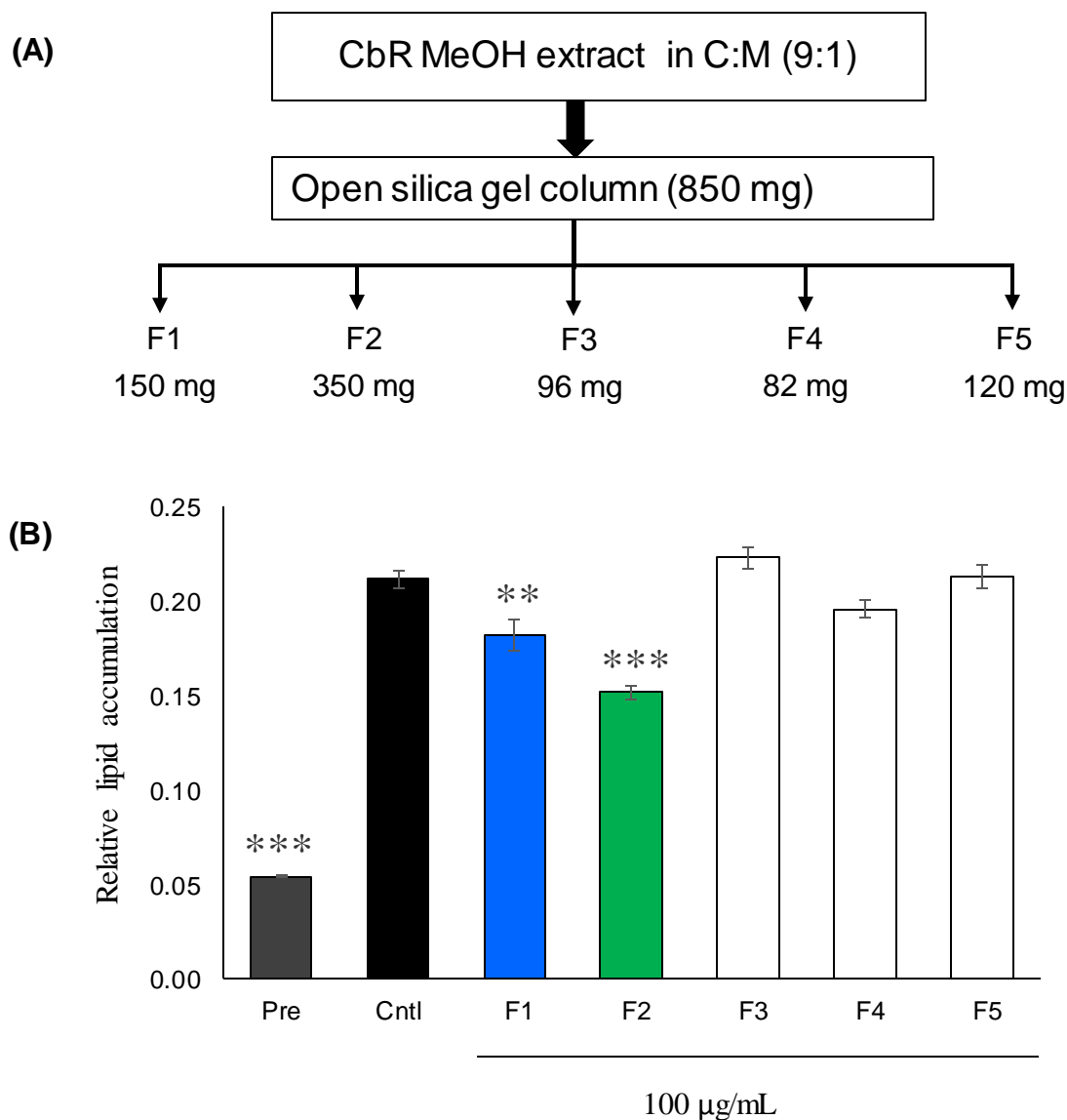


**Figure 3–6** Effect of CbR methanol extract fractions on 3T3–L1 cells. (A) A Flowchart for the partially purified by open silica gel column chromatography. (B) Inhibitory effects of the fractions derived from partially purified methanol extract on cellular lipid accumulation. The results are presented as means  $\pm$  SEM from three independent experiments. The asterisk (\*) indicates a significant difference between control and treatment groups by Dunnett's test. \*\* $p < 0.01$ , and \*\*\* $p < 0.001$  vs control (Cntl) and preadipocytes (pre) C=Chloroform and M=Methanol.



### 3.3.4. Screening of F1 fraction

In figure 3-6B shows the F-1 and F-2 inhibition of lipid accumulation first F-1 were selected for comparatively low polarity as mentioned above. F-1 was further fractionated in to three fractions (F1-1 to F1-3) using HPLC system. The screening of fraction of F1-2 shows the strongest inhibitory (Figure-3-8B).

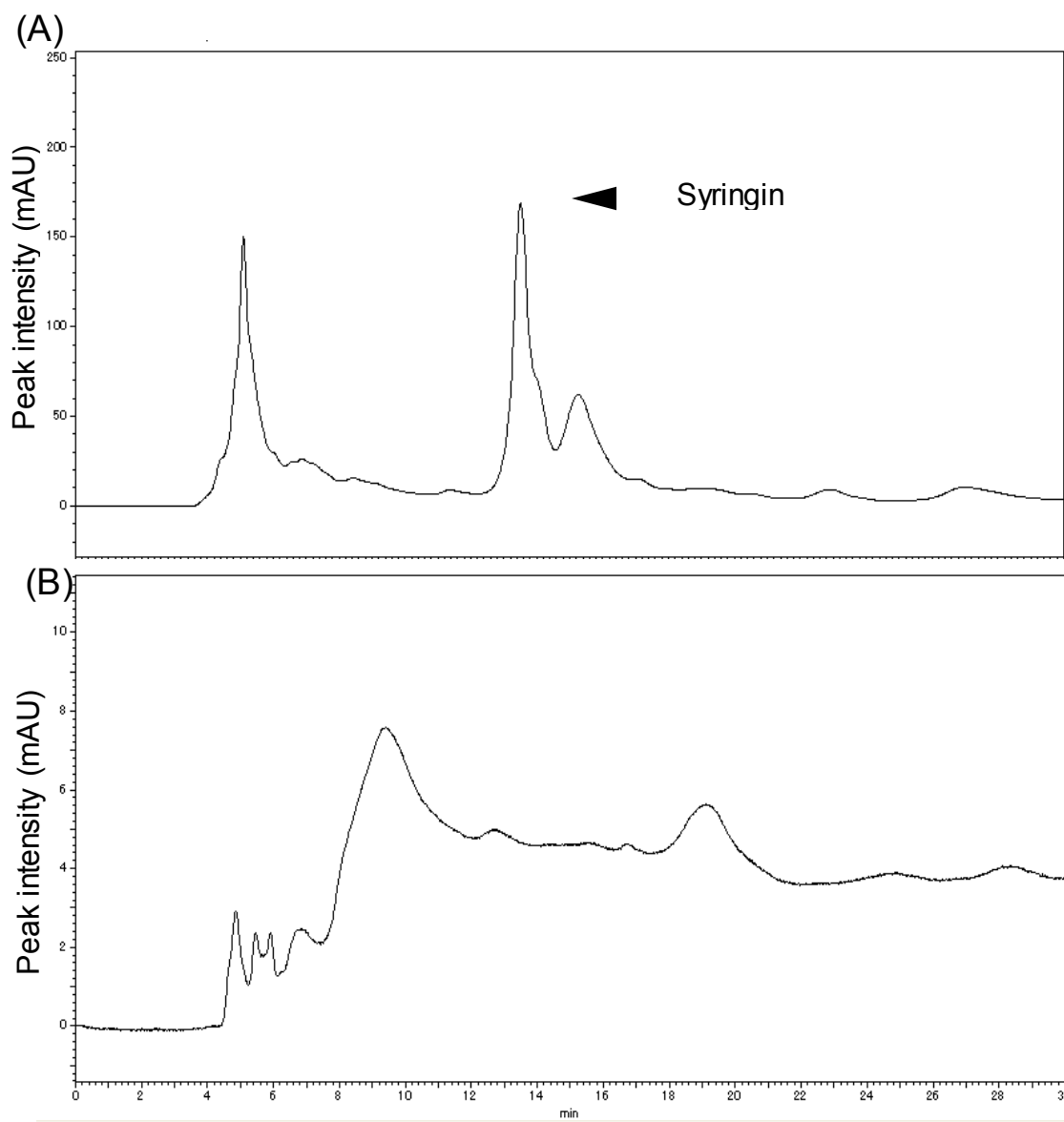


**Figure 3-7** 1 HPLC chromatogram of CbR methanol extract fractions detected at 271 nm (A) F-1 and (B) F-2 (Develosil column 4.6 x 250 mm) Chloroform : Methanol 9:1

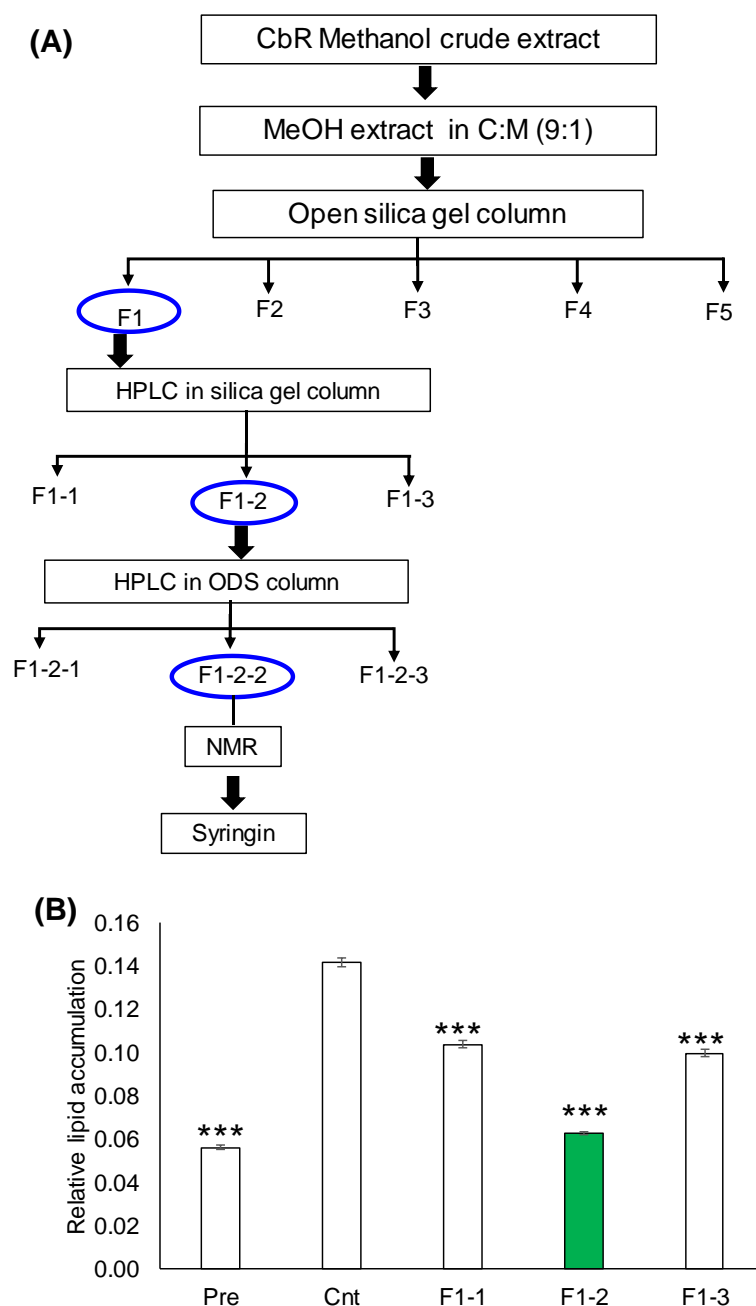


**Figure 3–8** Effect of fractions from CbR on 3T3–L1 cells. (A) A Flowchart for the isolation of active anti-obesity compounds from *Cirsium brevicaulis* A GRAY root (CbR) methanol extract. (B) Inhibitory effects of the fractions derived from partially purified methanol extract on cellular lipid accumulation. The results are presented as means  $\pm$  SEM from three independent experiments. The asterisk (\*) indicates a significant difference between control and treatment groups by Dunnett's test. \*\*\* $p < 0.001$  vs control (Cntl) and preadipocytes (pre). C=Chloroform, and M=Methanol

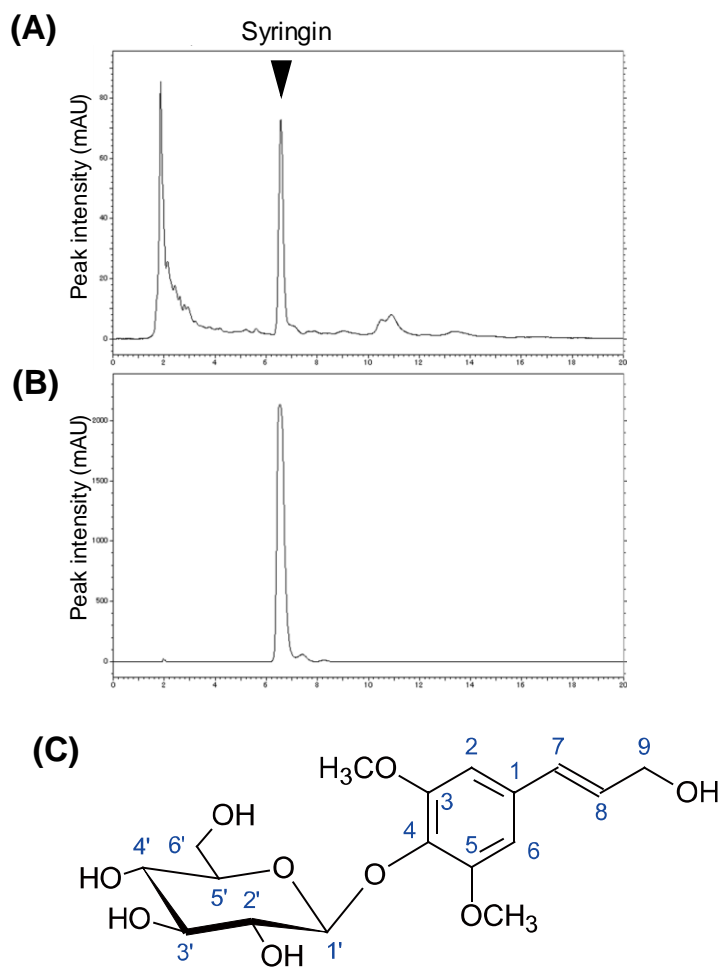


**Figure 3–9** Isolation of active components from CbR and their chemical structure. (A–B) Chromatograms of F–1 from crude methanol extract and purified syringin, respectively. (C) Chemical structure of syringin revealed by NMR analyses

### 3.3.5. Chemical structure identification of active compound from CbR

The active fraction, F1, was further fractionated through normal and reverse phase HPLC columns (Figure 3–9A). The purified active fraction was subjected to NMR analysis (Figure 3–9B). <sup>1</sup>H-NMR (CDCl<sub>3</sub>, 400 MHz): δ 6.75 (s, H-2, H-4, 2H), 6.55 (d, *J* = 15.9 Hz, H-7), 6.33 (dt, *J* = 15.9 Hz, 5.6 Hz, H-8), 4.87 (overlapped with solvent signal, H-1'), 4.22 (dd, *J* = 5.5 Hz, 1.2 Hz, H-9, 2H), 3.86 (s, 3-OCH<sub>3</sub> 5-OCH<sub>3</sub>, 6H), 3.81 (m, H-6'a), 3.70 (m, H-6'b), 3.50 (m, H-2'), 3.44 (m, H-4'), 3.43 (m, H-3'), 3.23 (m, H-5'). <sup>13</sup>C-NMR (CDCl<sub>3</sub>, 100 MHz): δ 154.41 (C-3, -5), 135.92 (C-4), 135.32 (C-1), 131.32 (C-7), 130.07 (C-8), 105.48 (C-2, -5), 105.37 (C-1'), 77.88 (C-5'), 75.77 (C-2'), 71.38 (C-4'), 63.62 (C-9), 62.62 (C-6'), 57.05 (3-OCH<sub>3</sub> 5-OCH<sub>3</sub>). ESI-MS analysis of the compound found the [M+Na]<sup>+</sup> ion at *m/z* 395.2. Interpretation of these spectral data identified the chemical structure of the active component as syringin (Figure 3–9C).

### 3.3.6. Screening of F2 fraction

In figure 3–6B shows the highest inhibition of lipid accumulation of the F2. HPLC chromatography were performed F1 and F2 (Figure 3–7) chromatogram representing that F2 contains high polarity compounds. Thus, F2 were further fractionated in to five fraction (F2–1 to F2–5) using open reverse phase column. F2–1 was further fractionated on the basis of elution yield (77%) and anti-adipogenic effect on 3T3–L1 cells. In the following fractions using HPLC system in first normal phase HPLC column were used for large separation then revers phase column for purified the active compound (Figure 3–10) on the basis of strongest lipid accumulation inhibition effect on 3T3–L1 cells (Figure 3–11D and F).

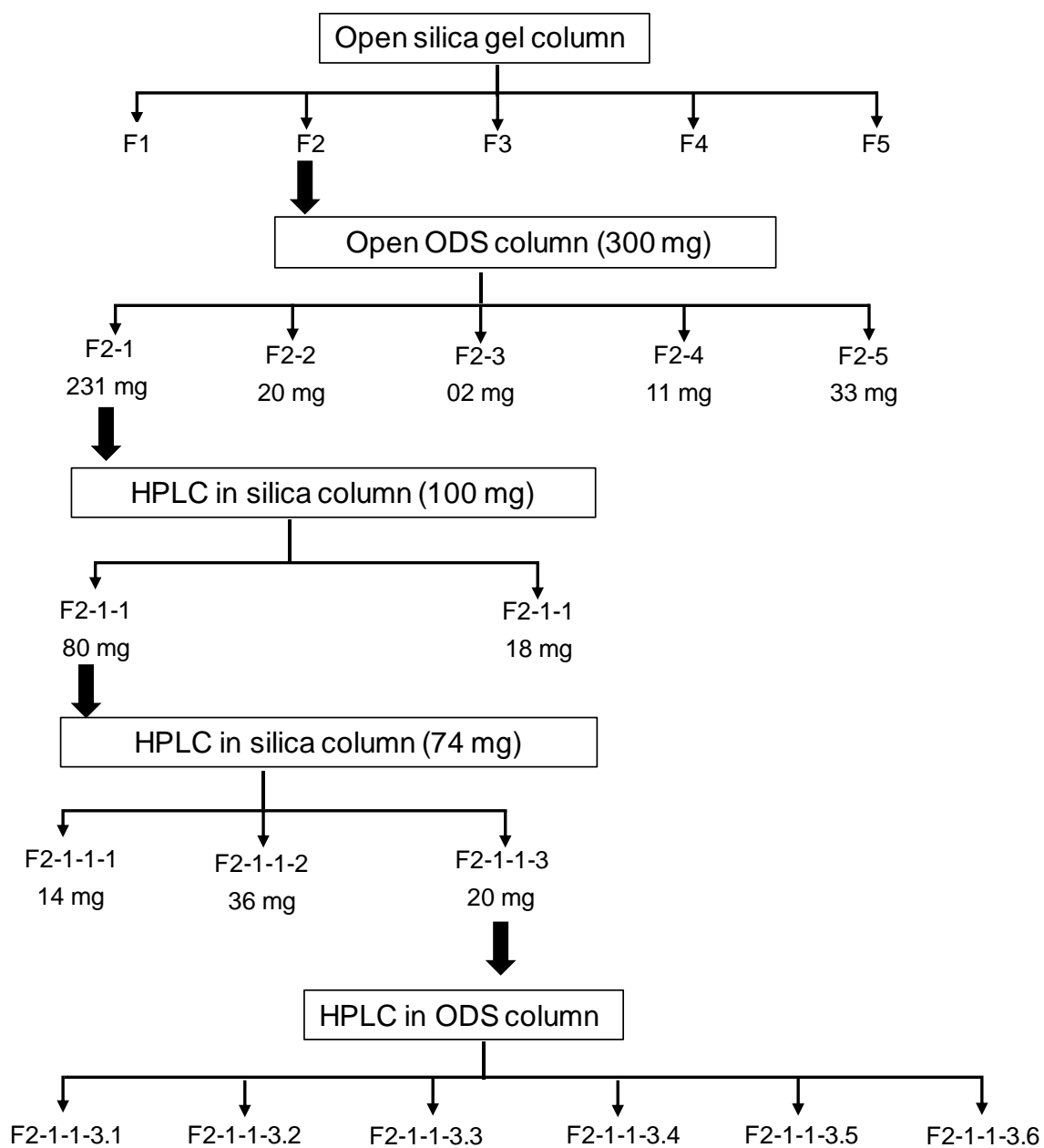


**Figure 3–10** Flowchart for the bioactivity-guided purification of anti-obesity compounds from CbR. Bioactivity was assessed on 3T3–L1 cells. Liquid chromatography was carried out on an open column and HPLC system.

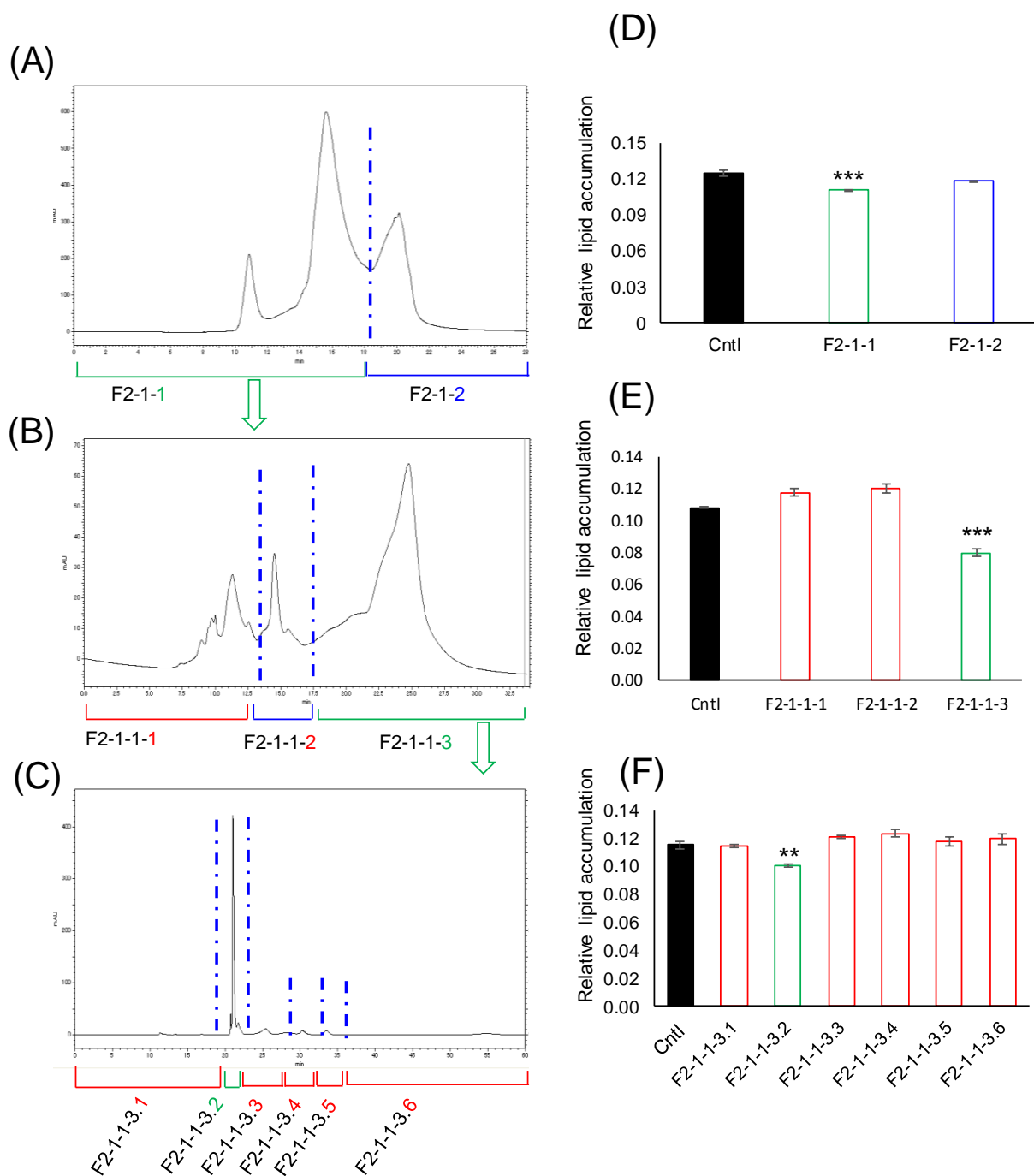


**Figure 3-11** HPLC profiling CbR methanol extract and effects of on intracellular lipid accumulation in 3T3-L1 cells. HPLC chromatograms of partially purified CbR methanol Extract (detected at PDA 371 nm) (A): F2-1, (B): F2-1-1 (C): F2-1-1-3 and D-F relative lipid accumulation in 3T3-L1. The results are presented as means  $\pm$  SEM from three independent experiments. The asterisk (\*) indicates a significant difference between control and treatment groups by Dunnett's test. \*\* $p < 0.01$ , and \*\*\* $p < 0.001$  vs control (Cntl).

### 3.4. Discussion:

As described above, CbR has been traditionally used as a food and herbal medicine in the Okinawa and Amami Islands of Japan [135]. A previous study investigated the antioxidant activities of methanol and water extracts from roots of *C. japonicum* and that both extracts have high phenolic and flavonoid contents, and antidiabetic activities [128]. The testing and screening of plant extracts against a variety of pharmacological targets in order to benefit from the immense natural chemical diversity is a concern in drug discovery from the natural products.

This study demonstrated that methanol extract of CbR and its minimally polar contents significantly inhibited cellular lipid accumulation in 3T3–L1 adipocytes, as a precursor to assess the effects of CbR on the development of obesity (Figure 3–4). Further fractionation suggested that CbR contains various anti-obesity active compounds (Figures 3–5, 3–4, 3–6, 3–8 and 3–11), and one of them was identified as a syringin (Figure 3–9). Syringin was also isolated from the roots of a different *Cirsium* plant, *C. japonicum*[136]; Many studies have reported the beneficial activities of syringin, such as hypoglycemic, anti-inflammatory, anti-oxidative, and immunomodulating effects [137-139]. However, few studies have investigated the effect of syringin on 3T3–L1 cells and adipose tissues [140]. Although additional studies are needed to elucidate the underlying molecular mechanism and reveal other active components in CbR, this study suggested that CbR could be used for the treatment of obesity and diabetes.

### 3.5. Conclusion

This study indicated that CbR chloroform and methanol crude extract have the potent anti-obesity activity and also partially purified of CbR methanol extract inhibit adipogenesis.

# **CHAPTER IV**

Anti-adipogenic effects of syringin via  
AMPK and Akt signaling pathways



#### 4.1. Introduction:

In the previous chapter, syringin was identified as one of the components contributing to the anti-adipogenic activity of crude methanol extract of CbR. Syringin, a phenylpropanoid glycoside was first isolated from lilac *Syringa vulgaris*, and is also called eleutheroside B[141]. Syringin was also isolated from the root of different *Cirsium* plant, *C. japonicum* [136]. This compound is distributed widely throughout various plants [142], and its beneficial activities, such as hypoglycemic, anti-inflammatory, anti-oxidative, and immunomodulating effect, have been reported [137-139]; however, few studies have investigated the effect of syringin on 3T3–L1 adipocyte and adipose tissues [140]. Therefore, it is essential to elucidate the molecular mechanisms of the anti-adipogenic activity of syringin. Here I have investigated the following:

- ❑ Effect of syringin on 3T3–L1 cells lipid accumulation in different stages of adipogenesis.
- ❑ Pattern of gene expression modulation when 3T3–L1 cells are treated with syringin at early stage of differentiation.
- ❑ Elucidation of the molecular mechanisms involved in the inhibition of lipid accumulation in 3T3–L1 adipocytes.

## **4.2. Materials and methods**

### **4.2.1. Syringin purification**

Syringin purification and identification procedure have been discussed in chapter III.

### **4.2.2. Cell culture and treatments**

3T3–L1 preadipocytes cells culture was described in chapter III. Cells were cultured in the culture media supplemented with syringin from day 0 to 6. On the other hand, to study the acting stage of active compound in the adipocyte development, the cell cultures were treated with syringin at different time intervals. On day 6, lipid droplets of 3T3–L1 cells were stained with Oil Red O discussed in chapter III. To visualize intracellular accumulated neutral lipids, after washing with PBS, 3T3–L1 adipocytes were fixed with 10% formalin solution and stained with Oil Red O solution, according to a method of Allott *et al.* [143], and observed under a light microscope. To elucidate cytotoxic effects of syringin on 3T3–L1 cells, cells were treated with 20  $\mu$ M syringin from day 0 to 6. At the end of the treatment period, cells were washed twice with PBS and lysed into 1% Triton X-100, and the double-strand DNA (dsDNA) content of cell lysates was determined using a Quanti-iT PicoGreen dsDNA Assay Kit (Thermo Fisher Scientific, MA, USA).

#### **4.2.3. Quantitative real-time polymerase chain reaction**

Cells were treated with 20  $\mu$ M syringin or DMSO (used as a vehicle) for 48 h followed by cells were two times washed with PBS and total RNA was extracted from 3T3–L1 cells, which were treated with 20  $\mu$ M syringin from day 0 to 2, by FastGene RNA Basic kit (NIPPON Genetics Co., Ltd., Tokyo, Japan). First-strand cDNA was synthesized using mRNA as a template. For quantitative real-time polymerase chain reaction, the primers and probe sets (Table 4–1) were purchased from Integrated DNA Technologies, Inc. (Coralville, IA, USA). To measure the relative abundance of target transcripts, amplifications were performed using PrimeTime Gene Expression Master Mix (Integrated DNA Technologies, Inc.) with the StepOne Real-Time PCR System (Thermo Fisher Scientific), and the amounts of the target transcripts were normalized to those of ACTB.

**Table 4-1** TaqMan gene expression assays used for the quantitative real time PCR analysis.

Gene	Description	Gene expression assay reference
ACC1	Acetyl-coenzymeA (CoA) carboxylase 1	Mm.PT.58.12492865
ADIPOQ	Adiponectin	Mm.PT.58.9719546
$\beta$ -actin	ACTB	Mm.PT.58.33257376.gs
C/EBP $\alpha$	CCAAT/enhancer binding protein (C/EBP), alpha	Mm.PT.58.30061639.g
CPT1a	Carnitine palmitoyltransferase 1A	Mm.PT.58.10147164
CPT2	Carnitine palmitoyltransferase 2	Mm.PT.58.13124655
FABP4	Fatty acid binding protein 4	Mm.PT.58.43866459
FASN	Fatty acid synthase	Mm.PT.58.14276063
LIPE	Hormone-sensitive lipase	m.PT.58.6342082
LPL	Lipoprotein lipase	Mm.PT.58.46006099
ACOX	Peroxisomal acyl-coenzyme A oxidase 1	Mm.PT.58.50503784
PPAR $\gamma$	Peroxisome proliferator activated receptor gamma	Mm.PT.58.31161924
PGC1a	PPAR $\gamma$ coactivator 1 $\alpha$	Mm.PT.58.16192665
SCD1	Stearoyl-Coenzyme A desaturase 1	Mm.PT.58.8351960
GLUT4	Glucose transporter type 4	Mm.PT.58.9683859
UCP2	Uncoupling protein 2	Mm.PT.58.11226903
UCP3	Uncoupling protein 3	Mm.PT.58.9090376

PrimeTime qPCR Probe Assays (Integrated DNA Technologies, Inc)

#### 4.2.4. Western blot analyses

3T3–L1 cells have been treated with 20  $\mu$ M syringin from day 0 to 2 were washed with PBS and their lysates were prepared with PRO-PREP™ Protein Extraction Solution (iNtRON Biotechnology, Gyeonggi-do, Kore). Proteins were extracted and separated using SDS-PAG electrophoresis and subsequently transferred onto Polyvinylidene difluoride (PVDF) membranes (GE Healthcare Life Sciences, Chalfont, UK). Membranes were blocked with ATTO EzBlock Chemi (ATTO Corp., Tokyo, Japan) at room temperature for 1 h and then reacted with the following monoclonal antibodies (mAb) or polyclonal antibodies (pAb) as primary antibodies (Table 4–2) and anti-rabbit IgG pAb linked with horseradish peroxidase (HRP) as secondary antibody. These antibodies were diluted with Bullet ImmunoReaction Buffer (Nacalai tesque) and reacted for 1 h at room temperature. After each reaction, the PVDF membrane was washed three times with Tris-buffered saline with tween 20, and the protein bands on them were detected with the ECL Advance Western Blotting Detection System (GE Healthcare). Their images were captured and visualized using ImageQuant LAS 4000 (GE Healthcare) and the band intensities were quantified with ImageJ software and density were normalized by the level of  $\beta$ -actin.

**Table 4–2** List of antibodies used in this western blotting

<b>Antibody name</b>	<b>Company</b>	<b>Source</b>	<b>Dilution</b>
anti-PPAR $\gamma$ mAb	Signaling Technology, Inc (81B8)	Rabbit	1:1000
anti-C/EBP $\alpha$ mAb	Signaling Technology, Inc (D56F10)	Rabbit	1:1000
anti-FABP4 mAb	Signaling Technology, Inc (D25B3)	Rabbit	1:1000
anti-AMPK1/2 pAb	Santa Cruz Biotechnology, Inc	Rabbit	1:500
anti-p-AMPK1/2 pAb	Santa Cruz Biotechnology, Inc	Rabbit	1:500
anti-ACC pAb	Signaling Technology, Inc	Rabbit	1:1000
anti-p-ACC pAb	Signaling Technology, Inc	Rabbit	1:1000
anti-Akt mAb	Signaling Technology, Inc (C67E7)	Rabbit	1:1000
anti-p-Akt mAb	Signaling Technology, Inc (D9E)	Rabbit	1:1000
anti-GLUT4 mAb	Signaling Technology, Inc (1F8)	Mouse	1:1000
anti-SCD1 pAb	Signaling Technology, Inc (M38)	Rabbit	1:1000
Anti-LIPE pAb	Signaling Technology, Inc (D6W5S)	Rabbit	1:1000
anti-CPT1a mAb	Abcam (Cambridge, UK)	Mouse	1:1000
anti- $\beta$ -actin	Signaling Technology, Inc (E135)	Rabbit	1:1000
anti-rabbit IgG	Signaling Technology, Inc	Goat	1:2000
anti-mouse IgG	Signaling Technology, Inc	Goat	1:2000

#### 4.2.5. Statistical Analyses

Data are expressed as the mean  $\pm$  standard error of the mean (SEM). The statistical significance of the difference between the two experimental groups was determined using the Student's *t*-test. To determine the significance of the differences among the means for more than three groups, the data were analyzed using one-way analysis of variance, and the differences among the mean values were subsequently inspected using the Dunnett's significant difference test. The level of significance was set to  $p < 0.05$ .

## 4.3. Results

### 4.3.1. Effect of syringin during the differentiation time points of adipogenesis

To gain insight on the mechanism of the suppressive effect of syringin on adipogenesis of 3T3-L1 cells, I investigated the time course of the adipocyte differentiation in the presence of syringin (Figure 4–1A). Cellular lipid accumulation was significantly inhibited when syringin-treatments at 20  $\mu$ M are administered from day 0 to day 2 or 6 (Figure 4–1B). On the other hand, the inhibitory effects were not shown when 3T3-L1 cells are treated with syringin only for the latter period, day 2–6 (Figure 4–1B).

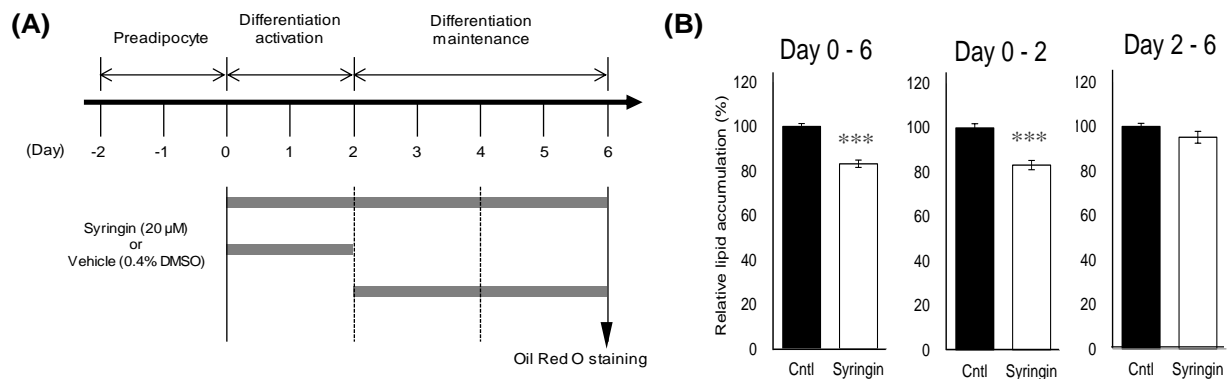


**Figure 4–1** Effect of syringin on intercellular lipid accumulation in 3T3–L1 cells. (A) Time schedule for the treatment with syringin during the cellular differentiation of 3T3–L1 cells (B) Inhibitory effects of the syringin on lipid accumulation in 3T3–L1 adipocytes. The results represent as the mean  $\pm$  SEM from three independent experiments. The asterisk (\*) indicates a significant difference between control and treatment groups tested by Student's *t*-test. \*\*\**p* < 0.001 vs control (Cntl).



#### **4.3.2. Effects of syringin on differentiation and lipid accumulation of 3T3–L1 cells**

The effect of syringin on intracellular lipid accumulation in mature 3T3–L1 adipocytes was visualized by Oil Red O staining as shown in (Figure 4–2C). Syringin treated groups decreased the amount of lipid in 3T3–L1 adipocytes. This observed reduction in lipid accumulation was confirmed by relative lipid quantification assay. As shown in (Figure 4–2B), compared to the differentiated control cells, 5 $\mu$ M, 10 $\mu$ M, and 20  $\mu$ M, treatment of syringin significantly decreased the lipid accumulation in 3T3–L1 adipocytes by 13, 18, and 29 %, respectively compared to control cells. There were no significant effects on lipid accumulation were observed in cells treated with 2.5  $\mu$ M versus control cells.

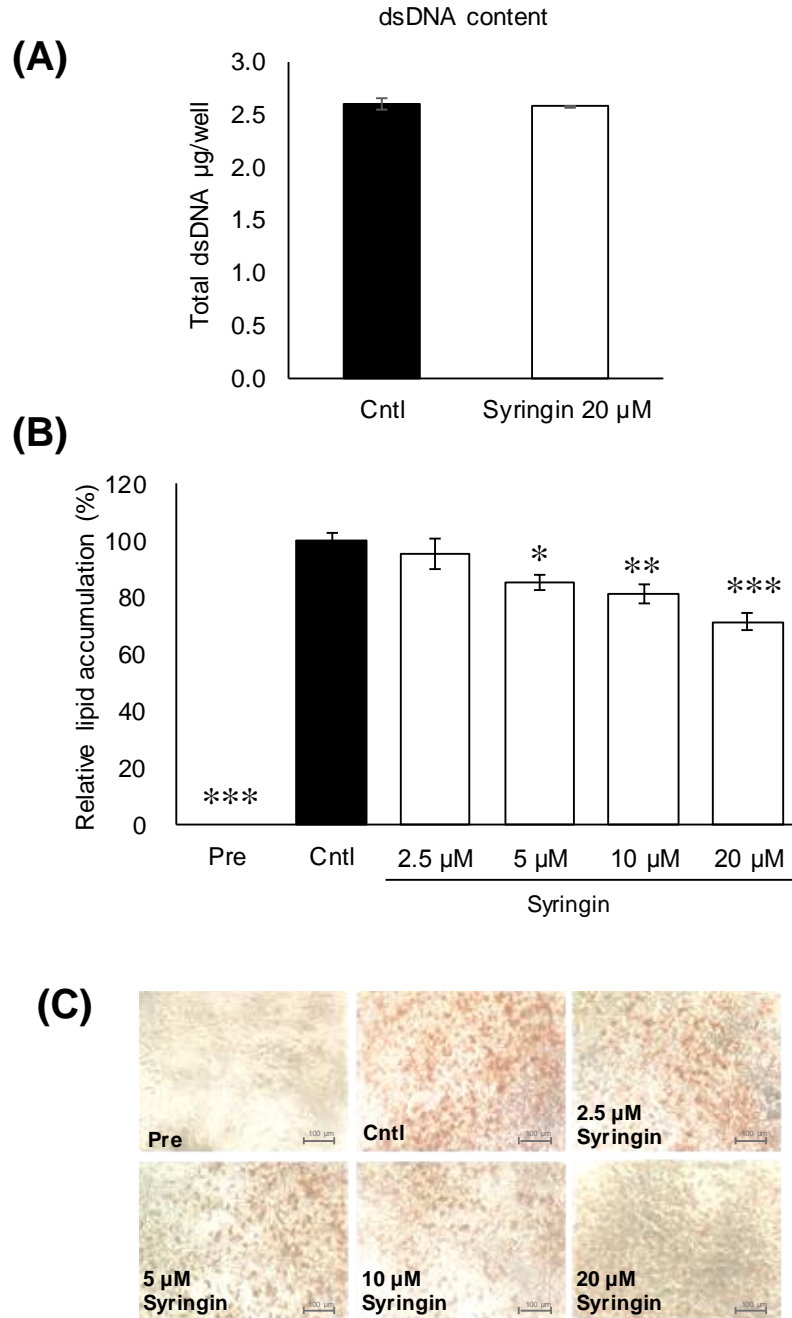


**Figure 4–2** Effect of syringin on adipogenic differentiation through the regulation of adipogenic factors in 3T3–L1 cells. (A) Cytotoxic effect of syringin on 3T3–L1 cells. (B & C) Cellular lipid accumulation by Oil Red O staining (image 20× magnification). The results are presented as means  $\pm$  SEM from three independent experiments. The asterisk (\*) indicates a significant difference between control and treatment groups by Dunnett’s test and Student’s *t*-tests. \* $p < 0.05$ , \*\* $p < 0.01$ , and \*\*\* $p < 0.001$  vs control (Cntl) and preadipocytes (pre).

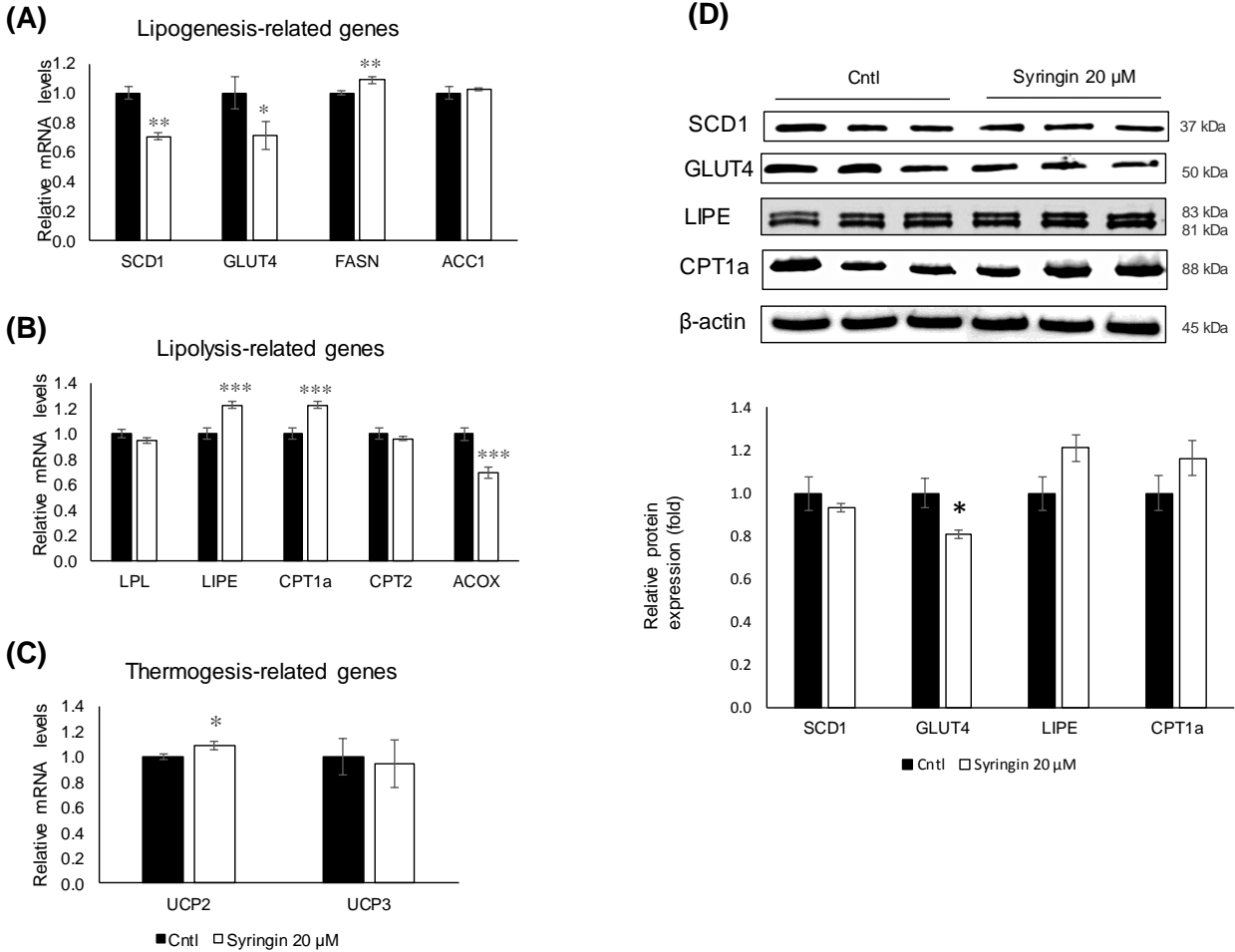


**Figure 4-3** Effect of syringin on adipogenic differentiation through the regulation of adipogenic factors in 3T3-L1 cells. (A–C) mRNA levels of (A) lipogenesis, (B) lipolysis, and (C) thermogenesis-related genes. (D) The expression of lipogenesis and lipolysis-related proteins. The results are presented as means  $\pm$  SEM from three independent experiments. The asterisk (\*) indicates a significant difference between control and treatment groups by Dunnett's test and Student's *t*-tests. \* $p < 0.05$ , \*\* $p < 0.01$ , and \*\*\* $p < 0.001$  vs control (Cntl) and preadipocytes (pre).

#### **4.3.3. Effects of syringin on lipid metabolism related genes and proteins regulation**

First 48 h of differentiation of 3T3-L1 cell has been generally considered as a critical window for assessment of anti-adipogenic effect [144]. To investigate the adipogenic effects of syringin, 3T3-L1 cells have been treated with syringin from day 0 to 2. Double-strand DNA (dsDNA) content of cellular lysate from 3T3-L1 cells cultured with syringin was highly similar compared to that from control cells in chapter III (Figure 4-2A). To understand the molecular mechanisms, assessed mRNA levels of lipid metabolism-related genes in 3T3-L1 cells. When comparing with mRNA levels of untreated control cells, treatment with syringin significantly decreased mRNA levels of the lipogenic-related genes, SCD1 and GLUT4. Whereas slightly increased mRNA level of FASN (Figure 4-3A). However, the protein level of SCD1 was suppressed with no significance, while GLUT4 protein level was significantly retarded as observed in its mRNA expression level. On the other hand, syringin significantly increased mRNA levels of lipolytic-related genes, LIPE and CPT1a, and thermogenic-related genes UCP2 (Figures 4-3B and 4-3C). The protein expression level of CPT1a and LIPE showed an increasing trend compared to control (Figure 4-3D). In lipolytic-related genes, mRNA level of ACOX was significantly decreased by syringin treatment (Figure 4-3B). Treatment with syringin significantly decreased mRNA levels of key adipogenic-specific gene PPAR $\gamma$  and adipocyte marker gene FABP4 and adiponectin, in comparison with untreated 3T3-L1 cells (Figure 4-4A). In protein expression levels, adipogenic-related proteins PPAR $\gamma$ , FABP4, and C/EBP $\alpha$  also significantly decreased by the treatment with syringin (Figure 4-4B).

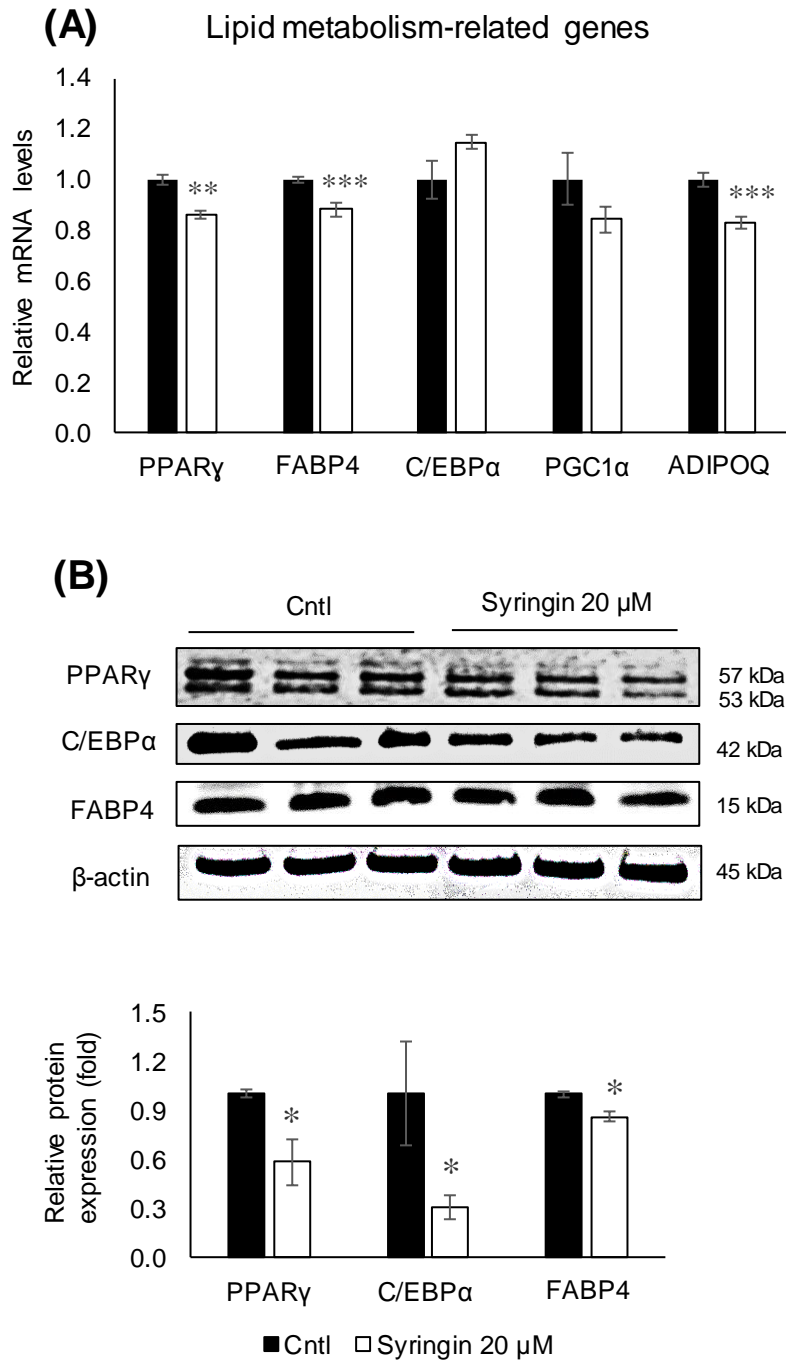


**Figure 4-4** Effect of syringin on the expression of adipogenesis-related genes. (A) mRNA levels of adipogenesis-related genes. (B) Representative Western blot of adipogenic protein factors. The results are presented as means  $\pm$  SEM from three independent experiments. The asterisk (\*) indicates a significant difference between control and treatment groups tested by Student's *t*-test. \* $p < 0.05$  and \*\* $p < 0.01$  vs control (Cntl)

#### **4.3.4. Effects of syringin on signaling pathways**

To elucidate how anti-adipogenic effects of syringin are exerted, I investigated the changes in signaling pathway related to adipogenesis. As shown in Figure 4–5, treatment with syringin significantly upregulated the levels of phosphorylated AMPK and ACC but not that of total ones, resulting in significant increases in phosphorylated protein ratios (Figures 4–4B and 4–5A). On the other hand, phosphorylated Akt ratio was significantly enhanced in 3T3–L1 cells treated with syringin (Figure 4–5C).

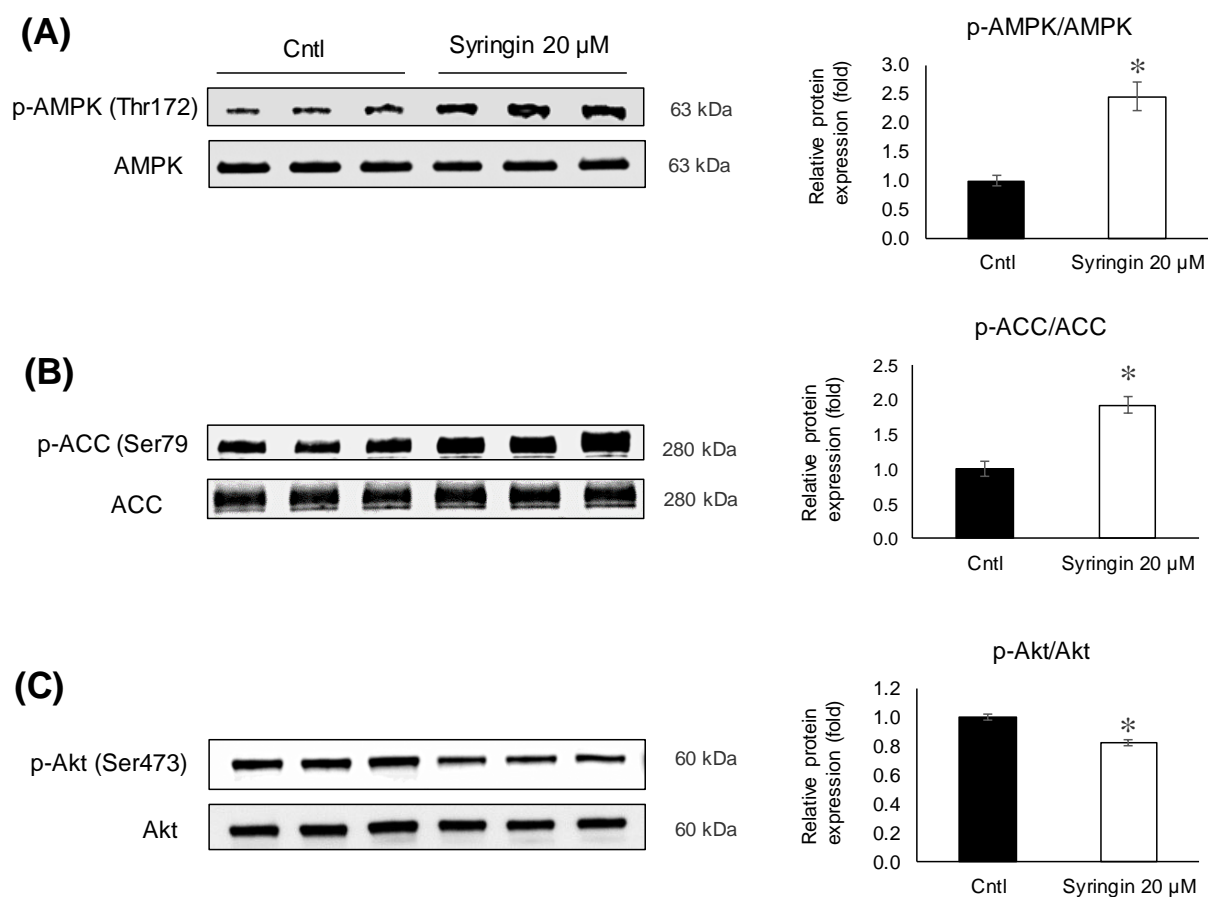


**Figure 4–5** Effects of syringin on AMPK, ACC, and Akt phosphorylation during the differentiation of 3T3–L1 adipocytes. (A–C) Ratios of relative phosphorylated to total protein levels of (A) p-AMPK/AMPK, (B) p-ACC/ACC, and (C) p-Akt/Akt. The results are presented as means  $\pm$  SEM from three independent experiments. The asterisk (\*) indicates a significant difference between control and treatment groups by Student's *t*-test. \**p* < 0.05 vs control (Cntl).

#### 4.4. Discussion

In the previous chapter syringin as a bioactive compound was identified in several plants [141]; however, this is the first time it is being reported that syringin presence in CbR. It has attracted wide attention for its considerable bioactivities such as neuroprotective, antioxidant, anti-diabetic, anti-allergic and anti-inflammatory properties[141]. Syringin significantly inhibited the fibroblast to adipocyte differentiation of 3T3–L1 cell. It was here shown that syringin affects the expression of several lipid metabolism and adipogenic-related genes on the transcriptional and posttranscriptional levels (Figures 4–2 to 4–5) respectively, resulting in anti-adipogenic activities.

It has been especially reported that syringin have potentially hypoglycemic and antidiabetic activities [145,146]. Which are strongly associated obesity related metabolic syndrome. To evaluate the anti-obesity effects of syringin and exposed to a range of syringin at 2.5 to 25  $\mu$ M treated in the later stage of adipocyte differentiation (day 2–6) resulting no significant inhibitory effects on cellular lipid accumulation. Although these results are consistent with (Figure 4–1). In here demonstrated that syringin has anti-adipogenic activity when treated in the early stage of differentiation of 3T3–L1 cells for the first time (Figures 4–1B, and 4–2B and C) without cytotoxicity (Figure 4–2A).

There are several mechanisms for reducing obesity, such as lipid accumulation inhibition, enhanced energy expenditure, thermogenesis and lipolytic enhancement [147]. Adipocyte is an endocrine organ which play a vital role in glucose and lipid metabolism. In addition it maintains physiological signal or metabolic stress by releasing endocrine factors that regulate diverse processes, such as energy expenditure, appetite control, glucose homeostasis, insulin sensitivity, inflammation and tissue repair [148]. Several studies found that, adipocyte differentiation and their



fat accumulation are positively correlated with the number and size of adipocytes which are associated with the development of obesity [149,150]. In this study, treatment with syringin of 3T3–L1 cells significantly decreased mRNA levels of major lipogenic-related genes, but enhanced mRNA levels of major lipolytic and thermogenic-related genes and proteins (Figure 4–3). Adipocyte differentiation is associated with a broad network including transcription factors, which are responsible for expression of adipogenic-related proteins. Among the transcription factors, PPAR $\gamma$  and C/EBP family are considered as a master regulators of adipogenesis [151,152]. As shown in (Figure 4–4A), syringin attenuated the mRNA levels of adipocyte specific markers such as FABP4 and adiponectin, which are regulated by C/EBP $\alpha$  or PPAR $\gamma$  during adipocyte differentiation [153]. Indeed, syringin suppressed mRNA levels of PPAR $\gamma$  and also protein expressions of PPAR $\gamma$  and C/EBP $\alpha$  (Figure 4–4B). Treatment with syringin on 3T3–L1 cells significantly reduced cellular lipid accumulation during early adipocyte differentiation (Figure 4–1B). These data suggested that syringin influence on adipogenesis in 3T3–L1 preadipocytes at an early phase by modulating the expression of adipocytes differentiation–related transcription factors.

Recent studies provided the protective effects of syringin against oxidative stress and inflammation in diabetic rats and considered that syringin could be a probable candidate to be used in the treatment of gestational diabetes. It was also shown that syringin improved insulin sensitivity by increasing AMP-activated protein kinase (AMPK) activity, decreasing expression of lipogenic genes in skeletal muscle cells, and suppressing the chronic inflammation and endoplasmic reticulum (ER) stress [154]. AMPK, a serine/threonine protein kinase, regulates the fatty acid synthesis and degradation according to sensor of cellular energy metabolism, and it has critical role in maintaining energy homeostasis in the body [155]. It has been well known that

AMPK plays a crucial role in regulating adipogenesis, and their activation in adipose tissue could prove beneficial in attenuating adipose tissue dysfunctionality because AMPK has a crucial role in the regulation of transcriptional factors related to adipogenesis and lipid synthesis [156-158]. Therefore, differentiation of pre-adipocytes into adipocytes inhibitory substrate and adipocytes associated with activation of AMPK signaling could be considered as a target for treatment of obesity [159-161]. In an attempt to elucidate the molecular mechanisms underlying syringin induced anti-adipogenesis of 3T3-L1 preadipocytes, protein levels of phosphorylated AMPK and its substrate, ACC were evaluated. Treatment with syringin induced the levels of p-AMPK (Thr172), and this activation resulted in the phosphorylation of ACC resulting in ACC inhibition, in turn, inhibited adipogenesis (Figures 4-5A and 4-5B). The present study also showed the decreases in lipogenic-related gene and proteins expressions (Figure 4-3A). These data therefore suggested that syringin inhibits adipogenesis through the enhanced AMPK activation in adipocyte. Significant decreases in pAkt/Akt ratio were observed in syringin-treated cell compared with the control cells (Figure 4-5C). It has been reported that inhibition of Akt phosphorylation/activation blocks adipocyte differentiation of 3T3-L1 cells, and suggested Akt signaling pathway is essential for adipogenesis [162,163]. Anti-adipogenic effects of syringin, therefore, may be exerted partly by inhibiting Akt activation.

#### **4.5. Conclusion**

Isolated syringin as an anti-adipogenic active compound in CbR, and demonstrated that syringin attenuated lipogenesis by direct modulation of the lipogenic gene network and significantly inhibited adipogenesis of 3T3–L1 cells when treated at early stage of differentiation. To the best of my knowledge, this is the first report on the anti-obesity properties of syringin. Although additional studies are needed to elucidate the underlying details of the molecular mechanisms and reveal the other active component (s) in CbR. This study suggests providing the evidence for promoting the development of natural and safe anti-obesity agents from CbR.

# **CHAPTER V**

## **General Conclusion**

Over the last few decades, obesity has become one of the most prevalent health issues worldwide and reaching pandemic levels. Therefore, it is essential to establish strategies for prevention and medication of obesity.

In previous studies, DPCs such as pteryxin (PTX) and peucedanocoumarin III (PCII) were isolated from *Peucedanum japonicum* Thunb (PJT) have reported anti-obesity properties in 3T3–L1 adipocytes. However, pure DPCs had limitation on *in vivo* study in-depth investigations on mechanisms related to anti-obesity. Thus, in this study found that DPCs consisting anti-obesity effect on HFD-induced obese mice. On the other hand, nanoparticulation of DPCs with PLGA dramatically increased its activity almost 100-fold compared to non-nanoparticulated DPCs. DPCs and nano-DPC modulate gene network showed anti-obesity activity as illustration in (Figure 5–1). I have summarized several important characteristics of PTX and PCIII in Table 5–1 and 5–2 respectively. Thus, this study suggests that DPCs is potential anti-obesity drug in the pharmaceutical industry.

*Cirsium brevicaule* A. GRAY is a wild perennial herb, and its roots (CbR) have traditionally been used as food and medicine in the Okinawa and Amami Islands of Japan. In this study characterized anti-obesity properties of CbR by testing its activities in the 3T3–L1 adipocyte. I have isolated syringin as an anti-obesity active compound for the first time. I have summarized several important characteristics of syringin (Table 5–3) and, syringin modulated the gene network to suppress adipogenesis as illustrated in (Figure 5–2).

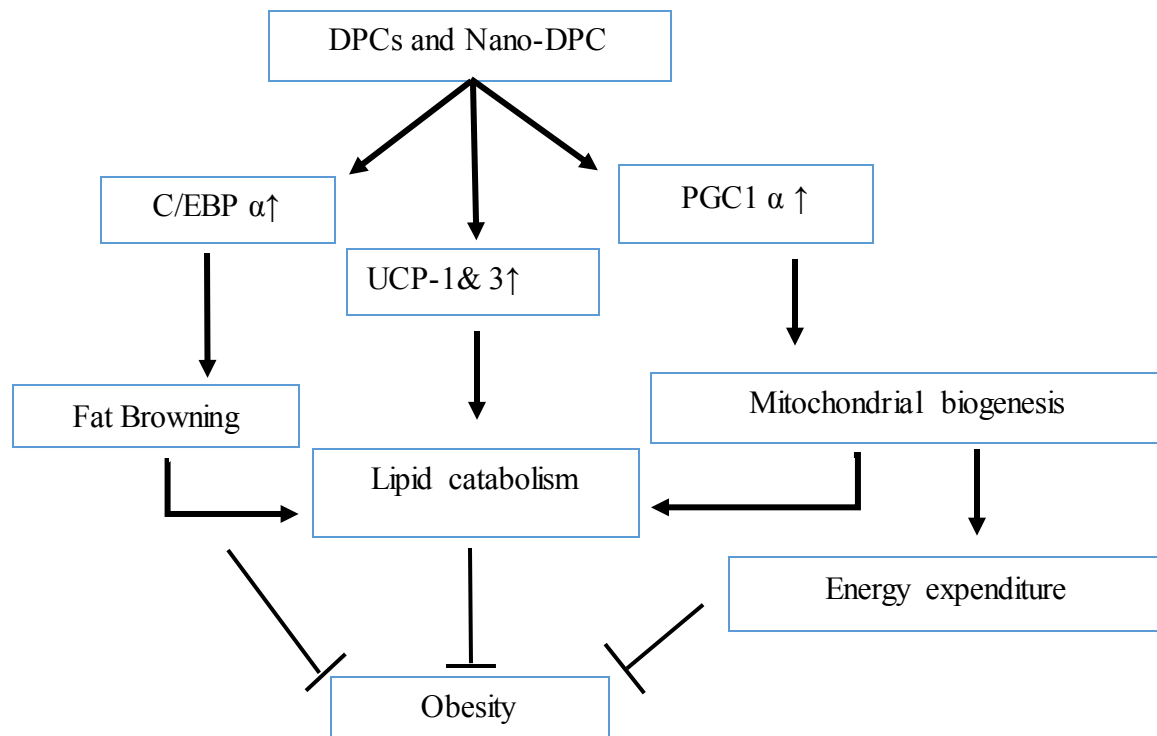


**Figure 5-1** Summary illustration of suppressive effects of DPCs and Nano-DPC on high fat diet induce obese mice fat burning pathway

Stimulatory =  $\rightarrow$   
 Inhibitory action =  $\perp$   
 Up-regulation =  $\uparrow$

**Table 5–1 Summary of pteryxin (PTX) characteristics**

Plant name		Identified Function		Literature
<i>Peucedanum japonicum</i> Formosan	(+)-pteryxin	Antiplatelet aggregation		[164]
<i>Angelica keiskei</i>	(+)-pteryxin	Antitumor-promoter Scavenging activity for against Nitric oxide		[165]
<i>Peucedanum japonicum</i> Thunb	(+)-pteryxin	Antioxidant protein HO-1 inducer		[166]
<i>Peucedanum japonicum</i> Thunb	(+)-pteryxin	Anti-obesity activity		[167]
	20 µg/mL (+)-pteryxin	<i>Upregulated genes</i>	<i>Downregulated genes</i>	[168]
		PPAR $\gamma$ , RORC, FABP4, UCP2	SREBP1c, FAS, ACC, MEST	
	50 µg/mL (+)-pteryxin	PGC1 $\alpha$ , CPT1 $\alpha$	PPAR $\gamma$ , C/EBP $\alpha$ , SREBP1c, MEST, FAS, Adiponectin	

**Table 5–2 Summary of peucedanocoumarin III (PCIII) characteristics**

Source	Name	Identified Function		Literature
Bioactive compound was determined in several plants or Synthetic.	Peucedanocoumarin III	Therapeutic effect on Parkinson's disease		[169]
		Anti-obesity activity		[170]
		<i>Upregulated genes</i>	<i>Downregulated genes</i>	[94]
			PPAR $\gamma$ , PPAR $\alpha$ , C/EBP $\alpha$ , SCD1, Slc2a4, UCP2	



**Table 5–3 Summary of syringin characteristics**

<b>Source</b>	<b>Name</b>	<b>Identified Function</b>	<b>Literature</b>
Bioactive compound was determined in several plants or Synthetic.	Syringin	Neuroprotective effect	[171]
		Antidiabetic effect	[145,146]
		Anti-ulcer effect	[172]
		anti-inflammatory effect	[173]
		Anti-allergic effect	[174]

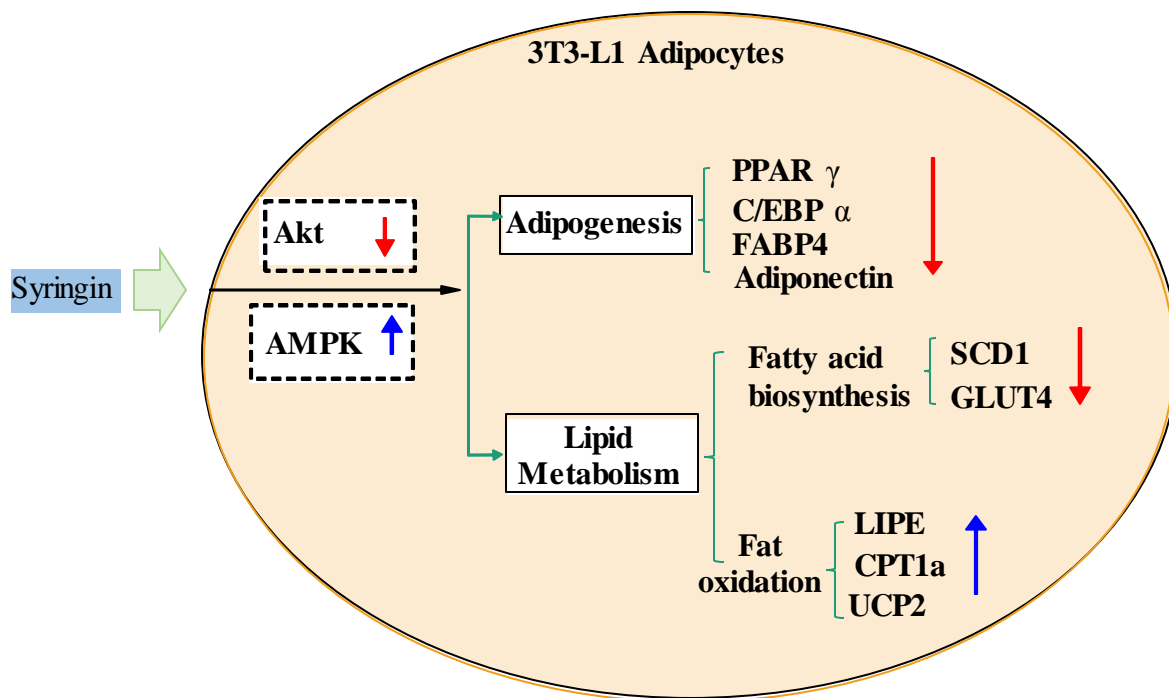


**Figure 5–2** Summary illustration of the suppressive effects of syringin on adipogenesis and lipogenesis related gene parameters *in vitro*

Up-regulation =  $\uparrow$   
 Down-regulation =  $\downarrow$

## References:

1. Vermeulen, S.J.; Park, T.; Khoury, C.K.; Béné, C. Changing diets and the transformation of the global food system. *Annals of the New York Academy of Sciences* **2020**, *1478*, 3, doi:org/10.1111/nyas.14446.
2. Panel, E. *Clinical guidelines on the identification, evaluation, and treatment of overweight and obesity in adults: the evidence report*; National Institutes of Health, National Heart, Lung, and Blood Institute: 1998; org/10.1002/j.1550-8528.1998.tb00690.x.
3. World Health Organization, Obesity and overweight. Available online: <https://www.who.int/news-room/fact-sheets/detail/obesity-and-overweight> (accessed on 15 June , 2021).
4. Stunkard, A.J.; Foch, T.T.; Hrubec, Z. A twin study of human obesity. *Jama* **1986**, *256*, 51-54, doi:10.1001/jama.1986.03380010055024.
5. Bouchard, C.; Tremblay, A.; Després, J.-P.; Nadeau, A.; Lupien, P.J.; Thériault, G.; Dussault, J.; Moorjani, S.; Pinault, S.; Fournier, G. The response to long-term overfeeding in identical twins. *New England Journal of Medicine* **1990**, *322*, 1477-1482, doi:10.1056/NEJM199005243222101.
6. Huang, T.; Hu, F.B. Gene-environment interactions and obesity: recent developments and future directions. *BMC medical genomics* **2015**, *8*, 1-6, doi:10.1186/1755-8794-8-S1-S2.
7. Gong, W.; Li, H.; Song, C.; Yuan, F.; Ma, Y.; Chen, Z.; Wang, R.; Fang, H.; Liu, A. Effects of Gene - Environment Interaction on Obesity among Chinese Adults Born in the Early 1960s. *Genes* **2021**, *12*, 270, doi:10.3390/genes12020270.
8. Guo, W.; Pan, B.; Sakkiyah, S.; Yavas, G.; Ge, W.; Zou, W.; Tong, W.; Hong, H. Persistent organic pollutants in food: contamination sources, health effects and detection methods. *International journal of environmental research and public health* **2019**, *16*, 4361, doi:10.3390/ijerph16224361.
9. Bourez, S.; Le Lay, S.; Van den Daelen, C.; Louis, C.; Larondelle, Y.; Thomé, J. -P.; Schneider, Y.-J.; Dugail, I.; Debier, C. Accumulation of polychlorinated biphenyls in adipocytes: selective targeting

- to lipid droplets and role of caveolin-1. *PLoS One* **2012**, 7, e31834, doi:org/10.1371/journal.pone.0031834.
10. Ruzzin, J.; Petersen, R.; Meugnier, E.; Madsen, L.; Lock, E.-J.; Lillefosse, H.; Ma, T.; Pesenti, S.; Sonne, S.B.; Marstrand, T.T. Persistent organic pollutant exposure leads to insulin resistance syndrome. *Environmental health perspectives* **2010**, 118, 465-471, doi:10.1289/ehp.0901321.
  11. Lim, S.; Cho, Y.M.; Park, K.S.; Lee, H.K. Persistent organic pollutants, mitochondrial dysfunction, and metabolic syndrome. *Annals of the New York Academy of Sciences* **2010**, 1201, 166-176, doi:10.1111/j.1749-6632.2010.05622.x.
  12. Blüher, M. Obesity: global epidemiology and pathogenesis. *Nature Reviews Endocrinology* **2019**, 15, 288-298, doi:org/10.1038/s41574-019-0176-8.
  13. Japan; Society; on; Obesity; Study. Available at <http://www.dm-net.co.jp/calendar/2014/021932.php> **2014**.
  14. Male Obesity Rising in Japan. Available online: <https://www.nippon.com/en/japan-data/h00853/> (accessed on 15 June ).
  15. Ministry; of; Health; Labour; Anderson, M.L.; Welfare. Available at <http://www.mhlw.go.jp/stf/houdou/> **2010**.
  16. Billon, N.; Dani, C. Developmental origins of the adipocyte lineage: new insights from genetics and genomics studies. *Stem Cell Reviews and Reports* **2012**, 8, 55-66, doi:10.1007/s12015-011-9242-x.
  17. Green, H.; Meuth, M. An established pre-adipose cell line and its differentiation in culture. *Cell* **1974**, 3, 127-133, doi: 10.1016/0092-8674(74)90116-0.
  18. Green, H.; Kehinde, O. An established preadipose cell line and its differentiation in culture II. Factors affecting the adipose conversion. *Cell* **1975**, 5, 19-27, doi:10.1016/0092-8674(75)90087-2.

19. Green, H.; Kehinde, O. Spontaneous heritable changes leading to increased adipose conversion in 3T3 cells. *Cell* **1976**, *7*, 105-113, doi:10.1016/0092-8674(76)90260-9.
20. Ross, S.R.; Choy, L.; Graves, R.A.; Fox, N.; Soleyeva, V.; Klaus, S.; Ricquier, D.; Spiegelman, B.M. Hibernoma formation in transgenic mice and isolation of a brown adipocyte cell line expressing the uncoupling protein gene. *Proceedings of the National Academy of Sciences* **1992**, *89*, 7561-7565, doi:10.1073/pnas.89.16.7561.
21. Wabitsch, M.; Brenner, R.; Melzner, I.; Braun, M.; Möller, P.; Heinze, E.; Debatin, K.-M.; Hauner, H. Characterization of a human preadipocyte cell strain with high capacity for adipose differentiation. *International journal of obesity* **2001**, *25*, 8-15, doi:10.1038/sj.ijo.0801520.
22. Rodriguez, A.-M.; Elabd, C.; Delteil, F.; Astier, J.; Vernochet, C.; Saint-Marc, P.; Guesnet, J.; Guezennec, A.; Amri, E.-Z.; Dani, C. Adipocyte differentiation of multipotent cells established from human adipose tissue. *Biochemical and biophysical research communications* **2004**, *315*, 255-263, doi:org/10.1016/j.bbrc.2004.01.053.
23. Pisani, D.F.; Djedaini, M.; Beranger, G.E.; Elabd, C.; Scheideler, M.; Ailhaud, G.P.; Amri, E.-Z. Differentiation of human adipose-derived stem cells into “brite” (brown-in-white) adipocytes. *Frontiers in endocrinology* **2011**, *2*, 87, doi:10.3389/fendo.2011.00087.
24. Farmer, S.R. Transcriptional control of adipocyte formation. *Cell metabolism* **2006**, *4*, 263-273, doi:org/10.1016/j.cmet.2006.07.001.
25. Cho, Y.-W.; Hong, S.; Jin, Q.; Wang, L.; Lee, J.-E.; Gavrilova, O.; Ge, K. Histone methylation regulator PTIP is required for PPAR $\gamma$  and C/EBP $\alpha$  expression and adipogenesis. *Cell metabolism* **2009**, *10*, 27-39, doi:org/10.1016/j.cmet.2009.05.010.
26. Liu, S.; Willett, W.C.; Manson, J.E.; Hu, F.B.; Rosner, B.; Colditz, G. Relation between changes in intakes of dietary fiber and grain products and changes in weight and development of obesity

- among middle-aged women. *American journal of clinical nutrition* **2003**, *78*, 920-927, doi:10.1093/ajcn/78.5.920.
27. Papandreou, D.; Rousso, I.; Mavromichalis, I. Update on non-alcoholic fatty liver disease in children. *Clinical nutrition* **2007**, *26*, 409-415, doi:10.1016/j.clnu.2007.02.002.
  28. Lin, Y.C.; Chang, P.F.; Yeh, S.J.; Liu, K.; Chen, H.C. Risk factors for liver steatosis in obese children and adolescents. *Pediatrics & Neonatology* **2010**, *51*, 149-154, doi:10.1016/S1875-9572(10)60028-9.
  29. Dixon, J.B.; Dixon, M.E.; Anderson, M.L.; Schachter, L.; O'brien, P.E. Daytime sleepiness in the obese: not as simple as obstructive sleep apnea. *Obesity* **2007**, *15*, 2504-2511, doi:org/10.1038/oby.2007.297.
  30. Uguz, F.; Sahingoz, M.; Gungor, B.; Aksoy, F.; Askin, R. Weight gain and associated factors in patients using newer antidepressant drugs. *General hospital psychiatry* **2015**, *37*, 46-48, doi:10.1016/j.genhosppsy.2014.10.011.
  31. Padwal, R.S.; Majumdar, S.R. Drug treatments for obesity: orlistat, sibutramine, and rimonabant. *Lancet* **2007**, *369*, 71-77, doi:10.1016/S0140-6736(07)60033-6.
  32. Ahmad, B.; Serpell, C.; Lim, I.F.; Wong, E.H. Molecular Mechanisms of Adipogenesis: The Anti-Obesogenic Role of AMP-Activated Protein Kinase and Recently Reported Plant Products. *Preprints* **2019**, 2019070040, doi:10.20944/preprints201907.0040.v2.
  33. Drew, B.S.; Dixon, A.F.; Dixon, J.B. Obesity management: update on orlistat. *Vascular health and risk management* **2007**, *3*, 817-821.
  34. Thuraiajah, P.H.; Syn, W.K.; Neil, D.A.; Stell, D.; Haydon, G. Orlistat (Xenical)-induced subacute liver failure. *European journal of gastroenterology & hepatology* **2005**, *17*, 1437-1438, doi:10.1097/01.meg.0000187680.53389.88.

35. Lean, M.E. How does sibutramine work? *International journal of obesity and related metabolic disorders* **2001**, 25 Suppl4, S8-11, doi:10.1038/sj.ijo.0801931.
36. De Simone, G.; D' Addeo, G. Sibutramine: balancing weight loss benefit and possible cardiovascular risk. *Nutrition, Metabolism & Cardiovascular Diseases* **2008**, 18, 337-341, doi:10.1016/j.numecd.2008.03.008.
37. Slovacek, L.; Pavlik, V.; Slovackova, B. The effect of sibutramine therapy on occurrence of depression symptoms among obese patients. *Nutrition, Metabolism & Cardiovascular Diseases* **2008**, 18, e43-44, doi:10.1016/j.numecd.2008.04.002.
38. Nakamura, Y.; Hinoi, E.; Iezaki, T.; Takada, S.; Hashizume, S.; Takahata, Y.; Tsuruta, E.; Takahashi, S.; Yoneda, Y. Repression of adipogenesis through promotion of Wnt/beta-catenin signaling by TIS7 up-regulated in adipocytes under hypoxia. *Biochimica et Biophysica Acta (BBA) - Molecular Basis of Disease* **2013**, 1832, 1117-1128, doi:10.1016/j.bbadis.2013.03.010.
39. Rosen, E.D.; Spiegelman, B.M. Molecular regulation of adipogenesis. *Annual review of cell and developmental biology* **2000**, 16, 145-171, doi:10.1146/annurev.cellbio.16.1.145.
40. Than, A.; Cheng, Y.; Foh, L.C.; Leow, M.K.; Lim, S.C.; Chuah, Y.J.; Kang, Y.; Chen, P. Apelin inhibits adipogenesis and lipolysis through distinct molecular pathways. *Molecular and cellular endocrinology* **2012**, 362, 227-241, doi:10.1016/j.mce.2012.07.002.
41. Park, U.H.; Jeong, H.S.; Jo, E.Y.; Park, T.; Yoon, S.K.; Kim, E.J.; Jeong, J.C.; Um, S.J. Piperine, a component of black pepper, inhibits adipogenesis by antagonizing PPAR $\gamma$  activity in 3T3-L1 cells. *Journal of agricultural and food chemistry* **2012**, 60, 3853-3860, doi:10.1021/jf204514a.
42. Hung, P.F.; Wu, B.T.; Chen, H.C.; Chen, Y.H.; Chen, C.L.; Wu, M.H.; Liu, H.C.; Lee, M.J.; Kao, Y.H. Antimitogenic effect of green tea (-)-epigallocatechin gallate on 3T3-L1 preadipocytes depends on the ERK and Cdk2 pathways. *American Journal of Physiology-Cell Physiology* **2005**, 288, C1094-1108, doi:10.1152/ajpcell.00569.2004.

43. Vitali, A.; Murano, I.; Zingaretti, M.C.; Frontini, A.; Ricquier, D.; Cinti, S. The adipose organ of obesity-prone C57BL/6J mice is composed of mixed white and brown adipocytes. *Journal of lipid research* **2012**, *53*, 619-629, doi:10.1194/jlr.M018846.
44. Fisher, F.M.; Kleiner, S.; Douris, N.; Fox, E.C.; Mepani, R.J.; Verdeguer, F.; Wu, J.; Kharitonov, A.; Flier, J.S.; Maratos-Flier, E., et al. FGF21 regulates PGC-1 $\alpha$  and browning of white adipose tissues in adaptive thermogenesis. *Genes & Development* **2012**, *26*, 271-281, doi:10.1101/gad.177857.111.
45. Bartelt, A.; Heeren, J. Adipose tissue browning and metabolic health. *Nature Reviews Endocrinology* **2014**, *10*, 24-36, doi:10.1038/nrendo.2013.204.
46. Oliver, P.; Lombardi, A.; De Matteis, R. Insights Into Brown Adipose Tissue Functions and Browning Phenomenon. *Frontiers in physiology* **2020**, *11*, 219, doi:10.3389/fphys.2020.00219.
47. Gaspar, R.C.; Pauli, J.R.; Shulman, G.I.; Muñoz, V.R. An update on brown adipose tissue biology: a discussion of recent findings. *American Journal of Physiology-Endocrinology and Metabolism* **2021**, *320*, E488-E495, doi:10.1152/ajpendo.00310.2020.
48. Sun, N.-N.; Wu, T.-Y.; Chau, C.-F. Natural dietary and herbal products in anti-obesity treatment. *Molecules* **2016**, *21*, 1351, doi:10.3390/molecules21101351.
49. Kajimura, S.; Saito, M. A new era in brown adipose tissue biology: molecular control of brown fat development and energy homeostasis. *Annual review of physiology* **2014**, *76*, 225-249, doi:10.1146/annurev-physiol-021113-170252.
50. Xiao, L.; Zhang, J.; Li, H.; Liu, J.; He, L.; Zhang, J.; Zhai, Y. Inhibition of adipocyte differentiation and adipogenesis by the traditional Chinese herb *Sibiraea angustata*. *Experimental Biology and Medicine* **2010**, *235*, 1442-1449, doi:org/10.1258/ebm.2010.010167.
51. Birari, R.B.; Bhutani, K.K. Pancreatic lipase inhibitors from natural sources: unexplored potential. *Drug discovery today* **2007**, *12*, 879-889, doi:10.1016/j.drudis.2007.07.024



52. Jamous, R.M.; Abu-Zaitoun, S.Y.; Akkawi, R.J.; Ali-Shtayeh, M.S. Antiobesity and antioxidant potentials of selected palestinian medicinal plants. *Evidence-Based Complementary and Alternative Medicine* **2018**, 2018, doi:10.1155/2018/8426752.
53. Kim, G.-N.; Shin, M.-R.; Shin, S.H.; Lee, A.R.; Lee, J.Y.; Seo, B.-I.; Kim, M.Y.; Kim, T.H.; Noh, J.S.; Rhee, M.H. Study of antiobesity effect through inhibition of pancreatic lipase activity of Diospyros kaki fruit and Citrus unshiu peel. *BioMed research international* **2016**, 2016, 2314-6133.
54. Marrelli, M.; Loizzo, M.R.; Nicoletti, M.; Menichini, F.; Conforti, F. Inhibition of key enzymes linked to obesity by preparations from Mediterranean dietary plants: effects on  $\alpha$ -amylase and pancreatic lipase activities. *Plant foods for human nutrition* **2013**, 68, 340-346, doi:10.1007/s11130-013-0390-9.
55. Morton, G.; Cummings, D.; Baskin, D.; Barsh, G.; Schwartz, M. Central nervous system control of food intake and body weight. *Nature* **2006**, 443, 289-295, doi:10.1038/nature05026.
56. Belza, A.; Frandsen, E.; Kondrup, J. Body fat loss achieved by stimulation of thermogenesis by a combination of bioactive food ingredients: a placebo-controlled, double-blind 8-week intervention in obese subjects. *International journal of obesity* **2007**, 31, 121-130, doi:org/10.1038/sj.ijo.0803351.
57. O'Neill, H.M.; Holloway, G.P.; Steinberg, G.R. AMPK regulation of fatty acid metabolism and mitochondrial biogenesis: implications for obesity. *Molecular and cellular endocrinology* **2013**, 366, 135-151, doi:10.1016/j.mce.2012.06.019.
58. Bordicchia, M.; Pocognoli, A.; D'Anzeo, M.; Siquini, W.; Minardi, D.; Muzzonigro, G.; Dessì-Fulgheri, P.; Sarzani, R. Nebivolol induces, via  $\beta_3$  adrenergic receptor, lipolysis, uncoupling protein 1, and reduction of lipid droplet size in human adipocytes. *Journal of hypertension* **2014**, 32, 389-396, doi:10.1097/HJH.000000000000024.

59. Sasidharan, S.; Chen, Y.; Saravanan, D.; Sundram, K.; Latha, L.Y. Extraction, isolation and characterization of bioactive compounds from plants' extracts. *African Journal of Traditional, Complementary and Alternative Medicines* **2011**, *8*.
60. Klop, B.; Elte, J.W.F.; Cabezas, M.C. Dyslipidemia in obesity: mechanisms and potential targets. *Nutrients* **2013**, *5*, 1218-1240, doi:10.3390/nu5041218.
61. de Freitas Junior, L.M.; de Almeida Jr, E.B. Medicinal plants for the treatment of obesity: ethnopharmacological approach and chemical and biological studies. *American journal of translational research* **2017**, *9*, 2050.
62. Parida, P.K.; Paul, D.; Chakravorty, D. The natural way forward: Molecular dynamics simulation analysis of phytochemicals from Indian medicinal plants as potential inhibitors of SARS - CoV - 2 targets. *Phytotherapy Research* **2020**, *34*, 3420-3433, doi:org/10.1002/ptr.6868.
63. Yang, L.; Wen, K.-S.; Ruan, X.; Zhao, Y.-X.; Wei, F.; Wang, Q. Response of plant secondary metabolites to environmental factors. *Molecules* **2018**, *23*, 762, doi:10.3390/molecules23040762.
64. Bernáth, J.; Tetenyi, P. The Effect of environmental factors on growth. Development and alkaloid production of Poppy (*Papaver somniferum* L.): I. Responses to day-length and light intensity. *Biochemie und Physiologie der Pflanzen* **1979**, *174*, 468-478, doi:org/10.1016/S0015-3796(17)31342-2.
65. Zoratti, L.; Karppinen, K.; Luengo Escobar, A.; Häggman, H.; Jaakola, L. Light-controlled flavonoid biosynthesis in fruits. *Frontiers in plant science* **2014**, *5*, 534, doi:10.3389/fpls.2014.00534.
66. Zobayed, S.; Afreen, F.; Kozai, T. Phytochemical and physiological changes in the leaves of St. John's wort plants under a water stress condition. *Environmental and Experimental Botany* **2007**, *59*, 109-116, doi:org/10.1016/j.envexpbot.2005.10.002.

67. Menezes-Benavente, L.; Kernodle, S.P.; Margis-Pinheiro, M.; Scandalios, J.G. Salt-induced antioxidant metabolism defenses in maize (*Zea mays* L.) seedlings. *Redox report* **2004**, *9*, 29-36, doi:10.1179/135100004225003888.
68. Murren, C.J.; Auld, J.R.; Callahan, H.; Ghalambor, C.K.; Handelsman, C.A.; Heskell, M.A.; Kingsolver, J.; Maclean, H.J.; Masel, J.; Maughan, H. Constraints on the evolution of phenotypic plasticity: limits and costs of phenotype and plasticity. *Heredity* **2015**, *115*, 293-301, doi:org/10.1038/hdy.2015.8.
69. Hossin, A.Y.; Inafuku, M.; Takara, K.; Nugara, R.N.; Oku, H. Syringin: A Phenylpropanoid Glycoside Compound in *Cirsium brevicaule* A. GRAY Root Modulates Adipogenesis. *Molecules* **2021**, *26*, 1531, doi:org/10.3390/molecules26061531.
70. Hossin, A.Y.; Inafuku, M.; Oku, H. Dihydropyranocoumarins Exerted Anti -Obesity Activity In Vivo and its Activity Was Enhanced by Nanoparticulation with Polylactic-Co-Glycolic Acid. *Nutrients* **2019**, *11*, 3053, doi:10.3390/nu11123053.
71. Anand, P.; Kunnumakkara, A.B.; Newman, R.A.; Aggarwal, B.B. Bioavailability of curcumin: problems and promises. *Molecular pharmaceutics* **2007**, *4*, 807-818, doi:10.1021/mp700113r.
72. Sharma, R. Steward WP, Gescher AJ. *Pharmacokinetics and pharmacodynamics of curcumin*. *Adv Exp Med Biol* **2007**, *595*, 453-470.
73. Alexis, F.; Pridgen, E.; Molnar, L.K.; Farokhzad, O.C. Factors affecting the clearance and biodistribution of polymeric nanoparticles. *Molecular pharmaceutics* **2008**, *5*, 505-515, doi:org/10.1021/mp800051m.
74. Khalil, N.M.; Carraro, E.; Cótica, L.F.; Mainardes, R.M. Potential of polymeric nanoparticles in AIDS treatment and prevention. *Expert opinion on drug delivery* **2011**, *8*, 95-112, doi:10.1517/17425247.2011.543673.

75. Khalil, N.M.; do Nascimento, T.C.F.; Casa, D.M.; Dalmolin, L.F.; de Mattos, A.C.; Hoss, I.; Romano, M.A.; Mainardes, R.M. Pharmacokinetics of curcumin-loaded PLGA and PLGA-PEG blend nanoparticles after oral administration in rats. *Colloids and Surfaces B: Biointerfaces* **2013**, *101*, 353-360, doi:10.1016/j.colsurfb.2012.06.024.
76. Leroux, J.-C.; Allémann, E.; De Jaeghere, F.; Doelker, E.; Gurny, R. Biodegradable nanoparticles—from sustained release formulations to improved site specific drug delivery. *Journal of Controlled Release* **1996**, *39*, 339-350, doi:org/10.1016/0168-3659(95)00164-6.
77. Hans, M.L.; Lowman, A.M. Biodegradable nanoparticles for drug delivery and targeting. *Current Opinion in Solid State and Materials Science* **2002**, *6*, 319-327, doi:org/10.1016/S1359-0286(02)00117-1.
78. Danhier, F.; Ansorena, E.; Silva, J.M.; Coco, R.; Le Breton, A.; Préat, V. PLGA-based nanoparticles: an overview of biomedical applications. *Journal of controlled release* **2012**, *161*, 505-522, doi:org/10.1016/j.jconrel.2012.01.043.
79. Watkins, R.; Wu, L.; Zhang, C.; Davis, R.M.; Xu, B. Natural product-based nanomedicine: recent advances and issues. *International journal of nanomedicine* **2015**, *10*, 6055, doi:10.2147/IJN.S92162.
80. Kondo, N.; Terakawa, M. Biodegradability of poly(lactic-co-glycolic acid) irradiated with femtosecond laser pulses without material removal. *Applied Physics A* **2019**, *125*, 135, doi:10.1007/s00339-019-2433-z.
81. Elmowafy, E.M.; Tiboni, M.; Soliman, M.E. Biocompatibility, biodegradation and biomedical applications of poly(lactic acid)/poly(lactic-co-glycolic acid) micro and nanoparticles. *Journal of Pharmaceutical Investigation* **2019**, *49*, 347-380, doi:10.1007/s40005-019-00439-x.
82. Hines, D.J.; Kaplan, D.L. Poly (lactic-co-glycolic) acid–controlled-release systems: experimental and modeling insights. *Critical Reviews™ in Therapeutic Drug Carrier Systems* **2013**, *30*.

83. Emami, F.; Mostafavi Yazdi, S.J.; Na, D.H. Poly(lactic acid)/poly(lactic-co-glycolic acid) particulate carriers for pulmonary drug delivery. *Journal of Pharmaceutical Investigation* **2019**, *49*, 427-442, doi:10.1007/s40005-019-00443-1.
84. Kumari, A.; Yadav, S.K.; Yadav, S.C. Biodegradable polymeric nanoparticles based drug delivery systems. *Colloids and surfaces B: biointerfaces* **2010**, *75*, 1-18, doi:org/10.1016/j.colsurfb.2009.09.001.
85. Silva, A.T.C.R.; Cardoso, B.C.O.; e Silva, M.E.S.R.; Freitas, R.F.S.; Sousa, R.G. Synthesis, characterization, and study of PLGA copolymer in vitro degradation. *Journal of Biomaterials and Nanobiotechnology* **2015**, *6*, 8, doi:10.4236/jbnnb.2015.61002.
86. Anand, P.; Nair, H.B.; Sung, B.; Kunnumakkara, A.B.; Yadav, V.R.; Tekmal, R.R.; Aggarwal, B.B. RETRACTED: Design of curcumin-loaded PLGA nanoparticles formulation with enhanced cellular uptake, and increased bioactivity in vitro and superior bioavailability in vivo. *Biochemical Pharmacology*: 2010; Vol. 79, pp 330-338.
87. Shaikh, J.; Ankola, D.; Beniwal, V.; Singh, D.; Kumar, M.R. Nanoparticle encapsulation improves oral bioavailability of curcumin by at least 9-fold when compared to curcumin administered with piperine as absorption enhancer. *European Journal of Pharmaceutical Sciences* **2009**, *37*, 223-230, doi:10.1016/j.ejps.2009.02.019.
88. Xie, X.; Tao, Q.; Zou, Y.; Zhang, F.; Guo, M.; Wang, Y.; Wang, H.; Zhou, Q.; Yu, S. PLGA nanoparticles improve the oral bioavailability of curcumin in rats: characterizations and mechanisms. *Journal of agricultural and food chemistry* **2011**, *59*, 9280-9289, doi:10.1021/jf202135j.
89. Yun, J.W. Possible anti-obesity therapeutics from nature—A review. *Phytochemistry* **2010**, *71*, 1625-1641, doi:org/10.1016/j.phytochem.2010.07.011.

90. Barja-Fernandez, S.; Leis, R.; Casanueva, F.F.; Seoane, L.M. Drug development strategies for the treatment of obesity: how to ensure efficacy, safety, and sustainable weight loss. *Drug Design, Development and Therapy* **2014**, *8*, 2391-2400, doi:10.2147/DDDT.S53129.
91. Lafontan, M.; Langin, D. Lipolysis and lipid mobilization in human adipose tissue. *Progress in Lipid Research* **2009**, *48*, 275-297, doi:10.1016/j.plipres.2009.05.001.
92. Nukitrangsan, N.; Okabe, T.; Toda, T.; Inafuku, M.; Iwasaki, H.; Yanagita, T.; Oku, H. Effect of *Peucedanum japonicum* Thunb on the expression of obesity-related genes in mice on a high-fat diet. *Journal of Oleo Science* **2011**, *60*, 527-536.
93. Okabe, T.; Toda, T.; Nukitrangsan, N.; Inafuku, M.; Iwasaki, H.; Oku, H. *Peucedanum japonicum* Thunb inhibits high-fat diet induced obesity in mice. *Phytotherapy Research* **2011**, *25*, 870-877, doi:10.1002/ptr.3355.
94. Taira, N.; Nugara, R.N.; Inafuku, M.; Takara, K.; Ogi, T.; Ichiba, T.; Iwasaki, H.; Okabe, T.; Oku, H. In vivo and in vitro anti-obesity activities of dihydropyrancoumarins derivatives from *Peucedanum japonicum* Thunb. *Journal of Functional Foods* **2017**, *29*, 19-28, doi:10.1016/j.jff.2016.11.030.
95. Chen, Y.-C.; Chen, P.-Y.; Wu, C.-C.; Chen, I.-S. Chemical constituents and anti-platelet aggregation activity from the root of *Peucedanum formosanum*. *Journal of Food and Drug Analysis* **2008**, *16*, doi:org/10.38212/2224-6614.2357.
96. Aida, Y.; Kasama, T.; Takeuchi, N.; Chiba, M.; Tobinaga, S. Pharmacological activities of khellactones, compounds isolated from *Peucedanum japonicum* THUNB. and *Peucedanum praeruptorium* DUNN. *Methods and findings in experimental and clinical pharmacology* **1998**, *20*, 343-352, doi:10.1358/mf.1998.20.4.485689.
97. Sarkhail, P.; Shafiee, A.; Sarkheil, P. Biological activities and pharmacokinetics of praeruptorins from *Peucedanum* species: a systematic review. *BioMed Research International* **2013**, *2013*, 343808, doi:10.1155/2013/343808.

98. Reiner, A.T.; Somoza, V. Extracellular Vesicles as Vehicles for the Delivery of Food Bioactives. *Journal of Agricultural and Food Chemistry* **2019**, *67*, 2113-2119, doi:10.1021/acs.jafc.8b06369.
99. Singh, H. Nanotechnology Applications in Functional Foods; Opportunities and Challenges. *Preventive Nutrition and Food Science* **2016**, *21*, 1-8, doi:10.3746/pnf.2016.21.1.1.
100. Swider, E.; Koshkina, O.; Tel, J.; Cruz, L.J.; de Vries, I.J.M.; Srinivas, M. Customizing poly(lactic-co-glycolic acid) particles for biomedical applications. *Acta Biomaterialia* **2018**, *73*, 38-51, doi:10.1016/j.actbio.2018.04.006.
101. Zakeri-Milani, P.; Loveymi, B.D.; Jelvehgari, M.; Valizadeh, H. The characteristics and improved intestinal permeability of vancomycin PLGA-nanoparticles as colloidal drug delivery system. *Colloids and Surfaces B: Biointerfaces* **2013**, *103*, 174-181, doi:10.1016/j.colsurfb.2012.10.021.
102. Folch, J.; Lees, M.; Sloane Stanley, G.H. A simple method for the isolation and purification of total lipides from animal tissues. *Journal of Biological Chemistry* **1957**, *226*, 497-509, doi:org/10.1016/S0021-9258(18)64849-5.
103. Chen, H.C.; Farese, R.V., Jr. Determination of adipocyte size by computer image analysis. *Journal of lipid research* **2002**, *43*, 986-989, doi:org/10.1016/S0022-2275(20)30474-0.
104. Jo, J.; Gavrilova, O.; Pack, S.; Jou, W.; Mullen, S.; Sumner, A.E.; Cushman, S.W.; Periwai, V. Hypertrophy and/or Hyperplasia: Dynamics of Adipose Tissue Growth. *PLOS Computational Biology* **2009**, *5*, e1000324, doi:10.1371/journal.pcbi.1000324.
105. Ghaben, A.L.; Scherer, P.E. Adipogenesis and metabolic health. *Nature Reviews Molecular Cell Biology* **2019**, *20*, 242-258, doi:10.1038/s41580-018-0093-z.
106. Longo, M.; Zatterale, F.; Naderi, J.; Parrillo, L.; Formisano, P.; Raciti, G.A.; Beguinot, F.; Miele, C. Adipose Tissue Dysfunction as Determinant of Obesity-Associated Metabolic Complications. *Int J Mol Sci* **2019**, *20*, doi:10.3390/ijms20092358.

107. Tandon, P.; Wafer, R.; Minchin, J.E.N. Adipose morphology and metabolic disease. *J Exp Biol* **2018**, *221*, doi:10.1242/jeb.164970.
108. Akazawa, S.; Sun, F.; Ito, M.; Kawasaki, E.; Eguchi, K. Efficacy of troglitazone on body fat distribution in type 2 diabetes. *Diabetes Care* **2000**, *23*, 1067-1071, doi:10.2337/diacare.23.8.1067.
109. Darlington, G.J.; Ross, S.E.; MacDougald, O.A. The role of C/EBP genes in adipocyte differentiation. *Journal of Biological Chemistry* **1998**, *273*, 30057-30060, doi:10.1074/jbc.273.46.30057.
110. Fajas, L.; Fruchart, J.C.; Auwerx, J. Transcriptional control of adipogenesis. *Current Opinion in Cell Biology* **1998**, *10*, 165-173, doi:org/10.1016/S0955-0674(98)80138-5.
111. Gustafson, B.; Gogg, S.; Hedjazifar, S.; Jenndahl, L.; Hammarstedt, A.; Smith, U. Inflammation and impaired adipogenesis in hypertrophic obesity in man. *American Journal of Physiology-Endocrinology and Metabolism* **2009**, *297*, E999-E1003, doi:10.1152/ajpendo.00377.2009.
112. Iwase, M.; Yamamoto, T.; Nishimura, K.; Takahashi, H.; Mohri, S.; Li, Y.; Jheng, H.F.; Nomura, W.; Takahashi, N.; Kim, C.S., et al. Suksdorfin Promotes Adipocyte Differentiation and Improves Abnormalities in Glucose Metabolism via PPARgamma Activation. *Lipids* **2017**, *52*, 657-664, doi:10.1007/s11745-017-4269-7.
113. Palou, A.; Pico, C.; Bonet, M.L.; Oliver, P. The uncoupling protein, thermogenin. *The International Journal of Biochemistry & Cell Biology* **1998**, *30*, 7-11, doi:10.1016/s1357-2725(97)00065-4.
114. Rosen, E.D.; Spiegelman, B.M. Adipocytes as regulators of energy balance and glucose homeostasis. *Nature* **2006**, *444*, 847, doi:org/10.1038/nature05483.
115. Cinti, S. The adipose organ at a glance. *Disease Models & Mechanisms* **2012**, *5*, 588-594, doi:10.1242/dmm.009662.



116. Almind, K.; Manieri, M.; Sivitz, W.I.; Cinti, S.; Kahn, C.R. Ectopic brown adipose tissue in muscle provides a mechanism for differences in risk of metabolic syndrome in mice. *Proceedings of the National Academy of Sciences* **2007**, *104*, 2366-2371, doi:org/10.1073/pnas.0610416104.
117. Wu, J.; Bostrom, P.; Sparks, L.M.; Ye, L.; Choi, J.H.; Giang, A.H.; Khandekar, M.; Virtanen, K.A.; Nuutila, P.; Schaart, G., et al. Beige adipocytes are a distinct type of thermogenic fat cell in mouse and human. *Cell* **2012**, *150*, 366-376, doi:10.1016/j.cell.2012.05.016.
118. Wu, J.; Cohen, P.; Spiegelman, B.M. Adaptive thermogenesis in adipocytes: is beige the new brown? *Genes and Development* **2013**, *27*, 234-250, doi:10.1101/gad.211649.112.
119. Puigserver, P.; Wu, Z.; Park, C.W.; Graves, R.; Wright, M.; Spiegelman, B.M. A cold-inducible coactivator of nuclear receptors linked to adaptive thermogenesis. *Cell* **1998**, *92*, 829-839, doi:10.1016/s0092-8674(00)81410-5.
120. Anand, P.; Nair, H.B.; Sung, B.; Kunnumakkara, A.B.; Yadav, V.R.; Tekmal, R.R.; Aggarwal, B.B. Design of curcumin-loaded PLGA nanoparticles formulation with enhanced cellular uptake, and increased bioactivity in vitro and superior bioavailability in vivo. *Biochemical Pharmacology* **2010**, *79*, 330-338, doi:10.1016/j.bcp.2009.09.003.
121. Xie, X.; Tao, Q.; Zou, Y.; Zhang, F.; Guo, M.; Wang, Y.; Wang, H.; Zhou, Q.; Yu, S. PLGA nanoparticles improve the oral bioavailability of curcumin in rats: characterizations and mechanisms. *J Agric Food Chem* **2011**, *59*, 9280-9289, doi:10.1021/jf202135j.
122. Kozuka, C.; Shimizu-Okabe, C.; Takayama, C.; Nakano, K.; Morinaga, H.; Kinjo, A.; Fukuda, K.; Kamei, A.; Yasuoka, A.; Kondo, T., et al. Marked augmentation of PLGA nanoparticle-induced metabolically beneficial impact of gamma-oryzanol on fuel dyshomeostasis in genetically obese-diabetic ob/ob mice. *Drug Delivery* **2017**, *24*, 558-568, doi:10.1080/10717544.2017.1279237.

123. Demirtas, I.; Tufekci, A.R.; Yaglioglu, A.S.; Elmastas, M. Studies on the antioxidant and antiproliferative potentials of *Cirsium arvense* subsp. vestitum. *Journal of Food Biochemistry* **2017**, *41*, e12299, doi:10.1111/JFBC.12299.
124. Sahli, R.; Rivière, C.; Dufloer, C.; Beaufay, C.; Neut, C.; Bero, J.; Hennebelle, T.; Roumy, V.; Ksouri, R.; Quetin-Leclercq, J. Antiproliferative and antibacterial activities of *Cirsium scabrum* from Tunisia. *Evidence-Based Complementary and Alternative Medicine* **2017**, *2017*, doi:org/10.1155/2017/7247016.
125. Jordon-Thaden, I.E.; Louda, S.M. Chemistry of *Cirsium* and *Carduus*: a role in ecological risk assessment for biological control of weeds? *Biochemical Systematics and Ecology* **2003**, *31*, 1353-1396, doi:10.1016/S0305-1978(03)00130-3.
126. He, X.-F.; He, Z.-W.; Jin, X.-J.; Pang, X.-Y.; Gao, J.-G.; Yao, X.-J.; Zhu, Y. Caryolane-type sesquiterpenes from *Cirsium souliei*. *Phytochemistry Letters* **2014**, *10*, 80-85, doi:10.1016/J.PHYTOL.2014.08.003.
127. Liao, Z.; Wu, Z.; Wu, M. *Cirsium japonicum* flavones enhance adipocyte differentiation and glucose uptake in 3T3-L1 cells. *Biological and Pharmaceutical Bulletin* **2012**, *35*, 855-860, doi:10.1248/bpb.35.855
128. Liao, Z.; Chen, X.; Wu, M. Antidiabetic effect of flavones from *Cirsium japonicum* DC in diabetic rats. *Archives of Pharmacal Research* **2010**, *33*, 353-362, doi:10.1007/s12272-010-0302-6.
129. Mori, S.; Satou, M.; Kanazawa, S.; Yoshizuka, N.; Hase, T.; Tokimitsu, I.; Takema, Y.; Nishizawa, Y.; Yada, T. Body fat mass reduction and up-regulation of uncoupling protein by novel lipolysis-promoting plant extract. *International journal of biological sciences* **2009**, *5*, 311, doi:10.7150/ijbs.5.311.

130. Perez G, R.; Ramirez LM, E.; Vargas S, R. Effect of *Cirsium pascuarens* on blood glucose levels of normoglycaemic and alloxan - diabetic mice. *Phytotherapy Research* **2001**, *15*, 552-554, doi:10.1002/ptr.882.
131. Fernández-Martínez, E.; Jiménez-Santana, M.; Centeno-Álvarez, M.; Torres-Valencia, J.M.; Shibayama, M.; Cariño-Cortés, R. Hepatoprotective effects of nonpolar extracts from inflorescences of thistles *Cirsium vulgare* and *Cirsium ehrenbergii* on acute liver damage in rat. *Pharmacognosy magazine* **2017**, *13*, S860, doi:10.4103/pm.pm\_260\_17.
132. Kadawaki, Y. Taxonomy and distribution of *Cirsium brevicaulis* A. GRAY and its related species (Asteraceae). *Memoirs of the National Science Museum (Tokyo)* **1990**, *23*, 51-61.
133. 門田裕一.シマアザミとその近縁種の分類と分布[英文](奄美諸島・トカラ列島の自然史科学的総合研究-2-). *国立科学博物館専報* **1990**, p51-61.
134. Inafuku, M.; Nugara, R.N.; Kamiyama, Y.; Futenma, I.; Inafuku, A.; Oku, H. *Cirsium brevicaulis* A. GRAY leaf inhibits adipogenesis in 3T3-L1 cells and C57BL/6 mice. *Lipids in health and disease* **2013**, *12*, 124, doi:org/10.1186/1476-511X-12-124.
135. Yin, J.; Heo, S.-I.; Wang, M.-H. Antioxidant and antidiabetic activities of extracts from *Cirsium japonicum* roots. *Nutrition Research and Practice* **2008**, *2*, 247-251, doi:10.4162/nrp.2008.2.4.247.
136. Miyaichi, Y.; Matsuura, M.; Tomimori, T. Phenolic compound from the roots of *Cirsium japonicum* DC. *Natural Medicines* **1995**, *49*, 92-94.
137. Yin, L.; Yang, Y.-h.; Wang, M.-y.; Zhang, X.; Duan, J.-a. Effects of syringin from *Phellodendron chinensis* on monosodium urate crystal-induced inflammation and intercellular adhesion molecule-1 (ICAM-1) expression. *African Journal of Pharmacy and Pharmacology* **2012**, *6*, 1515-1519, doi:10.5897/AJPP12.081.

138. Nakazawa, T.; Yasuda, T.; Ohsawa, K. Metabolites of orally administered *Magnolia officinalis* extract in rats and man and its antidepressant-like effects in mice. *Journal of pharmacy and pharmacology* **2003**, *55*, 1583-1591, doi:10.1211/0022357022188.
139. Es-Safi, N.-E.; Kollmann, A.; Khelifi, S.; Ducrot, P.-H. Antioxidative effect of compounds isolated from *Globularia alypum* L. structure–activity relationship. *LWT-Food science and technology* **2007**, *40*, 1246-1252, doi:10.1016/j.lwt.2006.08.019.
140. Jung, C.H.; Ahn, J.; Heo, S.H.; Ha, T.-Y. Eleutheroside E, an active compound from *Eleutherococcus senticosus*, regulates adipogenesis in 3T3-L1 cells. *Food Science and Biotechnology* **2014**, *23*, 889-893, doi:10.1007/s10068-014-0119-z.
141. US, M.R.; Zin, T.; ABDURRAZAK, M.; AHMAD, B.A. Chemistry and pharmacology of syringin, anovel bioglycoside: A review. *Asian Journal of Pharmaceutical and Clinical Research* **2015**, *8*, 20-25.
142. US, M.R.; Zin, T.; ABDURRAZAK, M.; AHMAD, B.A. Chemistry and pharmacology of syringin, anovel bioglycoside: A review. *CHEMISTRY* **2015**, *8*.
143. Allott, E.H.; Oliver, E.; Lysaght, J.; Gray, S.G.; Reynolds, J.V.; Roche, H.M.; Pidgeon, G.P. The SGBS cell strain as a model for the in vitro study of obesity and cancer. *Clinical and Translational Oncology* **2012**, *14*, 774-782, doi:10.1007/s12094-012-0863-6.
144. Jang, Y.J.; Son, H.J.; Ahn, J.; Jung, C.H.; Ha, T. Coumestrol modulates Akt and Wnt/ $\beta$ -catenin signaling during the attenuation of adipogenesis. *Food & function* **2016**, *7*, 4984-4991, doi:org/10.1039/C6FO01127F.
145. Krishnan, S.S.C.; Subramanian, I.P.; Subramanian, S.P. Isolation, characterization of syringin, phenylpropanoid glycoside from *Musa paradisiaca* tepal extract and evaluation of its antidiabetic effect in streptozotocin-induced diabetic rats. *Biomedicine & Preventive Nutrition* **2014**, *4*, 105-111, doi:org/10.1016/j.bionut.2013.12.009.

146. Niu, H.-S.; Liu, I.-M.; Cheng, J.-T.; Lin, C.-L.; Hsu, F.-L. Hypoglycemic effect of syringin from *Eleutherococcus senticosus* in streptozotocin-induced diabetic rats. *Planta medica* **2008**, *74*, 109-113, doi:10.1055/s-2008-1034275.
147. Evans, M.; Lin, X.; Odle, J.; McIntosh, M. Trans-10, cis-12 conjugated linoleic acid increases fatty acid oxidation in 3T3-L1 preadipocytes. *The Journal of nutrition* **2002**, *132*, 450-455, doi:org/10.1093/jn/132.3.450.
148. Scheja, L.; Heeren, J. The endocrine function of adipose tissues in health and cardiometabolic disease. *Nature reviews endocrinology* **2019**, *15*, 507-524, doi:org/10.1038/s41574-019-0230-6.
149. Jeon, T.; Hwang, S.G.; Hirai, S.; Matsui, T.; Yano, H.; Kawada, T.; Lim, B.O.; Park, D.K. Red yeast rice extracts suppress adipogenesis by down-regulating adipogenic transcription factors and gene expression in 3T3-L1 cells. *Life sciences* **2004**, *75*, 3195-3203, doi:10.1016/j.lfs.2004.06.012.
150. Furuyashiki, T.; Nagayasu, H.; Aoki, Y.; Bessho, H.; Hashimoto, T.; Kanazawa, K.; Ashida, H. Tea catechin suppresses adipocyte differentiation accompanied by down-regulation of PPAR $\gamma$ 2 and C/EBP $\alpha$  in 3T3-L1 cells. *Bioscience, biotechnology, and biochemistry* **2004**, *68*, 2353-2359, doi:org/10.1271/bbb.68.2353.
151. Darlington, G.J.; Ross, S.E.; MacDougald, O.A. The role of C/EBP genes in adipocyte differentiation. *Journal of Biological Chemistry* **1998**, *273*, 30057-30060, doi:10.1074/jbc.273.46.30057.
152. Morrison, R.F.; Farmer, S.R. Hormonal signaling and transcriptional control of adipocyte differentiation. *The Journal of nutrition* **2000**, *130*, 3116S-3121S, doi:10.1093/jn/130.12.3116S.
153. Tsuda, T.; Ueno, Y.; Kojo, H.; Yoshikawa, T.; Osawa, T. Gene expression profile of isolated rat adipocytes treated with anthocyanins. *Biochimica et Biophysica Acta (BBA)-Molecular and Cell Biology of Lipids* **2005**, *1733*, 137-147, doi:10.1016/j.bbalip.2004.12.014.
154. Kim, B.; Kim, M.-S.; Hyun, C.-K. Syringin attenuates insulin resistance via adiponectin-mediated suppression of low-grade chronic inflammation and ER stress in high-fat diet-fed mice.

- Biochemical and Biophysical Research Communications* **2017**, *488*, 40-45, doi:10.1016/j.bbrc.2017.05.003.
155. Kim, S.-K.; Kong, C.-S. Anti-adipogenic effect of dioxinohydroeckol via AMPK activation in 3T3-L1 adipocytes. *Chemico-biological interactions* **2010**, *186*, 24-29, doi:org/10.1016/j.cbi.2010.04.003.
  156. Horman, S.; Browne, G.J.; Krause, U.; Patel, J.V.; Vertommen, D.; Bertrand, L.; Lavoie, A.; Hue, L.; Proud, C.G.; Rider, M.H. Activation of AMP-activated protein kinase leads to the phosphorylation of elongation factor 2 and an inhibition of protein synthesis. *Current biology* **2002**, *12*, 1419-1423, doi:10.1016/s0960-9822(02)01077-1.
  157. Moon, H.S.; Chung, C.S.; Lee, H.G.; Kim, T.G.; Choi, Y.J.; Cho, C.S. Inhibitory effect of (-) - Epigallocatechin - 3 - gallate on lipid accumulation of 3T3 - L1 cells. *Obesity* **2007**, *15*, 2571-2582, doi:10.1038/oby.2007.309.
  158. Ahmad, B.; Serpell, C.J.; Fong, I.L.; Wong, E.H. Molecular Mechanisms of Adipogenesis: The Anti-adipogenic Role of AMP-Activated Protein Kinase. *Frontiers in Molecular Biosciences* **2020**, *7*, doi:org/10.3389/fmolb.2020.00076.
  159. Feng, S.; Reuss, L.; Wang, Y. Potential of natural products in the inhibition of adipogenesis through regulation of PPAR $\gamma$  expression and/or its transcriptional activity. *Molecules* **2016**, *21*, 1278, doi:10.3390/molecules21101278.
  160. Jeon, S.-M. Regulation and function of AMPK in physiology and diseases. *Experimental & molecular medicine* **2016**, *48*, e245-e245.
  161. Baek, J.-H.; Kim, N.-J.; Song, J.-K.; Chun, K.-H. Kahweol inhibits lipid accumulation and induces Glucose-uptake through activation of AMP-activated protein kinase (AMPK). *BMB reports* **2017**, *50(11)*, 566-571, doi:org/10.5483/BMBRep.2017.50.11.031.

162. Kim, G.-S.; Park, H.J.; Woo, J.-H.; Kim, M.-K.; Koh, P.-O.; Min, W.; Ko, Y.-G.; Kim, C.-H.; Won, C.-K.; Cho, J.-H. *Citrus aurantium* flavonoids inhibit adipogenesis through the Akt signaling pathway in 3T3-L1 cells. *BMC complementary and alternative medicine* **2012**, *12*, 31, doi:10.1186/1472-6882-12-31.
163. Choe, W.K.; Kang, B.T.; Kim, S.O. Water-extracted plum (*Prunus salicina* L. cv. Soldam) attenuates adipogenesis in murine 3T3-L1 adipocyte cells through the PI3K/Akt signaling pathway. *Experimental and therapeutic medicine* **2018**, *15*, 1608, doi:10.3892/etm.2017.5569.
164. Chen, I.S.; Chang, C.T.; Sheen, W.S.; Teng, C.M.; Tsai, I.L.; Duh, C.Y.; Ko, F.N. Coumarins and antiplatelet aggregation constituents from Formosan *Peucedanum japonicum*. *Phytochemistry* **1996**, *41*, 525-530, doi:10.1016/0031-9422(95)00625-7.
165. Akihisa, T.; Tokuda, H.; Ukiya, M.; Iizuka, M.; Schneider, S.; Ogasawara, K.; Mukainaka, T.; Iwatsuki, K.; Suzuki, T.; Nishino, H. Chalcones, coumarins, and flavanones from the exudate of *Angelica keiskei* and their chemopreventive effects. *Cancer letters* **2003**, *201*, 133-137, doi:10.1016/s0304-3835(03)00466-x.
166. Taira, J.; Ogi, T. Induction of antioxidant protein HO-1 through Nrf2-ARE signaling due to pteryxin in *Peucedanum japonicum* Thunb in RAW264. 7 macrophage cells. *Antioxidants* **2019**, *8*, 621, doi:10.3390/antiox8120621.
167. Nugara, R.N.; Inafuku, M.; Takara, K.; Iwasaki, H.; Oku, H. Pteryxin: a coumarin in *Peucedanum japonicum* Thunb leaves exerts antiobesity activity through modulation of adipogenic gene network. *Nutrition* **2014**, *30*, 1177-1184, doi:10.1016/j.nut.2014.01.015.
168. Nugara, R.N.; Oku, H.; Saitoh, S.; Inafuku, M.; Iwasaki, H.; Kumara, R.; Undugoda, L.; Lankasena, B. The dose-dependent pteryxin-mediated molecular mechanisms in suppressing adipogenesis in vitro. *Journal of Functional Foods* **2021**, *82*, 104508, doi:org/10.1016/j.jff.2021.104508.

169. Ham, S.; Kim, H.; Yoon, J.-H.; Kim, H.; Song, B.R.; Choi, J.-Y.; Lee, Y.-S.; Paek, S.-M.; Maeng, H.-J.; Lee, Y. Therapeutic Evaluation of Synthetic Peucedanocoumarin III in an Animal Model of Parkinson's Disease. *International Journal of Molecular Sciences* **2019**, *20*, 5481, doi:org/10.3390/ijms20215481.
170. Ham, S.; Kim, H.; Hwang, S.; Kang, H.; Yun, S.P.; Kim, S.; Kim, D.; Kwon, H.S.; Lee, Y.-S.; Cho, M. Cell-based screen using amyloid mimic  $\beta$ 23 expression identifies peucedanocoumarin III as a novel inhibitor of  $\alpha$ -synuclein and Huntingtin aggregates. *Molecules and cells* **2019**, *42*, 480, doi:10.14348/molcells.2019.0091.
171. Yang, E.-J.; Kim, S.-I.; Ku, H.-Y.; Lee, D.-S.; Lee, J.-W.; Kim, Y.-S.; Seong, Y.-H.; Song, K.-S. Syringin from stem bark of *Fraxinus rhynchophylla* protects A $\beta$  (25–35)-induced toxicity in neuronal cells. *Archives of pharmacal research* **2010**, *33*, 531-538, doi:10.1007/s12272-010-0406-z.
172. Huang, L.; Zhao, H.; Huang, B.; Zheng, C.; Peng, W.; Qin, L. *Acanthopanax senticosus*: review of botany, chemistry and pharmacology. *Die Pharmazie-An International Journal of Pharmaceutical Sciences* **2011**, *66*, 83-97.
173. Choi, J.; Shin, K.-M.; Park, H.-J.; Jung, H.-J.; Kim, H.J.; Lee, Y.S.; Rew, J.-H.; Lee, K.-T. Anti-inflammatory and antinociceptive effects of sinapyl alcohol and its glucoside syringin. *Planta medica* **2004**, *70*, 1027-1032, doi:10.1055/s-2004-832642.
174. Cho, J.Y.; Nam, K.H.; Kim, A.R.; Park, J.; Yoo, E.S.; Baik, K.U.; Yu, Y.H.; Park, M.H. In - vitro and in - vivo immunomodulatory effects of syringin. *Journal of Pharmacy and Pharmacology* **2001**, *53*, 1287-1294, doi:10.1211/0022357011776577